AD-A110 842 SHAKER RESEARCH CORP BALLSTON LAKE NY F/G 21/5
BASIC TECHNOLOGY OF SQUEEZE-FILM DAMPERS FOR ROTOR DYNAMICS CON--ETC(U)
NOV 81 C H PAN DAAG29-78-C-0027
UNCLASSIFIED SRC-81-TR-74 ARO-15657.4-E NL

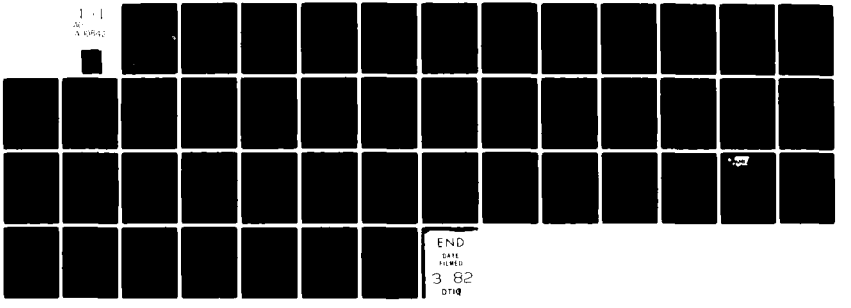

END
DATE FILMED
3 82
DTIC

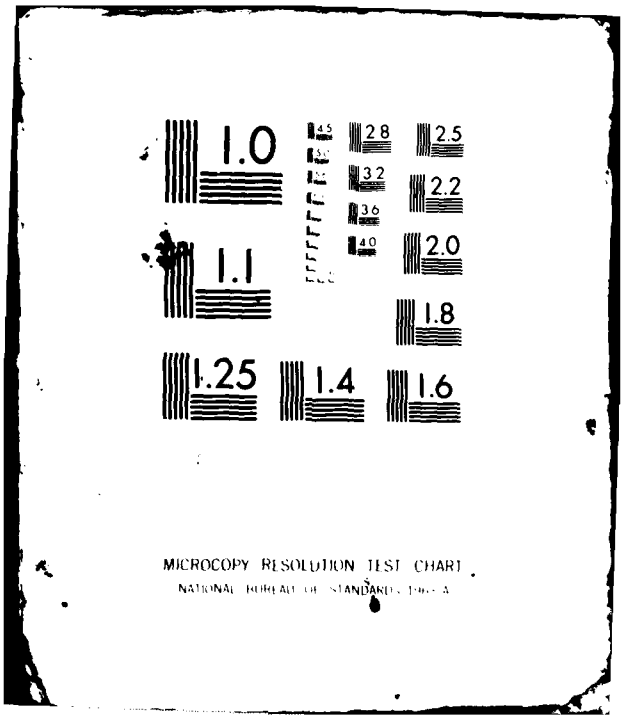
1.0
1.1
1.25
1.4
1.6
1.8
2.0
2.2
2.5
2.8
3.2
3.6
4.0
MICROCOPY RESOLUTION TEST CHART
NATIONAL BUREAU OF STANDARDS 1963-A

(12)

BASIC TECHNOLOGY OF SQUEEZE-FILM DAMPERS FOR ROTOR DYNAMICS CONTROL

By:

C. H. T. Pan

November 1981

U. S. ARMY RESEARCH OFFICE

Contract Number DAAG29-78-C-0027

Shaker Research Corporation
Northway 10 Executive Park
Ballston Lake, NY 12019

UNCLASSIFIED
SECURITY CLASSIFICATION OF THIS PAGE (When Data Entered)

REPORT DOCUMENTATION PAGE		READ INSTRUCTIONS BEFORE COMPLETING FORM
1. REPORT NUMBER SRC81TR74	2. GOVT ACCESSION NO. AD-A110842	3. RECIPIENT'S CATALOG NUMBER
4. TITLE (and Subtitle) BASIC TECHNOLOGY OF SQUEEZE-FILM DAMPERS FOR ROTOR DYNAMICS CONTROL		5. TYPE OF REPORT & PERIOD COVERED FINAL REPORT July 1978 to July 1981 6. PERFORMING ORG. REPORT NUMBER
7. AUTHOR(s) C. H. T. Pan		8. CONTRACT OR GRANT NUMBER(s) DAAG29-78-C-0027
9. PERFORMING ORGANIZATION NAME AND ADDRESS Shaker Research Corporation Northway 10 Executive Park Ballston Lake, NY 12019		10. PROGRAM ELEMENT, PROJECT, TASK AREA & WORK UNIT NUMBERS
11. CONTROLLING OFFICE NAME AND ADDRESS U. S. Army Research Office Post Office Box 12211 Research Triangle Park, NC 27709		12. REPORT DATE November 1981 13. NUMBER OF PAGES
14. MONITORING AGENCY NAME & ADDRESS(if different from Controlling Office)		15. SECURITY CLASS. (of this report) Unclassified 15a. DECLASSIFICATION/DOWNGRADING SCHEDULE

16. DISTRIBUTION STATEMENT (of this Report)

Approved for public release; distribution unlimited.

17. DISTRIBUTION STATEMENT (of the abstract entered in Block 20, if different from Report)

NA

18. SUPPLEMENTARY NOTES

The view, opinions, and/or findings contained in this report are those of the author(s) and should not be construed as an official Department of the Army position, policy, or decision, unless so designated by other documentation.

19. KEY WORDS (Continue on reverse side if necessary and identify by block number)

Squeeze-Film Damper
Rotor Dynamics
Film Rupture
Cavitation
Fluid Film Bearings

20. ABSTRACT (Continue on reverse side if necessary and identify by block number)

Research was performed to develop a rigorous treatment for the film rupture process in the squeeze-film damper. The short bearing analysis was generalized to accommodate a consistent treatment of the rupture domain for a squeeze-film damper, which is undergoing a circular orbit motion either in a submerged condition or with one end subjected to a pressurized feed condition. A closed form solution was found and a full compilation of numerical results was furnished. With appropriate scaling, these results are also valid for

DD FORM 1 JAN 73 1473 EDITION OF 1 NOV 65 IS OBSOLETE

UNCLASSIFIED
SECURITY CLASSIFICATION OF THIS PAGE (When Data Entered)

20. ABSTRACT CONTINUED

the static operation of a short journal bearing under similar lubricant supply conditions. Two publications covered these materials. A third publication gave a general treatment of the motion of the interfacial boundary as applicable to all kinematic circumstances of a thin lubricating film.

TABLE OF CONTENTS

I. INTRODUCTION

Squeeze-film dampers are used in the construction of modern aircraft turbo-engines to allow its rotor to pass through one or more critical speeds to reach its operating condition [1]. Typically, the damper is formed by an oil film which separates the outer race of a roller element bearing from the bearing housing. Due to space limitation, the axial length of the squeeze-film is in the order of the width of the bearing and is effectively quite short in comparison with its diameter. Usually, the damper is centered by a spring structure which represents a parallel connection between the bearing outer-race and the housing. The lubricating oil is typically fed to either or both ends of the squeeze-film through a circumferential distribution manifold.

Effective use of the damper for vibration control requires proper sizing of the damper to fit the flexibility characteristics of the rotor [2]. Obviously, a minimal damping capacity is needed if the kinetic energy of the flexible rotor as excited by a mass imbalance may be absorbed to avoid a cumulatively increasing amplitude of vibration as the critical speed is approached. At the same time, if the damping capacity is excessive, for a flexible rotor, the support bearing in effect becomes rigidly attached to the frame. The critical condition would be shifted to a higher speed. The inherent damping capacity is inoperative because of lack of motion of the support point. The vibrational response to rotor imbalance would increase unchecked as the higher critical speed is approached. Thus, use of damp-mounting to control imbalance response of a flexible rotor through critical speeds requires an optimum damping capacity. If the rotor is required to pass through several critical speeds, the optimum damping capacity is a compromise among all the modes of interest. To design such a damper system properly, it is necessary to carry out a thorough rotor dynamic analysis [3].

Due to inherent symmetry, the response of a centered damper to rotor imbalance is a circular orbit. According to the lubrication theory, there is a kinematic equivalance between a statically loaded journal bearing and a damper in circular orbit. Accordingly, the theory of plain journal bearings can be applied to dampers provided the following rules are observed:

- The static eccentricity of the journal bearing is equivalent to the orbit amplitude of the damper.
- The journal rotational speed ω of the journal bearing is to be replaced by twice the vibrational rate 2ν. Since the vibrational rate is also the rotational speed of the shaft for imbalance response, one in effect doubles the rotational speed when journal bearing data is used to obtain damper characteristics.
- The tangential force per unit static eccentricity of the journal bearing, upon rescaled for twice the rotational speed, is equivalent to the damping force per unit orbit amplitude of the damper.
- The radial force per unit eccentricity of the journal bearing, again upon rescaled for twice the rotational speed, is equivalent to the stiffness force per unit orbit amplitude of the damper, which is additive to the stiffness of the centering spring.

While the above-stated scaling law between a journal bearing and a squeeze-film damper is basically sound, it is ironical that commonly accepted journal bearing data and analysis are not suitable for use to describe damper characteristics. The commonly used Ocvirk-Gümbel analysis for short journal bearings [4,5] is not a suitable model for the squeeze-film damper. This is because a journal bearing usually receives its make-up lubricant supply through a feed-hole, which is within the bearing surface; whereas the lubricant flow in a damper must come in from either end. In order to remedy the situation, Shaker Research Corporation proposed to undertake a study to advance the technology of squeeze-film dampers by establishing the appropriate analysis for its characteristics in a manner consistent with the typical configurations and lubricant supply method. The work was sponsored by U.S. Army Research Office under Contract Number DAAG29-78-C-0027 for the period from July 15, 1978 to July 15, 1981, and was performed under the guidance of the Technical Representative, Dr. Edward A. Saibel of the Engineering Sciences Division, U.S. Army Research Office.

II. SUMMARY OF MAJOR FINDINGS

The theoretical study of a squeeze-film damper undergoing a circular orbital motion was performed in a manner which is also applicable to a statically loaded journal bearing, so long as the lubricant supply is fed through either end. It was established that the film rupture process must satisfy the flow continuity condition throughout the "cavitation domain". The Swift-Stieber condition [6,7] would govern the breakup boundary, whereas the fill-back boundary is established according to the flow balance between surface transport (through the cavitated domain) and the re-established film. It was further concluded that the short-bearing approximation originally advanced by Ocvirk and Dubois [4] can be adapted to satisfy the above-stated conditions around the film rupture boundary. Closed form solutions were found, from which a full set of numerical results was compiled and presented in the dimensionless form. The following general conclusions can be surmised.

- The state of a ruptured film is defined by three parameters; namely, the pressure in the ruptured domain (or the largest orbit size without rupture), the operating orbit size, and the axial location of the rupture axis.
- The pressure in the ruptured domain is an unknown parameter of the system. It can be fixed at the ambient level only if a "drain away condition" is maintained at the discharge side.
- If lubricant is allowed to drain away at both ends of the damper, the lubricant depletion process occurs with the evolution of a succession of "necking down" patterns.
- If the damper is driven into an orbit of an ever increasing orbit amplitude after film rupture has commenced, the overall extent of rupture would increase accordingly and can reach into the convergent portion of the gap. As a consequence of the enlarged rupture domain, the damper would be more "spring-like".
- With a free draining discharge at one end, an appropriate supply pressure fed to the other end would effectively fix the operating characteristics of the damper.

Experimental observations were made by direct viewing of the rupture pattern through a transparent damper bushing. It was found that minor details in the outboard flow passageways can prevent free draining of lubricant discharge. When this happens, the rupture process appeared to be associated with local nucleation sites and developed slowly with the aggregation of void pockets which fluctuate as the dynamic load passes by.

The unsteady motion of a rupture boundary was also treated theoretically. This was done in a manner consistent with the lubrication theory. Flow in the ruptured domain was modeled as an adhered film. Inertia and body forces were neglected as well as meniscus surface tension and interfacial phase transfer. A constant "cavity pressure" was assumed but was allowed to be either higher or lower than the film pressure bordering the rupture boundary. A "law of independent action" was proposed so that the thickness of the adhered film and the sweeping rate of the rupture boundary may be separate interfacial parameters. The commonly used Swift-Stieber condition was shown to be a special case of the "law of independent" action for the quiescent time-independent state. Computation of the adhered film field in the ruptured domain would have to proceed simultaneously with the computation of the film pressure. The former was governed by a real characteristic in the world diagram of the sliding motion and would have to be reconciled in the determination of the sweeping rate of the rupture boundary. The new theory can be used conjunctively with any combination of the surface sliding velocities and with the presence of the squeeze-film action. It can be used as the basis for the numerical simulation of large amplitude, motion of a ruptured film, with or without sliding, including the non-circular orbit of the squeeze film.

III. LIST OF PUBLICATIONS

Four publications are credited to the research supported by ARO. They are listed as follows:

Pan, C. H. T.
"Squeeze-Film Damper Technology. An Overview of Squeeze-Film Dampers, Applications, and Technological Status"
Workshop on Stability and Dynamic Response of Rotors with Squeeze-Film Bearings
May 8-9, 1979
Charlottesville, VA

Pan, C. H. T.
"An Improved Short Bearing Analysis for the Submerged Operation of Plain Journal Bearings and Squeeze-Film Dampers"
ASME Paper No. 79-Lub-33
ASME-ASLE Lubrication Conference
October 16-18, 1979
Dayton, OH
ASME Journal of Lubrication Technology
Vol. 102, No. 3, July 1980
pp. 320-332
1979 Lubrication Division Best Paper

Pan, C. H. T. and Ibrahim, R. A.
"Cavitation in a Short Bearing with Pressurized Lubricant Supply"
ASME Paper No. 80-C2/Lub-47
ASME-ASLE International Lubrication Conference
August 18-21, 1980
San Francisco, CA
ASME Journal of Lubrication Technology
Vol. 103, No. 3, July 1981
pp. 337-349

Pan, C. H. T.
"Dynamic Analysis of Rupture in Thin Fluid Films. I - A Noninertial Theory"
ASME Paper No. 81-Lub-24
ASLE-ASME Joint Lubrication Conference
October 4-7, 1981
New Orleans, LA

Reprints of the last three are included in the Appendix.

IV. PARTICIPATING SCIENTIFIC PERSONNEL

The research was performed by the Principal Investigator, Dr. C. H. T. Pan, with the assistance of other participating scientific personnel of Shaker Research Corporation, who are listed below:

David C. Brower

B. Geren

R. A. Ibrahim

A. I. Krauter

W. D. Waldron

V. REFERENCES

1. Pan, C. H. T., "Squeeze-Film Damper Technology. An Overview of Squeeze-Film Dampers, Applications, and Technological Status," Proceedings of the Conference on the Stability and Dynamic Response of Rotors with Squeeze-Film Bearings, May 8-9, 1979, Charlottesville, VA, Applied Technology Laboratory, AVRADCOM, Fort Eustis, VA, pp. 251-268.

2. Gunter, E. J., Li, D. F., and Barrett, L. E., "Dynamic Characteristics of a Two-Spool Gas Turbine Helicopter Engine," Proceedings of the Conference on the Stability and Dynamic Response of Rotors with Squeeze-Film Bearings, May 8-9, 1979, Charlottesville, VA, Applied Technology Laboratory, AVRADCOM, Fort Eustis, VA, pp. 24-52.

3. Wilson, D. S. and Pan, C. H. T., "Rotor-Bearing Dynamics Technology Design Guide. Part IX - User's Manual," AFAPL-TR-78-6, Part IX, Interim Report for Period November 1979 to October 1980, Aero Propulsion Laboratory, Air Force Wright Aeronautical Laboratories, Air Force Systems Command, Wright-Patterson Air Force Base, OH 45433.

4. Dubois, G. B. and Ocvirk, F. W., "Analytical Derivation of Short Bearing Approximation for Full Journal Bearings," NACA Report 1157, 1953.

5. Gümbel, L. and Everling, E., "Das Problem der Lagerreibung," VDI, Vol. 5, 1914, pp. 87-104.

6. Swift, H. W., "The Stability of Lubricating Films in Journal Bearings," Proceedings Institution of Civil Engineers (London), Vol. 233, 1932, pp. 267-288.

7. Stieber, W., "Das Schwimmlager," VDI, Berlin, 1933.

APPENDIX

Re/Pre-Prints
of
Journal Articles

Reprinted from the JOURNAL OF LUBRICATION TECHNOLOGY, *Vol. 102, No. 3, July 1980*

C. H. T. Pan
Shaker Research Corporation, Ballston Lake, N. Y. 12019. Fellow ASME

An Improved Short Bearing Analysis for the Submerged Operation of Plain Journal Bearings and Squeeze-Film Dampers[1]

By allowing the film pressure to assume some subambient value and by allowing natural boundaries of the film to form in the unloaded region, the short-bearing theory of Ocvirk and Dubois is extended to include a detailed description of the cavitation zone. Two alternative cavitation configurations are shown to be possible, rendering different eccentricity (orbit size), attitude angle (phase), for the same load and minimum film pressure. The first configuration features an enclosed cavity maintained at a subambient level and is called "0" cavitation, which is crudely emulated by the conventional "half-film" approximation. The second configuration features ambient level side cavities, the boundaries of which are drawn inside the bearing ends by a sub-cavity film pressure, and is called "1" cavitation. The "1" cavitation, which is initiated by the aggregation of entrained bubbles in the ambient fluid, can present itself in the form of multiple striations causing substantial loss of load capacity.

I Introduction

The short bearing approximation is a powerful analytical device for the estimation of journal bearing forces. Recent interest in the use of squeeze-film damper for vibration control has drawn considerable attention to its use. The geometrical constraint of a small (L/D) ratio turns out to be commonly quite acceptable. The conventional short-bearing formulae for the bearing forces, however, are also based on an additional heuristic hypothesis that the subambient portion of the film pressure would not be realized. Under the disguise of this "reasonable" model concerning film pressure, a gross inconsistency concerning the lubricant circulation pattern is often overlooked. By neglecting the subambient film pressure, axial flow at the bearing ends can only be outward. In actual practice, the flow leakages through the bearing ends are usually made up by the supply of lubricant through a feed hole in the unloaded portion of the bearing gap. However, the journal bearing may also be used in a submerged arrangement. The squeeze film damper often operates in this manner. In a submerged arrangement, lubricant end leakage from the loaded portion of the bearing film must be made up by the re-entry of the lubricant into the bearing gap on the unloaded side. Thus, the presence of some subambient pressure in the bearing film cannot be avoided.

Ever since the formulation of the lubrication theory by Osborne Reynolds [1], the question of subambient film pressure has been a matter of much controversy. Gumbel [2] pioneered the popular notion that an adequate approximation is attained by discarding that portion of the full solution of the film pressure, which is subambient. After the short bearing approximation was introduced [3], it became immediately linked to Gumbel's idea, the short bearing film is usually taken to be the convergent portion only. Meanwhile, more precise treatment of the film cavitation process, which is presumably the mechanism for preventing the film pressure to fall much below the ambient level, had been attempted in various ways. Swift [4] and Stieber [5] independently revived Reynolds' idea that at a film rupture boundary, the gradient of the film pressure must vanish. Jakobsson and Floberg [6] demonstrated the procedure to treat the rupture boundary in a two dimensional field. Etsion and Pinkus [7] gave computed results including a detailed account for the feeding slot or hole. Wakurai et al. [8] considered a journal bearing with a circumferential feeding slot; they introduced the idea that a short bearing type analysis can be combined with the treatment of the film rupture condition of Swift and Stieber. While Jakobsson and Floberg brought out the significance of a subambient condition through an assumed vapor pressure, the recent efforts [7, 8] still dealt with situations where the film pressure could not be subambient. The cavitation boundary conditions were also re-examined with respect to local flow fields, including the roles of the separation streamline [9] and the surface tension in the meniscus [10]. Floberg returned to the question of minimum film pressure, this time via the concept of liquid tensile strength [11], he sought to determine the pattern of striation

[1] Supported by the U. S. Army Research Office under Contract Number DAAG29-78-C-0027, Project Number P-15657-E.
Contributed by the Lubrication Division of THE AMERICAN SOCIETY OF MECHANICAL ENGINEERS and presented at the ASME-ASLE Lubrication Conference, Dayton, Ohio, October 16-18, 1979. Manuscript received by the Lubrication Division, July 10, 1979. Paper No. 79-Lub-33.

streamers, which have been seen from photographs of the cavitation domain. In contrast to the rupture condition, Floberg's striation streamer analysis depends on the assumption of zero net flow across the boundary. Nau examined experimental evidence of cavitation on face seals [12]. He concluded that there is a distinction between the "separation cavitation" which is associated with a direct communication between the cavitation domain and the ambient, and the "ligament cavitation" which features an enclosed cavitation domain. Interest in vibration control by means of squeeze-film dampers led to experimental information pertaining to the submerged operation of short squeeze journal bearings [13, 14]. Both White and Tonnesen found abrupt changes in the bearing characteristics. Marsh [15], referring to White's data, suggested that subdivision of the fluid film can take place to cause reduction of the dynamic load capacity of the damper.

It is clear that Gumbel's simple model is not always adequate to cope with cavitation phenomena in industrial machine elements. It also became evident that one may not be able to describe all cavitation phenomena in fluid films with a single model such as the Swift-Stieber (or Reynolds) boundary condition, even if one is willing to remain ignorant about processes which pertain to local flow fields. At the same time, although the short bearing formulae as derived with Gumbel's hypothesis are not suitable for a submerged journal bearing, there is no fundamental reason to preclude the use of the short bearing approximation with a more appropriate treatment of the cavitation process. The work of Wakurai, et al already demonstrated the feasibility of treating ambient cavitation with the Reynold's condition. The present work represents another step in this direction.

II Review of Background

Conventional Short Bearing Analysis. With the approximation of a constant viscosity, the laminar, incompressible lubrication theory applicable to a thin fluid film in a cylindrical annular gap is represented by

$$-\frac{1}{12\mu}\frac{\partial}{\partial z}\left(h^3\frac{\partial p}{\partial z}\right)+\frac{\partial}{R\partial\theta}\left(\frac{\omega Rh}{2}-\frac{h^3}{12\mu R}\frac{\partial p}{\partial\theta}\right)+\frac{\partial h}{\partial t}=0 \qquad (1)$$

For two circumstances, (a) the static displacement of a rotating journal, and (b) the steady circular orbit motion of a squeeze-film damper, Equation (1) can be reduced to a single dimensionless form:

$$\frac{1}{\lambda^2}\frac{\partial}{\partial\zeta}\left(H^3\frac{\partial P}{\partial\zeta}\right)+\frac{\partial}{\partial\eta}\left(H^3\frac{\partial P}{\partial\eta}-H\right)=0 \qquad (2)$$

The respective description of the film thickness is, for the static displacement of a rotating journal

$$h=C-e\cos\theta \qquad (3a)$$

and for the circular orbit motion of a squeeze-film damper

$$h=C-e\cos(\theta-\nu t) \qquad (3b)$$

Definitions of the dimensionless variables for the two circumstances are indicated below:

	Static Journal	*Circular Orbit of Damper*
λ	L/D	L/D
H	$h/C=1-\epsilon\cos\eta$	$h/C=1-\epsilon\cos\eta$
P	$p(C^2/(6\mu\omega R^2)$	$p(C^2/(12\mu\nu R^2)$
η	θ	$-(\theta-\nu t)$
ζ	$2z/L$	$2z/L$

The film pressure is measured above the ambient reference. In the case of the damper in a circular orbit, the equivalent sliding vector is in the opposite direction with the amplitude $2\nu R$, thus resulting in the corresponding definitions of P and η.

The short bearing approximation presumes $\partial/\partial\zeta\,(H^3\partial P/\partial\zeta)$ and $\partial/\partial\eta\,(H^3\partial P/\partial\eta)$ to be of a similar magnitude so that in the limit $\lambda\to 0$, equation (2) is reduced to

$$\frac{\partial}{\partial\zeta}\left(H^3\frac{\partial\Pi}{\partial\zeta}\right)-\frac{\partial H}{\partial\eta}=0;\quad \Pi=\lambda^{-2}P \qquad (4)$$

For the axially uniform film, $\partial H/\partial\zeta=0$, equation (4) has the solution

$$\Pi=\Pi_0+\zeta\Pi_1+\frac{\zeta^2}{2}Q(\eta) \qquad (5)$$

where

$$Q(\eta)=H^{-3}\frac{dH}{d\eta}=\frac{\epsilon\sin\eta}{(1-\epsilon\cos\eta)^3} \qquad (6)$$

(Π_0, Π_1) are invariant with respect to ζ and are determined from suitable boundary conditions. The most commonly accepted boundary conditions are associated with the imposition of the ambient pressure of the ends; i.e.

$$\Pi(\zeta=\pm 1)=0$$

so that

$$\Pi_1=0;\quad \Pi_0=-\frac{Q}{2} \qquad (7)$$

Nomenclature

A_n = constant of integration in the neckdown region for "I" cavitation
C = radial clearance
D = diameter of journal
e = eccentricity of journal
F = function of η_f given by equation (27)
F_R, F_T = dimensionless radial and tangential force components, equation (47)
H = dimensionless lubricant film thickness or bearing gap, h/C
h = lubricant film thickness or bearing gap
L = bearing axial length
P = dimensionless film pressure; $p(C^2/(6\mu\omega R^2)$ for static journal bearing, $p(C^2/(12\mu\nu R^2)$ for squeeze-film damper
p = film pressure above ambient
$Q=\frac{1}{H^3}\frac{dH}{d\eta}$
R = journal radius, $D/2$
t = time
z = axial coordinate
α_n = fractional Couette transport across neck-down boundary
ϵ = operating eccentricity ratio, e/C
ϵ_i = eccentricity ratio for cavitation incipience
ζ = dimensionless axial coordinate, $2z/L$
ζ_0 = dimensionless axial distance from film center to cavitation boundary
η = generalized circumferential coordinate
θ = circumferential angular coordinate
λ = slenderness parameter, L/D
μ = viscosity coefficient of fluid
ν = frequency of oscillation of damper
Π = short bearing dimensionless pressure, $P(D/L)^2$
Π_0, Π_1 = integration constants in generalized short bearing solution
Π_C = value of Π in cavity
Π_{min} = lower bound of Π for fluid film
χ = Sommerfeld angle, $2\tan^{-1}\left[\sqrt{\frac{1+\epsilon}{1-\epsilon}}\tan\left(\frac{\eta}{2}\right)\right]$

Subscripts for η

0 = widest point of "0" cavitation
b = break-up boundary in "0" cavitation
b_i = break-up initiation in "0" cavitation
c_i = cavitation incipience point
f = fill back boundary in "0" cavitation
N = minimum pressure point in "I" cavitation
n = neck-down boundary in "I" cavitation
n_i = neck-down initiation in "I" cavitation
u = widening boundary in "I" cavitation

Subscripts for H and Q

H_b, Q_b
etc. = $H(\eta_b)$, $Q(\eta_b)$ etc.

Subscripts for F_R and F_T

FF = full film
CD = cavitation domain

and thus, the so-called "short bearing solution" is given by

$$\Pi = -\frac{1}{2}(1-\zeta^2)Q \tag{8}$$

This equation shows that the lubricant film pressure would be subambient in the interval $0 < \eta < \pi$. Since the latter condition is generally believed to be unlikely in an industrial environment, the "short bearing solution" is often accompanied by the "half-film approximation" by setting

$$\Pi(0 < \eta < \pi) = 0 \tag{9}$$

The "*half film approximation*" removes the perfect antisymmetry with respect to η of Π. Accordingly, the global characteristics of the lubricant as defined by

$$F_R = \int_{-1}^{1} d\zeta \int_{-\pi}^{\pi} \Pi \cos\eta \, d\eta \tag{10a}$$

$$F_T = -\int_{-1}^{1} d\zeta \int_{-\pi}^{\pi} \Pi \sin\eta \, d\eta \tag{10b}$$

are drastically altered. In the case of the "half-film approximation," the above integrals are calculated only in the interval $-\pi \le \eta \le 0$. The integrated results are well known:

	F_R	F_T
Full Film	0	$\frac{2\pi}{3}\frac{\epsilon}{(1-\epsilon^2)^{3/2}}$
Half Film	$\frac{4}{3}\frac{\epsilon^2}{(1-\epsilon^2)^2}$	$\frac{\pi}{3}\frac{\epsilon}{(1-\epsilon^2)^{3/2}}$

(11)

Rationale for the Half Film Approximation. Fixation of the film inlet at $\eta = -\pi$ and the exit at $\eta = 0$ is a fair approximation for most industrial situations. The exit location is justified on the assumption that the lubricant film cannot sustain any significant subambient condition. With the lubricant feedhole placed in the unloaded portion of the bearing gap, the inlet film would be formed not too far from the maximum gap. While it is realized that the inlet location would vary somewhat depending on the specific feeding arrangement, the overall film force does not depend on the precise inlet location.

Sum of end leakages and the exit flow are made up by the flow through the inlet film. Any excess in the flow supply through the feedhole would be discharged to the ambient in the unloaded gap. Thus the total flow through the feedhole ultimately reaches the ambient in the form of axial flow at the bearing ends.

Peculiarity of the Submerged Bearing. In a submerged bearing, because there is no separate feedhole, the net flow through the bearing ends has to be zero. The end flow in the loaded region is necessarily outward, which must be balanced by inward end flow in the unloaded region. The precise flow balance of flow determines the extent of the load carrying film. Some degree of subambient condition is unavoidable. The desired operating characteristics of a submerged bearing may very well require the lubricant film to develop a significant subambient level. Regardless of the magnitude of the subambient condition, the structure of the fluid film on the unloaded side will have a strong influence on the overall film force. If some form of cavitation should develop, the fluid film in the unloaded gap should be narrower than the bearing width. Thus one should expect the short bearing approximation to be at least equally applicable in the unloaded gap as in the loaded gap.

III A New Model of Cavitation for a Submerged Bearing

The conceptual discrepancies in the conventional short bearing solution ("half-film approximation") can be overcome by the following hypotheses.

1. The lubricant film can sustain some subambient and even tensile condition but is bounded by a lower limit

$$\Pi \ge \Pi_{min}; \quad \Pi_{min} < 0 \tag{12}$$

2. The film pressure in the cavitation region is governed by the range

$$\Pi_{min} \le \Pi_c \le 0 \tag{13}$$

Implied along with the second condition, inertia and capillary effects would be neglected. The general short bearing solution, neglecting misalignment, as given by equation (5), will be retained.

One must also give some attention to the conditions at the cavitation boundary. The commonly accepted Reynolds' condition for the lubricant to enter the cavitation boundary is (grad $\Pi = 0$ at $\Pi = \Pi_c$). While no explicit description regarding the flow field inside the cavitation region is associated with the Reynolds' condition, it is usually presumed that the velocity profile is a straight line in approaching the boundary, but, upon crossing over, lubricant is transported through the cavitation region in a thin layer which adheres to the moving surface. Since pressure gradient is negligible within the cavitation region, the lubricant cannot be redistributed in the direction transverse to the surface motion. To satisfy continuity, the film thickness at the re-establishment boundary (relative to that at the break-up boundary) must be consistent with the pressure gradient which would require a concavity in the velocity profile. This description is illustrated in Fig. 1.

Strictly speaking, according to such reasoning, the cavitated domain is not capable to transfer shear stress from one surface to the other. However, it is a common practice to invoke an alternate model, in which fluid transport through the cavitated region is contained in a multitude of striation streamers. Thus the cavitation boundary actually is not smooth, but displays a fluctuating pattern corresponding to the spacing of the striation streamers. The fluid contained in the striation streamers develops little pressure gradient, but contributes to a transfer of shear between the bearing surfaces. Figure 2 shows an illustration of cavitation streamers.

One may further indulge in the dichotomous description of the fluid structure (in the event of cavitation) in the global scale. In the case of a submerged plain journal under load, the condition of equation (13) can be satisfied in two distinct configurations. The central region may break up and give way to an isobaric region at $\Pi_c = \Pi_{min} < 0$. The central cavitation region, however, is separated from the ambient ends by "side bands," through which transverse pressure drop from the ambient continually feeds the lubricant with make-up flow. Such a configuration for cavitation will be referred to as the "0" pattern.

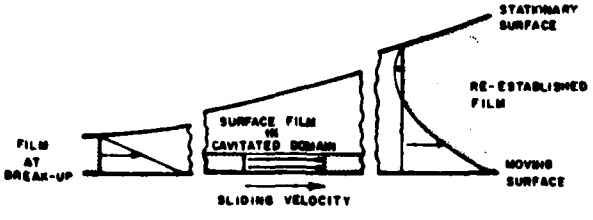

Fig. 1 Fluid transport through a cavitated domain via a surface-film

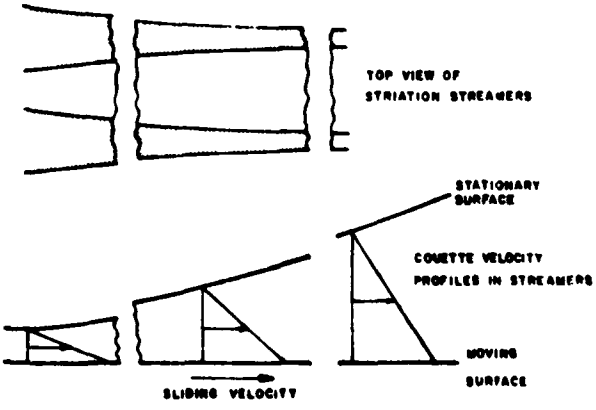

Fig. 2 Shear transmitting striation streamers in a cavitated domain

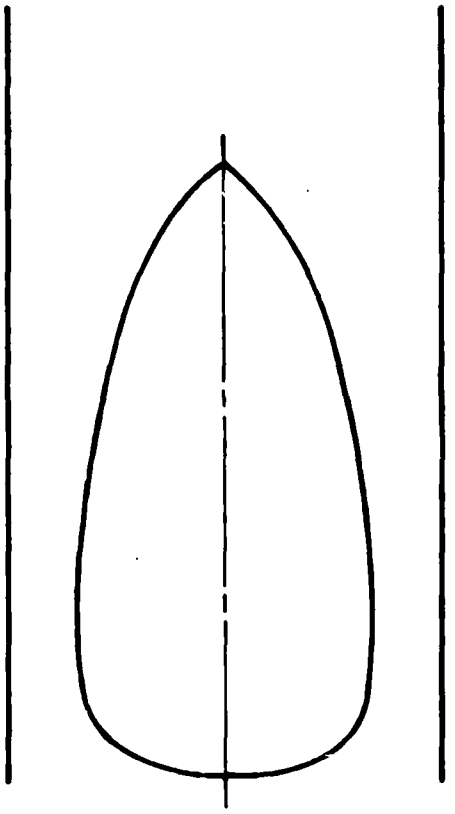

Fig. 3 Film cavitation of the "0" configuration

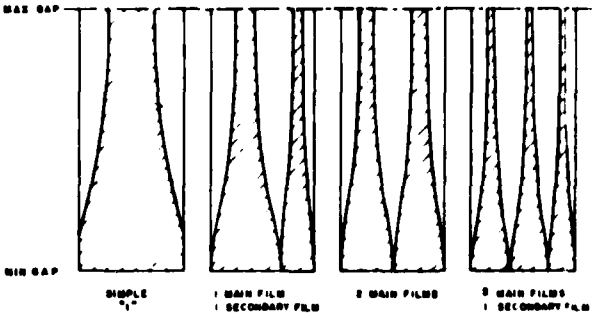

Fig. 4 "I" cavitation configurations, single and multiple striations

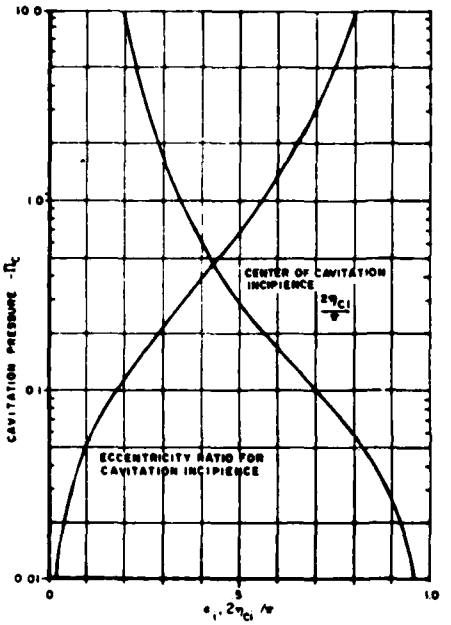

Fig. 5 Eccentricity ratio and center for cavitation incipience

One may retain the "dichotomy" of the flow structure at the micro-scale. That is, Reynolds' condition for film break up can be imposed where applicable, while the streamer concept can be retained to render a conservative estimate for the friction torque. Alternately, side boundaries of the unloaded portion of the fluid film may recede from the bearing ends. Presumably gaseous constituents will fill up the two side regions between the bearing ends and the necked down film. The pressure in the necked down region will be subambient, but the degree of necking down ensures the condition $\Pi_{min} \leq \Pi \leq \Pi_C = 0$. The latter form of cavitation will be designated "*I*." The lower bound value of pressure may require the film to be subdivided into a multiple "*I*" pattern consisting of more than one film strip. For the present purpose, symmetry about the mid-plane prevails in either case, therefore it is sufficient to limit our attention to one half the axial extent, i.e. $0 \leq \zeta \leq 1$. In the case of a multiple "*I*" pattern, $\zeta = 0$ would be the centerline of each film strip. Figs 3 and 4 show the film patterns of the two configurations; the respective analyses for the two cavitations will be dealt with separately in subsequent sections.

IV Analyses of the "0" Cavitation Configuration

Cavitation can commence at the midplane when the lubricant film enters into the divergent gap so that the midplane pressure reaches the condition

$$\Pi(\eta_{bi}, \zeta = 0) = -\frac{Q_{bi}}{2} = \Pi_C < 0 \tag{14}$$

where, η_{bi} locates the initiation of the "break-up" boundary, and

$$Q_{bi} = Q(\eta_{bi}) = \frac{\epsilon \sin \eta_{bi}}{(1 - \epsilon \cos \eta_{bi})^3}$$

Clearly, given Π_C, this condition can exist only if ϵ exceeds a lower bound, which can be called the cavitation incipience eccentricity ratio (for the "0" pattern), $\epsilon_i(\Pi_C)$. When ϵ_i is being exceeded, cavitation begins as a spot which centers around the location of the minimum pressure of the full film solution. The location of the spot from which cavitation grows can be called the cavitation incipience center, η_{Ci}, which is the root of the stationary point of Π in the divergent portion of the full film solution. (ϵ_i, η_{Ci}) as functions of Π_C are given by

$$-\frac{\epsilon_i \sin \eta_{Ci}}{2(1 - \epsilon_i \cos \eta_{Ci})^3} = \Pi_C; \quad \epsilon_i \cos \eta_{Ci} = \frac{1}{4}\left[\sqrt{1 + 24\epsilon_i^2} - 1\right] \tag{15}$$

They are shown as graphs in Fig. 5.

Suppose that $\epsilon > \epsilon_i$ for a given Π_C, the film break-up location η_{bi} can be solved from equation (14), then, for $\eta_b > \eta_{bi}$, the break-up boundary $\zeta_0(\eta_b)$ is to be found. The short bearing solution, Equation (5) is applicable for $\zeta_0 \leq \zeta \leq 1$. The boundary conditions are

$$\Pi(\zeta_0) = \Pi_C; \quad \Pi(1) = 0 \tag{16}$$

η_b is the circumferential coordinate of the break-up boundary.

Furthermore, Reynolds' cavitation condition requires

$$\left(\frac{\partial \Pi}{\partial \zeta}\right)_{\zeta_0} = 0 \tag{17}$$

Therefore

$$\Pi = \left(\frac{1 - \zeta}{1 - \zeta_0}\right)\Pi_C + \frac{1}{2}(1 - \zeta)(\zeta_0 - \zeta)Q \tag{18}$$

and

$$\zeta_0 = 1 - \sqrt{\frac{-2\Pi_C}{Q_b}} \tag{19}$$

Q_b is $Q(\eta_b)$

Making use of equation (14),

$$\zeta_0 = 1 - \sqrt{\frac{Q_{b_0}}{Q_b}} \tag{20}$$

The stationary condition of ζ_0 turns out to coincide with the location of the minimum pressure of the full film solution, i.e.

$$\epsilon \cos \eta_0 = \frac{1}{3}\left[\sqrt{1 + 24\epsilon^2} - 1\right] \tag{21}$$

η_0 locates the widest point of the "0" cavity or the narrowest point of the "side band," which terminates the "break up" boundary, rendering

$$(\zeta_0)_{max} = 1 - \sqrt{\frac{Q_{b_0}}{Q_0}} \tag{22}$$

Q_0 is $Q(\eta_0)$. Representative solutions of the break-up region of the "0" cavitation are shown in Fig. 6.

For $\eta > \eta_0$, the "side band" widens and equation (17) no longer applies. Instead, the sum of the transverse pressure flow and the transport through the "0" cavity should become the required full film flow, which, in the case of the short bearing theory, is simply the Couette flow as illustrated in Fig. 7, the necessary condition is

$$\frac{d\zeta_0}{d\eta_f} = -\frac{(1 - \epsilon\cos\eta_f)^3}{\epsilon(\cos\eta_b - \cos\eta_f)}\left(\frac{\partial\Pi}{\partial\zeta}\right)_{\eta_0} \tag{23}$$

The circumferential coordinate is designated η_f to indicate the "fill-back" process. Together with the pressure boundary conditions, equation (16), the short bearing theory now reduces to

$$\epsilon\left\{(\cos\eta_b - \cos\eta_f)\frac{d}{d\eta_f} + \sin\eta_f\right\}(1 - \zeta_0)^2 = -2(1 - \epsilon\cos\eta_f)^3\Pi_C \tag{24}$$

which describes the geometry of the "fill-back" boundary. The upper limit of η_f is reached when ζ_0 reduces to zero again.

Equation (24) is an ordinary differential equation and can be integrated for $\eta_f \geq \eta_0$ from the initial condition

$$\zeta_0(\eta_f = \eta_0) = (\zeta_0)_{max} \tag{25}$$

which is given by equation (22). η_b is a function of ζ_0 according to equation (20), therefore, the differential equation is *nonlinear*, and its rigorous solution can only be obtained numerically. However, as shown in Fig. 6, for most part of $\zeta_0 < (\zeta_0)_{max}$, η_b deviates very little from η_{b_0}. Therefore, one would expect that linearization of equation (24), obtained by replacing η_b with a suitable constant η_{b_m}, can be quite satisfactory. A reasonable choice for this constant is given by

$$\cos\eta_{b_m} = \frac{1}{(\zeta_0)_{max}}\int_0^{(\zeta_0)_{max}} \cos\eta_b d\zeta_0 \tag{26}$$

which defines the correct total "Couette transport" across the entire breakup boundary. The linearized problem has a closed form solution

$$(1 - \zeta_0)^2 = \left(\frac{H_0 - H_{b_0}}{H - H_{b_m}}\right)(1 - (\zeta_0)_{max})^2 - \frac{2\Pi_C}{(H - H_{b_m})}[F(\eta_f) - F_0] \tag{27}$$

where

$$F(\eta_f) = \left(1 + \frac{3}{2}\epsilon^2\right)\eta_f - 3\epsilon\left(1 + \frac{1}{4}\epsilon^2\right)\sin\eta_f + \frac{3}{4}\epsilon^2\sin 2\eta_f - \frac{1}{12}\epsilon^3\sin 3\eta_f$$

$$F_0 = F(\eta_f = \eta_0)$$

$$H_0 = 1 - \epsilon\cos\eta_0; \quad H_{b_m} = 1 - \epsilon\cos\eta_{b_m}$$

The above relations for the "fill-back" domain holds for $(\zeta_0)_{max} > \zeta_0(\eta_f) > 0$. The latter condition is reached at $\eta_f = \eta_r$, where a full film across the entire bearing width is re-established. η_r is solved numerically from equation (27) by setting $\zeta_0 = 0$.

This approximate solution can be called the "mean transport approximation." The full cavitation pattern calculated according to this approximation is shown for various combinations of (ϵ_r, ϵ) in Fig. 8.

V Analysis of the "I" Cavitation Configuration

The new model for cavitation proposed in Section III admits a second cavitation configuration. Suppose the fluid film remains intact at the midplane while the film pressure is maintained above the lower bound Π_{min} by drawing in liquid-gas interfacial meniscuses from the ends. Such a physical condition is quite reasonable if gaseous sub-

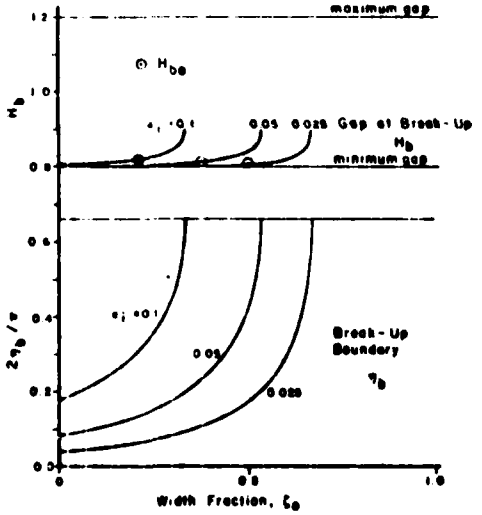

Fig. 6 Break-up boundary of the "0" cavitation configuration

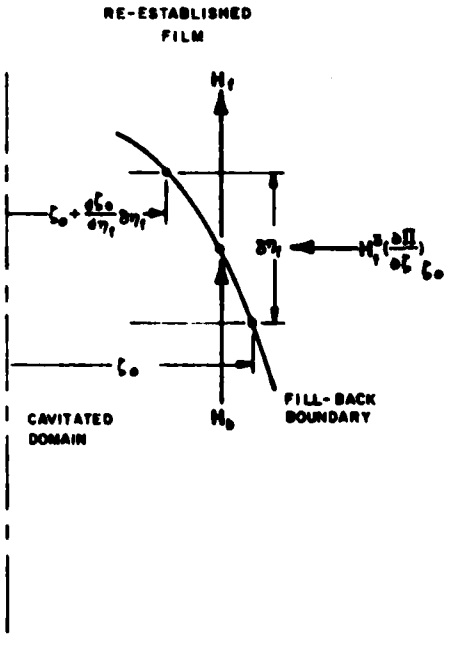

Fig. 7 Continuity across a fill-back boundary in a "0" cavitation configuration

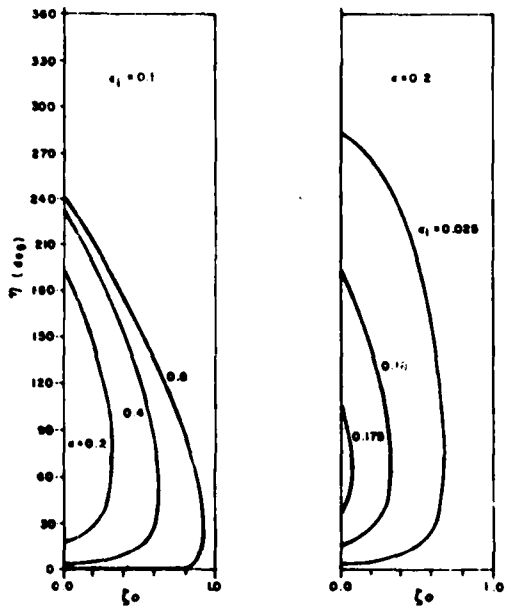

Fig. 8 Boundary patterns of "0" cavitation configuration

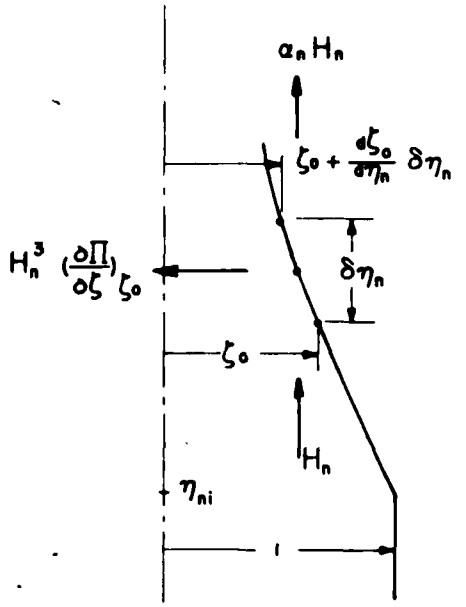

Fig. 9 Continuity across the necking-down boundary in an "I" cavitation configuration

stance is allowed to cumulate near the edges of the bearing film. The corresponding short bearing solution (neglecting surface tension) is

$$\Pi = \frac{-1}{2}(\zeta_0^2 - \zeta^2)Q_n \tag{28}$$

applicable in a yet unspecified range $0 < \eta < \pi$. $\zeta_0(\eta_n)$ is the location of the meniscus boundary, and $Q_n = Q(\eta_n)$, η_n being the circumferential coordinate of the necking-down boundary. It is important to recognize that

$$\frac{\partial \Pi}{\partial \zeta} = \zeta Q \tag{29}$$

varies linearly with the distance from the midplane and assumes its largest amplitude at the meniscus boundary for any value of η_n. This edge film pressure gradient is responsible for feeding the "necked-down" film which centers at the midplane. A crucial question to be settled at this point is the degree-of-fluid transport in the side voids once the "necking-down" process has started. This issue does not exist with the "0" configuration because the Reynolds' cavitation condition was imposed so that $\partial\Pi/\partial\zeta$ vanishes at the break-up boundary. Since axial fluid transport in the side voids cannot be sustained, the overall circumferential fluid transport, including both that through the "necked-down" film and that through the side voids, must be invariant once the necking-down process starts. At a differential scale the flow balance condition across the necking-down boundary is depicted in Fig. 9. Accordingly, the axial coordinate of the necking-down boundary must satisfy

$$H_n^3\left(\frac{\partial \Pi}{\partial \zeta}\right)_{\zeta_0} = -(1-\alpha_n)H_n\frac{d\zeta_0}{d\eta_n}$$

α_n represents "fractional Couette transport" at the necking-down boundary. Since the side voids represent the interruption of ambient feeding of the subambient film, they would be dried up. Therefore the correct value is $\alpha_n = 0$. Accordingly, the continuity condition across the necking-down boundary is

$$H_n^3\left(\frac{\partial \Pi}{\partial \Pi}\right)_{\zeta_0} = -H_n\frac{d\zeta_0}{d\eta_n} \tag{30}$$

Making use of Equation (29) and recalling the definition of Q, one obtains the differential equation for η_n:

$$H_n\frac{d\zeta_0}{d\eta_n} + \zeta_0\frac{dH_n}{d\eta_n} = 0 \tag{31}$$

Its solution is

$$H_n\zeta_0(\eta_n) = \text{const.} = A_n \tag{32}$$

Substituting into equation (28) and setting $\zeta = 0$, the center-line pressure becomes

$$\Pi(\zeta = 0, \eta_n) = -\frac{1}{2}A_n^2\frac{dH_n}{d\eta_n}\Big/H_n^5 \tag{33}$$

The right-hand side has a minimal condition given by

$$4\epsilon^2\cos^2\eta_N + \epsilon\cos\eta_N - 5\epsilon^2 = 0 \tag{34}$$

where η_N designates the location of the minimum film pressure. Solving for $\epsilon\cos\eta_N$, one finds

$$\epsilon\cos\eta_N = \frac{1}{8}[\sqrt{1+80\epsilon^2} - 1] \tag{35}$$

One can then calculate, writing Q_N for $Q(\eta_N)$

$$\Pi(\zeta = 0, \eta_N) = -\frac{1}{2}[\zeta_0(\eta_N)]^2 Q_N \tag{36}$$

One may observe that

$$\eta_N < \eta_{ci}: \quad Q_N < Q_{ci} \tag{37}$$

Consequently, incipience of necking-down depends on

$$-\frac{Q_{ci}}{2} = \Pi_{\min}$$

or

$$\epsilon = \epsilon_i$$

which is essentially the same as the incipience of breaking-up in the "0" cavitation process. An important characteristic of the "I" cavitation is that the extent of necking-down is finite, as soon as the condition for its initiation is satisfied. In contrast, upon incipience of "0" cavitation, the extent of cavitation grows gradually beginning with an infinitesimal amount. The neck-down initiation point η_{ni} coincides with η_{ci} for $\epsilon = \epsilon_i$. The corresponding centerline pressure

is the lower bound value. As ϵ exceeds ϵ_c, η_m moves toward the minimum gap while the corresponding centerline pressure stays at Π_{min} until η_m reaches η_N. $\eta_m \geq \eta_N$ is determined by the condition

$$Q_m = Q(\eta_m) = \frac{\epsilon \sin \eta_m}{(1 - \epsilon \cos \eta_m)^3} = -2\,\Pi_{min} \tag{38}$$

with further increase of ϵ, η_m falls below η_N while the minimum film pressure stays at η_N, so that

$$\zeta_0(\eta_N) = \sqrt{-\frac{2\Pi_{min}}{Q_N}} \tag{39}$$

Together with equation (32), one can calculate

$$\zeta_0(\eta_n) = \zeta_0(\eta_N)\left(\frac{H_N}{H_n}\right) \tag{40}$$

Since H_n cannot be smaller than the minimum gap $H(\eta = 0) = 1 - \epsilon$, it follows that

$$\zeta_0(\eta_r) < \left(\frac{H_N}{1-\epsilon}\right)\zeta_0(\eta_N) \tag{41}$$

If the right-hand side of equation (41) is larger than unity, then the neck-down initiation point $\eta_n > 0$ can be found as

$$\eta_n = \cos^{-1}\left[1 - H_N\zeta_0(\eta_N)\right]/\epsilon \tag{42}$$

for the solution of a simple "*I*" configuration. If the right-hand side of equation (41) should be less than unity, then the maximum width of the film

$$\zeta_0(\eta_r = 0) = \frac{H_N\theta_0(\eta_N)}{1-\epsilon} \tag{43}$$

is only a fraction of the bearing length. The spare length would then be occupied by one or more additional film strip(s) as illustrated in Fig. 4.

The necking-down process terminates at the maximal condition of H_n, which occurs at $\eta_r = \pi$ yielding

$$\zeta_0(\eta_n)_{max} = \zeta_0(\pi) = \left(\frac{H_N}{1+\epsilon}\right)\zeta_0(\eta_N) \tag{44}$$

Widening of the film then commences. Because the side-voids are dry, a relation similar to equation (32) holds, i.e.

$$H_u\,\zeta_0(\eta_u) = const. = A_u \tag{45}$$

η_u is the circumferential coordinate of the widening boundary and $H_u = H(\eta_u)$. It is clear, to maintain continuity, $\zeta_0(\eta_u = \pi) = \zeta_0(\eta_r = \pi)$ and $H_u(\eta_u = \pi) = H_r(\eta_r = \pi)$, one must require $A_u = A_n$. Because

$$H_u = H_\eta(2\pi - \eta_u) \tag{46}$$

the geometry of $\zeta_0(\eta_u)$ is an exact mirror image of $\zeta_0(\eta_n)$ about the line of centers. The domain of the widening process is $\pi \leq \eta_u \leq 2\pi - \eta_m$.

An essential distinctive feature which is common to all simple and multiple "*I*" configurations is the precise symmetry of the film boundaries (and antisymmetry of the pressure field) with respect to the line of centers. This is however in part due to the omission of curvature in the circumferential velocity profile by the short bearing theory.

VI Film Force Calculation

The film force can be calculated in terms of its radial and tangential components relative to the line of centers. In accordance with the common geometrical convention, they can be expressed nondimensionally as

$$(F_R, F_T) = -\frac{(W_R, W_T)}{\left(\frac{1}{2}\right)\mu\omega\left(\frac{R}{C}\right)^2\left(\frac{L}{D}\right)^2(LD)}$$

$$= 2\int_0^{2\pi}(\cos\eta, -\sin\eta)d\eta\int_0^1 \Pi d\zeta \tag{47}$$

Both from the standpoint of computational convenience and from the standpoint of physical interpretations, different procedures for the computation of film force components are devised.

"0" Configuration. For the "0" configuration, it is useful to subdivide the film force components into those in the "full-film" domain covered by $\eta_r \leq \eta \leq \eta_{bi}$ and those in the cavitated domain covered by $\eta_{bi} \leq \eta \leq \eta_r + 2\pi$. Thus

$$(F_R, F_T) = (F_R, F_T)_{FF} + (F_R, F_T)_{CD} \tag{48}$$

Closed form expressions are found for

$$(F_R)_{FF} = \frac{\epsilon(\cos\eta_{bi} - \cos\eta_r)(\cos\eta_{bi} + \cos\eta_r - 2\epsilon\cos\eta_{bi}\cos\eta_r}{3(1-\epsilon\cos\eta_{bi})^2(1-\epsilon\cos\eta_r)^2} \tag{49}$$

$$(F_T)_{FF} = \frac{(1-\epsilon^2)^{-3/2}}{3}\left[(\chi_{bi} - \chi_r) - \frac{1}{2}(\sin 2\chi_{bi} - \sin 2\chi_r)\right] \tag{50}$$

where,

$$\chi = 2\tan^{-1}\left(\sqrt{\frac{1+\epsilon}{1-\epsilon}}\tan\frac{\eta}{2}\right)$$

In the cavitated domain, one may use $\Pi_C = \Pi_{min}$ as the reference pressure. From equation (18)

$$\int_0^1(\Pi - \Pi_C)d\zeta = \int_{\zeta_0}^1(\Pi - \Pi_C)d\zeta$$

$$= -\frac{(1-\zeta_0)}{2}\left[\Pi_C + \frac{(1-\zeta_0)^2}{6}Q\right] \tag{51}$$

For the break-up region, equation (19) applies, therefore

$$\int_0^1(\Pi - \Pi_C)d\zeta = -\frac{1}{3}(1-\zeta_0)\Pi_C \text{ for } \eta_{bi} \leq \eta_b \leq \eta_{bo} \tag{52}$$

In the fill-back region, $\zeta_0(\eta_f)$ is given by equation (27). Thus,

$$(F_R, F_T)_{CD} = 2\left[(\sin\eta_r - \sin\eta_{bi}), (\cos\eta_r - \cos\eta_{bi})\right]\Pi_C$$
$$-\frac{2\Pi_C}{3}\int_{\eta_{bi}}^{\eta_{bo}}(1-\zeta_0)(\cos\eta_b, -\sin\eta_b)d\eta_b$$
$$-\Pi_C\int_{\eta_{bo}}^{\eta_r+2\pi}\left[(1-\zeta_0) + \frac{(1-\zeta_0)^3}{6}\frac{Q}{\Pi_C}\right]$$
$$\times(\cos\eta_f, -\sin\eta_f)d\eta_f \tag{53}$$

which can be readily computed by numerical quadrature with the aid of equations (19) and (27).

"I" Configuration. Consider, first, the simple "*I*" configuration. For the "full-film" domain, $-\eta_{ni} \leq \eta \leq \eta_{ni}$. Equations (49) and (50) apply, upon replacing (η_{bi}, η_r) by $(\eta_{ni}, -\eta_{ni})$, respectively. Thus

$$(F_R)_{FF} = 0$$

$$(F_T)_{FF} = \frac{2}{3}(1-\epsilon^2)^{-3/2}\left(\chi_{ni} - \frac{1}{2}\sin 2\chi_{ni}\right) \tag{54}$$

where,

$$\chi_{ni} = 2\tan^{-1}\left(\sqrt{\frac{1+\epsilon}{1-\epsilon}}\tan\frac{\eta_{ni}}{2}\right)$$

For the necked-down region, $\eta_{ni} \leq \eta_n \leq \pi$, from equation (28),

$$\int_0^1 \Pi d\zeta = \int_0^{\Pi_n}\Pi d\zeta$$

$$= -\frac{\zeta_0^3}{3}Q_n \tag{55}$$

Because of the antisymmetrical character of the film pressure, it is not necessary to treat the widening region, $\pi \leq \eta_w \leq 2\pi - \eta_{ni}$, sep-

arately. Making use of equation (40)

$$(F_R)_{cD} = 0$$

$$(F_T)_{cD} = \frac{4}{3}\epsilon[H_n\zeta_0(\eta_N)]^3 \int_{\eta_{ni}}^{\pi} \frac{\sin^2\eta_n}{H_n^6}\, d\eta_n \tag{56}$$

A closed form integral can be written for

$$\int \frac{\sin^2\eta}{H^6}\, d\eta$$

$$= (1-\epsilon^2)^{-9/2}\left\{\frac{1}{2}\left(1+\frac{3}{4}\epsilon^2\right)\chi - \frac{1}{4}\sin 2\chi - \frac{3\epsilon^2}{32}\sin 4\chi + \epsilon\left(1+\frac{\epsilon^2}{3}\right)\sin^3\chi - \frac{\epsilon^3}{5}\sin^5\chi\right\} \tag{57}$$

where,

$$\chi = 2\tan^{-1}\left[\sqrt{\frac{1+\epsilon}{1-\epsilon}}\left(\tan\frac{\eta}{2}\right)\right]$$

If a multiple "*I*" configuration prevails, $\eta_{ni} = 0$. Then

$$\int_0^{\pi} \frac{\sin^2}{H^6}\, d\eta = \frac{(4+3\epsilon^2)\pi}{8(1-\epsilon^2)^{9/2}} \tag{58}$$

The corresponding film force components are

$$F_R = 0$$

$$F_T = \frac{\epsilon(1-\epsilon)^3(4+3\epsilon^2)\pi}{6(1-\epsilon^2)^{9/2}} \sum [\mu_0(\eta_N)]^3 \tag{59}$$

The summation covers all film strips for the multiple "*I*" pattern.

VII Results

The incipience of cavitation is governed by the lowest pressure which can be sustained by the lubricant film. It is convenient to translate this threshold condition into the cavitation incipience eccentricity, ϵ_i, as given in Fig. 5.

When the operating eccentricity exceeds the incipience condition, $\epsilon > \epsilon_i$, the film on the unloaded side can break up to form a cavitation pattern of the "0" configuration. The essential geometrical parameters of this pattern are the locations of the breakup and re-establishment points and the width fraction of the cavitation domain. They are functions of $\epsilon > \epsilon_i$ as shown in Fig. 10. The break-up point is always located in the divergent part of the bearing gap. As $\epsilon > \epsilon_i$ increases, the break-up point accordingly shifts toward the minimum gap; meanwhile, the re-establishment point extends into the large gap area and the width of the cavitation domain assumes a larger fraction of the bearing length. The re-establishment point ultimately would pass the maximum gap and would be located in the convergent part of the bearing gap. The "far extending cavitation condition," with the film re-established in the convergent gap, can occur even at a very modest operating eccentricity if ϵ_i is small, for instance, at ($\epsilon = 0.1$, $\epsilon_i = 0.065$).

The axial pressure profiles for the "0" cavitation configuration can be classified into three main groups as illustrated in Figure 11. In the full film region, $\eta_i \le \eta \le \eta_{bi}$, the familiar symmetrical parabolic profiles apply. The center-line pressure is above ambient in the converging film and is negative in the divergent film. In the break-up region, $\eta_{bi} \le \eta \le \eta_o$, the parabolic profile is split by the cavitation domain, and it has a zero slope at the break-up boundary according to the Reynolds' boundary condition. In the fill-back region while the ends of the pressure profile are fixed respectively at the cavity and ambient pressures, its shape may be concave or convex depending on whether it is located in the divergent or in the convergent portion of the bearing gap. In fact, for the combination of a large ϵ and a small ϵ_i, it is possible for the pressure to be above ambient so that the film may be losing fluid to both the cavity and the ambient.

The overall film forces for the "0" cavitation configuration are shown graphically in Figs. 12 and 13. In Fig. 12, the tangential force for various values of ϵ_i are plotted against ϵ together with the "complete film" and the "half film" results for comparison. For all $\epsilon > \epsilon_i$, the "complete film" curve is approached as cavitation is either wholly suppressed or is of an insignificant extent. On the other hand, for moderate values of ϵ, if ϵ_i is less than 0.05, the tangential force can be significantly smaller than the value based on the "half film" approximation. Thus, depending on the value of the minimum film pressure, which is associated with the value of ϵ_i according to Figure 5, the "half film" tangential force may be in error by a factor of two

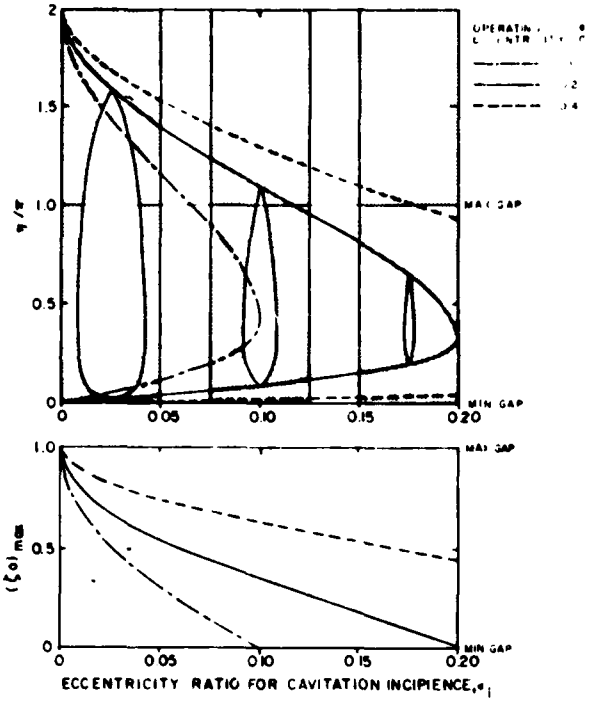

Fig. 10 Geometrical parameters of "0" cavitation

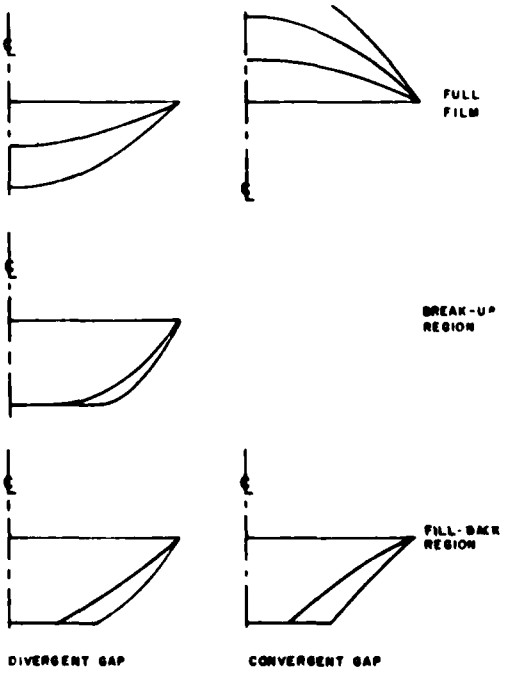

Fig. 11 Axial pressure profiles for "0" cavitation

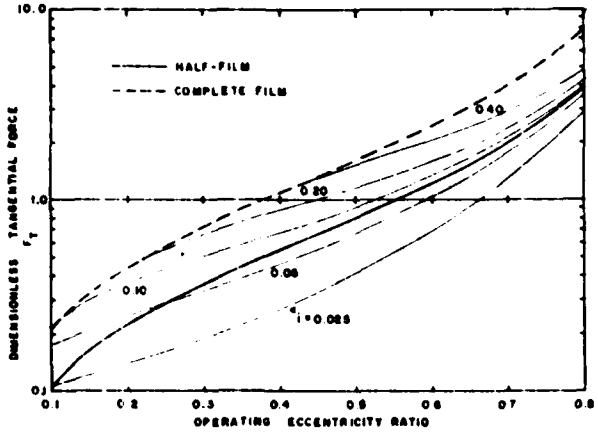

Fig. 12 Tangential force for "0" cavitation

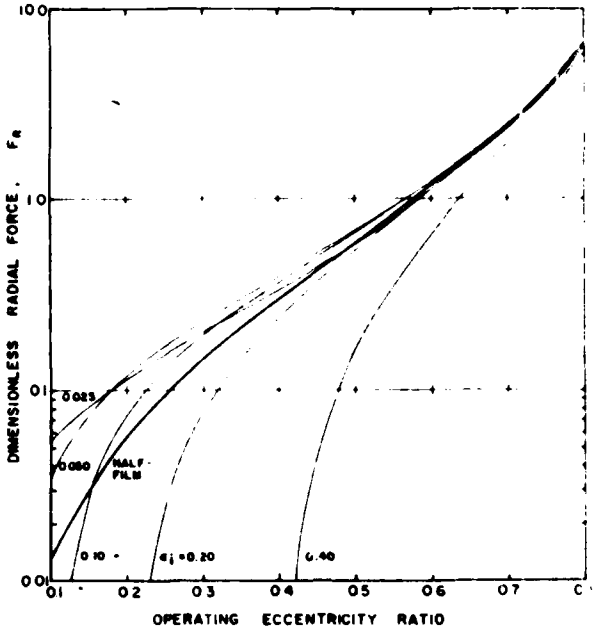

Fig. 13 Radial force for "0" cavitation

either way. In Fig. 13, the radial force is compared with the "half film" result. Again, for $\epsilon \leq \epsilon_i$, the radial force along with the influence of cavitation becomes negligible. For very small values of ϵ the cavitated force can be larger than the "half film" result. In short, the [illegible] solution may be deficient either by overlooking the cavitation incipience threshold or by disregarding the "far extending" [illegible] condition.

The "*I*" cavitation process may take place instead of the "0" pattern, with the film boundaries receding from the bearing ends to form a necked-down central film. Depending on the magnitude of the operating eccentricity ϵ relative to that for cavitation incipience, a variety of film patterns may develop. These possibilities are described below. As ϵ first exceeds ϵ_i, film neck-down commences at $\eta_m = \eta_c$, according to equation (15) where the center-line pressure is lowest. The film continues to neck down as the gap increases with the film width varying inversely as the gap. The neck of the film is located at the maximum gap, beyond which the film width increases. The film geometry is symmetrical about the line of centers while the film pressure is antisymmetrical, consequently the film force is purely tangential. Because such a necking-down process causes an abrupt change in the film pattern as ϵ exceeds ϵ_i, the film force accordingly decreases abruptly. As ϵ becomes larger, η_m moves toward the minimum gap, carrying with it the minimum center-line pressure which is at the lower bound value. As η_m passes below η_N, which is given by equation (35), with further increase of ϵ, the minimum center-line pressure (still maintained at the lower bound value) stays at η_N; the center-line pressure at η_m is higher.

Ultimately the neck-down initiation point would reach the minimum gap. Further increase of ϵ requires the appearance of a narrower secondary strip which contacts the main film strip at the minimum gap. Minimum pressure points are fixed at η_N in both strips. The minimum pressure in the main film strip stays at the lower bound value while that in the secondary strip is higher. With increasing ϵ, the widths of the main and secondary strips respectively decreases and increases until they become equal. A still larger ϵ would then require another secondary strip to appear, starting a new cycle. While the film pattern takes on such variations as illustrated in Fig. 4, the axial pressure profiles remain as simple parabolas with the only stipulation that the minimum pressure remains no less than the lower bound value. The film force, which is purely tangential for the entire family of the "*I*" patterns, is shown in Fig. 14. For $\epsilon < \epsilon_i$, the lubricant film is complete, the corresponding film force is shown as a dashed line. As ϵ reaches ϵ_i, the film force abruptly drops to correspond to the abrupt change of the film pattern, the neck-down region now spans $\eta_{ci} \leq \eta \leq 2\pi - \eta_{ci}$. Further increase of ϵ curiously is accompanied by a reduction of the film force. This trend continues through the double-striation condition. When the double-striation pattern approaches the condition of strips of equal width, the film force actually rises somewhat with ϵ but turns downward again after the third strip has been formed. Again it resumes the upward trend when all three strips approach an equal width, then down-turn again with the formation of the fourth striation strip. This process continues indefinitely while ϵ increases toward unity. The numeral at the right margin designates the number of striation strips in the film pattern. One may observe that for a given ϵ_i, the film force is always smaller than that at the cavitation initiation condition ($\epsilon = \epsilon_i$) in the case of the "*I*" configuration. For the "0" configuration, in contrast, the film forces always increase with ϵ despite the growth of the cavitation domain as shown in Figs. 12 and 13.

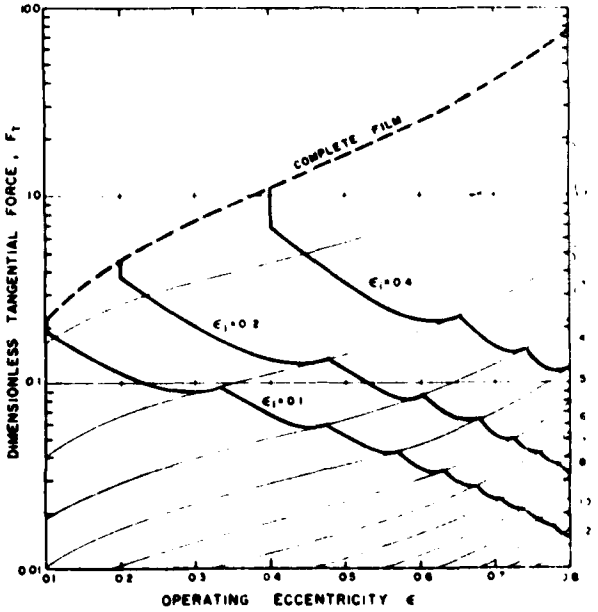

Fig. 14 Film force for "*I*" cavitation

VIII Discussions

The present work extended the applicability of the short-bearing

approximation to treat cavitation domains. Irrespective of the short bearing approximation, however, important questions are raised regarding the existence of subambient film pressure and the appropriate choice of cavitation boundary conditions.

Allowance of a subambient pressure is essential in the analysis of submerged journal bearing in order that the overall continuity of lubricant flow can be satisfied. Jakobsson and Floberg had correctly stated the case [6] and presented results which are equivalent to the "0" cavitation problem. Floberg further recognized that the flow structure in the cavitation domain is not smooth, but comprises of a number of striation streamers; he associated the number of striation streamers with the tensile strength of the lubricant [11]. Floberg, however, restricted the latter point of view to a scale which is much smaller than the overall cavitation domain. Nau distinguished separation cavitation from ligament cavitation [12], which roughly correspond to the "*I*" and "0" cavitation configurations treated in the present work. The present point of view may be regarded as a consolidation of these ideas. The possibility of a subambient pressure and the proper choice of cavitation boundary conditions cannot be separated. The total picture consists of the collection of the following points:

1. The cavitation boundary can be identified as a break-up boundary or a re-establishment boundary according to its geometrical relationship with the sliding vector. In crossing a break-up boundary, the sliding vector leaves a fluid film; while crossing a re-establishment boundary, it enters a fluid film.

2. In approaching a break-up boundary, if the film pressure is higher than the pressure in the cavitation domain then it must attain a zero gradient upon reaching the break-up boundary. This corresponds to the Swift-Stieber or the Reynolds' condition.

3. If the film pressure is subcavity in the neighborhood of the break-up boundary, a nonzero pressure gradient must exist at the boundary such that there is no net flow across it. An exception to this rule is when the break-up boundary has become parallel to the sliding vector and is turning into a re-establishment boundary.

4. Fluid transport across the cavitation domain follows the sliding vector and must be conserved between the break-up and the re-establishment points. If the break-up boundary borders on a subcavity film, then the cavitation domain must be a dry void and the re-establishment boundary must be followed by a film pressure rise; again, there can be no net flow across such a re-establishment boundary.

Note that the above conditions concern only thin film parameters.

Inaccuracies associated with the use of the short bearing approximation are present in the internal field and along the cavitation boundaries. The field inaccuracy is associated with the omission of the circumferential Poiseuille component of the film flow relative to the Couette component. Its magnitude can readily be estimated by computing and comparing these components from the solution of the film pressure. In terms of flow rate, the field inaccuracy is $O[L/D]$ but in terms of film pressure, $O[L/D]^2$. The field inaccuracy also affects the break-up boundary of "0" cavitation directly in that there is a residual circumferential pressure gradient, which amounts to $O[L/D]$ when scaled by the axial pressure gradient. At the re-establishment boundary, because the circumferential pressure gradient would facilitate filling up the gap, the boundary would shift more toward the maximum gap than the short bearing result. From this point of view one might expect that the deficiency of the "half film" approximation is probably somewhat overestimated in the present work. For "*I*" cavitation, the circumferential pressure gradient would upset the precise symmetry between the necking-down and the widening boundaries. The slope of the necking-down boundary should be reduced while that of the widening boundary should be increased. Consequently, the pressure field would not be precisely anti-symmetrical, so that the film force would have a radial component.

A more disconcerting feature of the short bearing approximation is revealed in the pressure field of the film with "0" cavitation. The situation is clearly illustrated in Fig. 11. The subambient pressure profile changes from the simple parabola in the full film to the split parabola in the break-up region. The split parabolas still have a zero slope at the cavitation boundary, and the pressure profile negotiates the transition smoothly. Upon entering the full back region, the pressure profile attains a finite slope at the boundary, still the change takes place smoothly. This happy situation unfortunately is not assured everywhere. The cavitation boundary keeps the film pressure at the lower bound value. Where the re-establishment boundaries join each other at the center line, the following pressure profile resumes the full film character of a parabola with zero slope at the center line in contrast to the finite slope at the neighboring re-establishment boundary. The situation is actually a little worse. The center line pressure of the re-established full film is always higher than the lower bound value; in fact, it can be above ambient if the re-establishment point is in the converging portion of the gap. Thus, not only smoothness but also continuity of the pressure profile is violated in the circumferential direction at this particular location. Such an anomaly is usually associated with the solution of a singular perturbation analysis [16] which reduces the order of the differential field equation when the asymptotic limit of an infinitesimal numerical parameter is carried out. The short bearing approximation is an application of the singular perturbation analysis. The solution is an asymptotically valid solution everywhere except on the line of film re-establishment. In this case, the deficiency is the jump in the pressure profile. A "boundary layer" type correction to the short bearing solution can be found by the method of matched asymptotic expansion [16]. The circumferential extent of the "boundary layer" is $O[L/D]$. Within the "boundary layer," a differential equation of the full order applies. The "boundary layer" correction smoothly, albeit, rapidly blends the two pressure profiles found in short bearing approximation on either side of the re-establishment point. One may note that because the width of the "boundary layer" is $O[L/D]$, the deficiency in the film force found by the short bearing approximation is also limited to $O[L/D]$.

The two cavitation configurations are both mathematically valid solutions (irrespective of the short bearing approximation). Experiments of White and Tonnesen on squeeze-film dampers [13, 14] independently lend some credence to the possibility of two different modes of operation. It is therefore useful to query what physical circumferences may promote the presence of one over the other? The clue to the answer is found in the concept of dry voids which cling to the sides of the necked-down film(s) in the "*I*" configuration. The possible presence of these voids would be associated with the abundance of entrained gas in the supply fluid and a stagnant state in the immediate neighborhood of the bearing ends. The squeeze film damper is more likely to operate with the "*I*" cavitation configuration than the rotating journal because journal rotation is likely to cause enough local circulation to prevent the formation of the voids. In any case a high through flow rate without excessive agitation (to avoid gas entrainment) is probably a feasible approach to forestall the "*I*" configuration which would cause a substantial reduction in the film force.

The natural short bearing cavitation parameter is

$$\Pi_{min} = \frac{p_{min} C^2}{\mu \omega R^2 (L/D)^2}$$

The scaling parameter (L/D), however, may not be involved in the physical process. Therefore it is useful to examine the results with a fixed value of the "universal cavitation parameter"

$$\frac{p_{min} C^2}{\mu \omega R^2}$$

instead of Π_{min}. One may also take the opportunity to further scrutinize the significance of the short bearing approximation by comparing the results for "0" cavitation with the results of Jakobsson and Floberg [6]. The curves in Figs 15 and 16 show such comparisons for two values of the universal cavitation parameter

$$\left(\frac{p_{min} C^2}{\mu \omega R^2} = 0.10, 0.01\right)$$

in terms of the eccentricity locus and the load capacity, respectively. As compared to the half-film approximation, present analysis brings out the lack of cavitation at small eccentricities as indicated by the

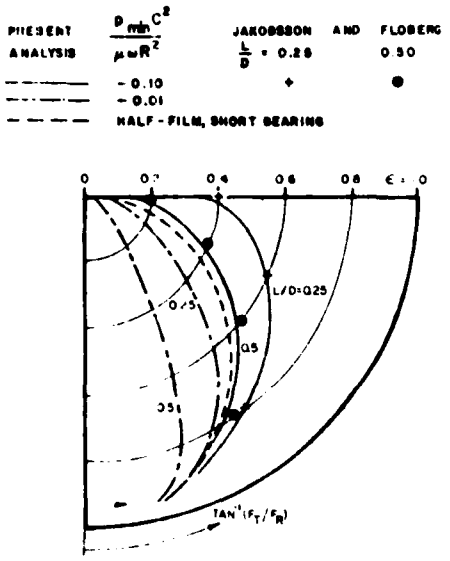

Fig. 15 Effects of L/D and cavitation parameter on eccentricity locus in "0" cavitation

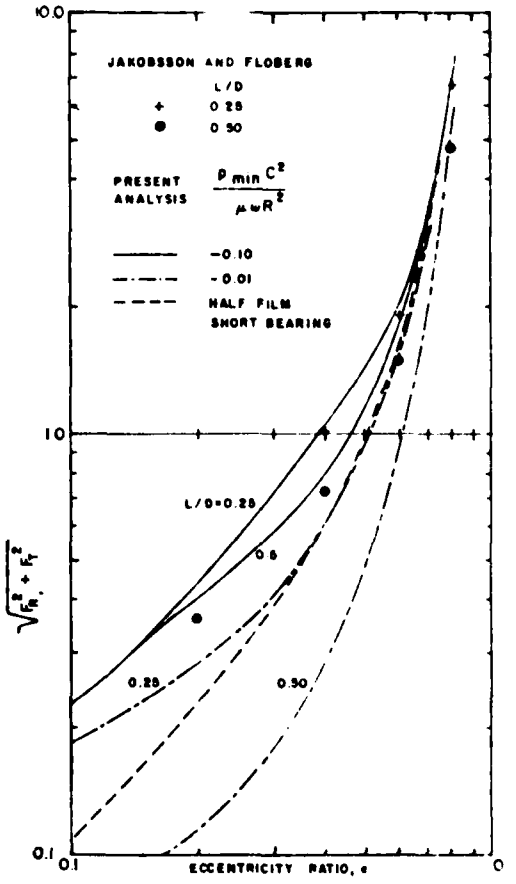

Fig. 16 Effects of L/D and cavitation pressure on load capacity in "0" cavitation

flat portion of the locus near the origin. This discrepancy of the half film approximation is more prevalent for a small L/D. The results of Jakobsson and Floberg [6] are in very good agreement with the present results so far as the eccentricity locii are concerned. For the smaller cavitation parameter, although the locii still leave the origin in the horizontal direction, they rapidly turn around and fall under the half-film results. The load capacity curves in Figure 16 reveals the deficiency of the half-film approximation in estimating load capacity throughout the small and moderate values of eccentricity, $\epsilon < 0.6$. Present results, expressed in terms of the second power law (with respect to L/D), shows that the effect due to the dependence of L/D on L/D is moderately prominent in the range $0.2 < \epsilon < 0.5$ for the two values ($L/D = 0.25, 0.5$) considered at the larger cavitation parameter (-0.10). The results of Jakobsson and Floberg indicate a stronger effect of L/D. At $L/D = 0.25$, the short bearing approximation is quite satisfactory. At $L/D = 0.5$, the short bearing approximation overestimates the load capacity by 12 percent up to $\epsilon = 0.5$, at $\epsilon = 0.6$ by 26 percent, and at $\epsilon = 0.8$ by 45 percent. At the smaller cavitation parameter (-0.01), the load capacity is significantly reduced by the "far extending" cavity.

IX Conclusions

The present analysis has shown that the level of subambient pressure level, which can be sustained by the fluid film, is an important parameter which controls the operating characteristics of a submerged journal bearing. The commonly used "half film" solution turns out to be a crude approximation for the solution with cavitation in the "0" configuration.

With "0" cavitation, the lower bound of film pressure sets the pressure level in the cavitated domain and determines the amount of fluid feeding from the ambient to the fluid film. With a low cavity pressure (large ϵ_c), there is a copius amount of feed flow and the full film condition can be readily re-established, keeping the extent of cavitation to a small area. With the cavity pressure only slightly below the ambient (small ϵ_c), a far extending cavitation region would exist, the full-film re-establishment point may reach deeply into the converging portion of the bearing gap. In between these extreme conditions, the "half film" solution represents a fair approximation.

"Γ" cavitation causes the minimum pressure to exist at an internal point of the fluid film. A requisite condition for the existence of this cavitation configuration is the aggregation of gas or vapor-filled voids in the ambient fluid. The fluid film boundaries recede away from the bearing ends allowing dry voids to occupy the wide gap portion of the end regions of the bearing. The void extent may be stretched to the full circumference, thus preventing feeding of fluid film from the ambient entirely. In addition, the voids may intersperse narrow film strips to form a multiple striation pattern. The occurrence of "Γ" cavitation is accompanied by a significant reduction of the fluid film force and thus may be regarded as a pathological mode of operation. With the short bearing approximation, the fluid film force for "Γ" cavitation is purely tangential.

A generalized cavitation model allows the two different cavitation configurations to exist. The new model is a consolidation of the boundary condition of Swift-Stieber for film rupture and that of Floberg for striation streamers. Either one of these conditions is allowed to prevail depending on the film pressure level near the boundary relative to that in the cavitation domain.

Successful use of the short bearing analysis in conjunction with the two cavitation configurations underscores the important pre requisite of satisfying overall flow continuity of the lubricant film prior to the determination of the film pressure field and the associated fluid film force. Imposition of the short bearing approximation is necessarily accompanied by the presence of abrupt lines in the pressure fields for the "0" cavitation pattern since the short bearing analysis is inherently a singular perturbation technique. The approach presented here, however, is much more realistic than the conventional "half film" short bearing approximation and permits further improvement by the technique of matched asymptotic expansions.

Present results for "0" cavitation agree closely with earlier results of Jakobsson and Floberg for $L/D = 0.25$ in the entire range of eccentricity. For $L/D = 0.5$, the agreement is still within 26 percent for all $\epsilon < 0.6$.

References

1 Reynolds, O., "On the Theory of Lubrication and Its Application to Mr

Beauchamp Tower's Experiments, Including an Experimental Determination of the Viscosity of Olive Oil," *Phil. Trans. Roy. Soc.*, Series A, Vol. 177, 1886, p. 157.

2 Gumbel, L., and Everling, E., "Monatsblatter Berliner Bezirksver," *VDI*, Vol. 5, 1914, pp. 87–104.

3 Dubois, G. B., and Ocvirk, F. W., "Analytical Derivation of Short Bearing Approximation for Full Journal Bearings," NACA Report 1157, 1953.

4 Swift, H. W., "The Stability of Lubricating Films in Journal Bearings," *Proceedings Institute of Civil Engineers* (London), Vol. 233, 1932, pp. 267–288.

5 Stieber, W., "Das Schwimmlager," *VDI*, Berlin, 1933.

6 Jakobsson, B. and Floberg, L., "The Finite Journal Bearing, Considering Vaporization," *Trans. Chalmers University Tech.*, Nr. 190, Goteborg, 1957.

7 Pinkus, O. and Etsion, "Solutions of Finite Journal Bearings with Incomplete Films," ASME JOURNAL OF LUBRICATION TECHNOLOGY, Vol. 97, 1975, p. 236.

8 Wakuri, Yutaro, et al., "Oil Flow in Short Bearing with Circumferential Groove," *Bulletin of the JSME*, Vol. 16, No. 92, Feb. 1973, pp. 441–446.

9 Birkhoff, G. and Hays, D. F., "Free Boundaries in Partial Lubrication," *Journal of Mathematics and Physics*, Vol. 42, No. 2, 1963, pp. 126–138.

10 Coyne, J. C. and Elrod, H. G., "Conditions for the Rupture of a Lubricating Film Part I: Theoretical Model," ASME, JOURNAL OF LUBRICATION TECHNOLOGY, Vol. 92, No. 3, 1970, pp. 451–456.

11 Floberg, L., "On Hydrodynamic Lubrication with Special Reference of Sub-Cavity Pressures and Number of Streamers in Cavitation Regions," Acta Poly. Scan., 1965, ME 19.

12 Nau, B. S., "Cavitation in Thin Films," BHRA, 1964, TN 832.

13 White, D. C., "Squeeze Film Journal Bearings," PhD dissertation, Cambridge University, 1970.

14 Tonnesen, J., "Experimental Parametric Study of a Squeeze Film Bearing," *Trans.* ASME JOURNAL OF LUBRICATION TECHNOLOGY, Vol. 98, 1976, p. 206.

15 Marsh, H., "Cavitation in Dynamically Loaded Bearings," *Cavitation and Related Phenomena in Lubrication*, Proceedings of the 1st Leeds Lyon Symposium on Tribology, September 1974, edited by D. Dowson, M. Godet and C. M. Taylor, pp. 91–95.

16 Van Dyck, Milton, *Perturbation Methods in Fluid Mechanics*, Academic Press, New York, N.Y., 1964.

DISCUSSION

I. Etsion[3]

The paper treats an important problem which, as was pointed out correctly, has been a matter of much controversy ever since the formulation of the lubrication theory. The submerged bearing is in many aspects similar to a face seal. Indeed the concept of the "0" cavitation configuration is known in the seal literature since the work by Findlay [17] in 1968. Findlay used the same approach as in the present work to show a cavitation region extending into the converging film of a face seal. The rationale behind these analyses is the required net zero end flow in the case of submerged operation. The "0" cavitation concept preserves this requirement and maintains flow continuity on the cavitation boundaries as well. It results, however, in a pressure discontinuity across the fluid film at $\eta = \eta_r$. Another possible solution which preserves both the net zero end flow and the pressure continuity can be obtained from equation (8) by setting $\Pi = \Pi$ at $\zeta = \zeta_0$. This solution, however, does not comply with the flow continuity on the cavitation boundaries. An inevitable question is which of the above two deficiencies is more severe?

The results presented in Figs. 15 and 16 show good correlation between the "0" cavity concept and the results of Jakobson and Floberg for a "universal cavitation parameter" of −0.10. Unfortunately, these results are compared with "half film" solution which is based on a cavitation parameter that equals zero. A more realistic comparison would require the same value of the cavitation parameter for all the solutions compared. If this is done, the solution of the cavitation region based on equation (8) becomes

$$\zeta_0 = \left(1 + \frac{2\,\Pi_{min}}{Q}\right)^{1/2} \tag{D-1}$$

where

$$\Pi_{min} = \frac{p_{min}\,C^2}{6\,\mu\omega R(L/D)^2}$$

Hence, for a cavitation parameter −0.1 and L/D ratios 0.25 and 0.5 Π_{min} becomes −1.6 and −0.4, respectively. It is clear that a cavitation region thus obtained from (D-1) depends on L/D. Therefore, the eccentricity locus and load capacity are also L/D dependent similar to the results shown in Figs. 15 and 16 for the "0" cavitation.

Additional Reference

17 Findlay, J. A., "Cavitation in Mechanical Face Seals," JOURNAL OF LUBRICATION TECHNOLOGY, Vol. 90, No. 2, Apr. 1968.

[3] Department of Mechanical Engineering, Technion, I Haifa, Israel.

N. Tipei[4]

The author is to be commended for this paper which introduces new concepts for a better understanding of cavitation phenomena in bearings. The initial limitations, regarding the short bearing approximation and the submerged arrangement of the journal bearing, only partially affect the validity of the analysis which should be extended to other conditions.

The previous work of Geoffrey Taylor, Pearson and Pitts and Greiller has provided up to a certain point, valuable information on the generation and on the number of streamers in subcavitated regions. However, the present analysis yields specific and detailed calculations, to be applied in lubrication problems.

This discusser would like the author's comments on the following points:

1. How much of an effect does the surface tension have on the boundary conditions at the liquid-gas interface?
2. The usual nonslip boundary conditions let a thin film of lubricant to be carried by the journal, even in subcavitation regions. Can the assumption of dry surfaces be critical in some cases?
3. For "I" cavitation the diagrams, Fig. 14, do not show values for $\epsilon > 0.8$. In opposition to short bearing theory, should the circumferential pressure gradient also be considered at higher ϵ values?

In conclusion, the present work is a significant contribution in a still not well understood chapter of lubrication. The extension of this analysis to other types of bearings should be welcome.

Author's Closure

The author is grateful to Dr. Etsion's addition of a reference to the earlier work of Findlay, who was concerned with the lift and leakage of a face seal as affected by waviness induced cavitation. It may be mentioned that the tracking dynamics of face and shaft seals would be dependent on the cavitation process.

The alternate solution suggested by Dr. Etsion is in essence an adaptation of the Gumbel approximation [2], which is at best a convenient short cut. The author can see no merit in offering it as a likely improvement. The crucial concepts to be emphasized here are that (1) The Swift-Stieber condition [4, 5] is reconcilable with the short bearing approximation and thus should be asserted; and (2) Unless

[4] General Motors Research Laboratories, Mechanical Research Department, Warren, Mich. 48090.

the gap is filled with lubricant, no pressure can be developed. As to the issue of pressure discontinuity at the film re-establishment point, it need only be said that it is inevitable to allow such a solution if one accepts the physical reality of a short partial arc journal bearing. Clearly, one must again rely on matched asymptotic expansion [16] to remove the pressure discontinuity at both entrance and exit edges.

One can examine the possible merits of equation (D-1) as a partial improvement over the conventional short bearing approximation. This idea had already been tried in a study of squeeze-film dampers [13]. While there was a definite improvement over the conventional short bearing approximation, there remained significant inexplicable discrepancies from experimental facts. One inherent fault in the Gumbel-Etsion proposition is that the cavitation domain would be always contained within the divergent portion of the gap. Figure 10 clearly shows that the reestablishment point may be in the convergent portion of the gap, depending on the precise value of ϵ (which fixes $\pi_{\min}$). For instance, if the numerical value of $\pi_{\min}$ should be quite small, the Gumbel-Etsion approach should yield results very close to the half film approximation, which are contradicted by the author's results for $\Pi_{\min} = -0.01$. Thus, one may safely conclude that, with whatever partial improvement may be offered by the use of equation (D-1), some uncertainty associated with the precise location of the film re-establishment point will result. The argument can only be resolved by a subjective cost-benefit judgment.

The author is flattered to receive the kind remarks from Dr. Tipei, whose contributions to the field of lubrication theory have been the source of inspiration of the author's own efforts. Specific questions raised by Dr. Tipei are answered as follows.

1. Assuming that perfect wetting takes place between the lubricant and the bearing wall, then the meniscus may have a radius of curvature which is lower-bounded by one fourth of the gap where cavitation breakup takes place. One immediate consequence is that the film pressure at the meniscus can be lower than the cavity pressure by the amount of $4\sigma/h$, where σ is the surface tension of the lubricant void interface. Typically, σ has a value of about 30 dynes/cm. Thus, if the gap is 2.5 μm (1/10 mil), then the associated pressure jump at the meniscus may approach 0.12×10^6 dynes/cm^2 (1.74 psi). However, pressure jump is only one facet of the total phenomenon. At the breakup meniscus, using the local gap as the geometric scale, the lubrication theory provides the upstream far-field asymptotic limit. On the downstream side, the flow (assuming absence of stream ers) ultimately becomes a thin film free surface flow over a moving wall. Transition between these two vastly different flow fields takes place in the vicinity of the meniscus [10]; inertia effects, in addition to surface tension, may be important because shear stress effects are minimal on the downstream side. Instability of the meniscus flow field with respect to a transverse wave is probably the cause of the streamer structure. Consequently, the precise platform of the meniscus boundary cannot be resolved to a scale of the bearing gap and may further be altered by the streamer structure which should have a wave length somewhere between the bearing gap and the bearing length. There is also reason to believe that the Swift-Stieber condition should be corrected for surface tension effects.

2. The nonslip boundary conditions can be reconciled with the "dry cavity" model (associated with the "I" configuration) by accepting wetness to be satisfied by a film of molecular dimensions. Inertia effects, however, can be responsible for residual films in the "dry cavity."

3. Circumferential pressure gradient is proportional to H^{-3}. Therefore, given a small but finite L/D, the short bearing approximation would eventually become inadequate if ϵ is allowed to approach unity. The author would recommend caution against using short bearing results at very large values of ϵ. A value of 0.8 is a reasonable upper bound for trusting short bearing results.

Reprinted from July 1981, Vol. 103, Journal of Lubrication Te

Cavitation in a Short Bearing With Pressurized Lubricant Supply

C. H. T. Pan

R. A. Ibrahim

Shaker Research Corporation,
Ballston Lake, N.Y. 12019

This work is a generalization of previous treatments of the cavitation problem for short journal bearings [1, 2]. Cavitation incipience and the cavitation pattern are dependent on both supply and cavitation pressure levels. The geometrical pattern of the cavity boundary is found to satisfy a universal solution which depends uniquely on the cavitation incipience eccentricity and the operating eccentricity. The same eccentricity parameters also uniquely determine the friction and through-flow characteristics. Radial and tangential force components are dependent on the supply/cavitation pressure ratio in addition to the eccentricity parameters. The results are applicable to journal bearings, shaft-seals, and squeeze-film dampers.

Introduction

The short bearing analysis of Dubois and Ocvirk [3] is a rare combination of extreme simplicity and near validity. For over a quarter of a century, lubrication engineers have used the short bearing formulas to estimate load capacity and friction loss of plain journal bearings. It has been as common notion that even for not-so-short bearings, these formulas are fair approximations. Although numerical computation has become standard engineering practice, the short bearing analysis remains a favorite approach not only for bearing designs but also for studying rotor-bearing dynamics, and for design evaluations of shaft seals and dampers.

It is a common practice that the short bearing analysis is performed with the additional approximation of retaining only the computed film pressure in the converging portion of the bearing gap (π-film). This turns out to be a reasonable assumption in most not-so-short bearing designs because lubricant is usually copiously supplied with the feed port located in the bearing wall somewhere in the divergent portion of the bearing gap. The rate of lubricant flow depends on the reservoir pressure level and the flow impedance upstream of the feed port. The reservoir pressure is nominally maintained above the ambient. A meniscus boundary is formed around the feed port. Even though the miniscus boundary is not precisely the maximum gap location, the overall film pressure distribution does not deviate substantially from the π-film approximation. Ironically, for a truly short configuration (as may be in the case of a journal bearing, a shaft seal, or a damper), the realities concerning lubricant supply and the film extent need more attention. Typically, there is no feed port in the bearing wall. The lubricant can reach the gap at either end and can enter to form a thin film only if there is a region where the film pressure is lower. Consequently, the lowest pressure level which can be sustained by the lubricant film becomes a crucial issue.

Unfortunately there is no simple and practical way to predict the cavitation incipience pressure in fluid film devices despite continued interests in the profession [4, 5]. The best estimate for the cavitation incipience pressure is somewhere between absolute zero and the discharge ambient. In the present work, the cavitation incipience pressure is regarded to be a given constant, which not only decides where the rupture of the lubricant film to take place but also governs the location of the full film formation point and thus the extent of cavitation.

The submerged short journal bearing represents a simple theoretical model to allow a consistent flow balance between lubricant flow into the divergent gap and the end leakage flow from the convergent gap. This problem was thoroughly treated in a recent work [1]. It was found that if a submerged journal bearing is to carry any load, the cavitation pressure must be subambient and that the extent of cavitation depends on both the cavitation pressure and the operating eccentricity. Comparison with the numerical results given by Jakobsson and Floberg for a submerged journal bearing of finite length [6] demonstrated that the improved short bearing analysis is valid for not-so-short configurations. According to the same analysis, the submerged short bearing has been found to be vulnerable to a condition of lubricant depletion if voids at the ambient pressure are allowed to aggregate near the bearing ends.

The submerged journal bearing configuration may not be a realistic model. Sometimes lubricant is delivered to one end of the bearing at a more or less elevated pressure. As a whole the lubricant passes through the bearing gap and is discharged to

Contributed by the Lubrication Division of THE AMERICAN SOCIETY OF MECHANICAL ENGINEERS and presented at the Century 2 ASME ASLE International Lubrication Conference, San Francisco, Calif., August 18-21, 1980. Revised manuscript received by the Lubrication Division, February 29, 1980. Paper No. 80-C/LUB-47.

the ambient conditon at the other end. The discharge end may or may not be flooded. Shaft seals operate precisely in this manner. It is also a likely configuration for squeeze-film dampers. The elevated feed pressure would postpone cavitation incipience to a higher eccentricity and would reduce the extent of cavitation at a given eccentricity as compared to that of an equivalent submerged bearing. The flow requirement of a short bearing fed from one end was studied by Wakuri, et al., [2]; an ambient cavity was assumed to exist at the discharge end of the short bearing. In the case of an internal cavity, the feed pressure directly influences the extent of cavitation; consequently, the through flow impedance varies accordingly. The present work is a direct extension of earlier studies [1, 2] by allowing the pressure at the feeding end to become elevated, by including the possibility of a flooded discharge end, and by rounding out the results to include film force components and bearing friction torque together with the through flow impedance.

Analysis

General Short Bearing Theory. Lubrication theory for a short journal bearing with an incompressible, isoviscous fluid obeys the following differential equation: [3]

$$\frac{\partial}{\partial \zeta}\left(H^3 \frac{\partial \Pi}{\partial \zeta}\right) - \frac{\partial H}{\partial \eta} = 0\{\lambda^2\} \tag{1}$$

where

$$\Pi = \frac{pC^2}{6\mu\omega R^2 (L/D)^2}$$

is the dimensionless film pressure measured above ambient. For an axially uniform film, $H = 1 - \epsilon\cos\eta$, equation (1) has the general solution

$$\Pi = \Pi_0 + \zeta\Pi_1 + \frac{\zeta^2}{2} Q(\eta) \tag{2}$$

where

$$Q(\eta) = H^{-3}\frac{\partial H}{\partial \eta} = \frac{\epsilon\sin\eta}{(1-\epsilon\cos\eta)^3} \tag{3}$$

(Π_0, Π_1) are invariant with respect to ζ and are determined from suitable boundary conditions.

This formulation is also applicable to the squeeze-film damper undergoing a circular whirl motion. The coordinates are fixed to the whirl motion with the angular coordinate aimed against the sense of whirl. ω should be replaced by 2ν, twice the whirl frequency, and ϵ now represents the ratio of the orbit radius to the damper clearance.

Full Width Film With Circumferential Feeding. If there is no cavitation and one end of the bearing is maintained at $\Pi_S > 0$, then upon satisfying the boundary conditions

$$\Pi(\zeta = -1) = \Pi_S; \qquad \Pi(\zeta = 1) = 0$$

the film pressure is determined by a special form of equation (2):

$$\Pi = \frac{1}{2}(1-\zeta)\Pi_S - \frac{1}{2}(1-\zeta^2)Q \tag{4}$$

The location of the minimum pressure is of special interest in consideration of cavitation since the value of the minimum film pressure determines whether or not cavitation would take place. The minimum pressure is located by the conditions

$$0 = \frac{\partial \Pi}{\partial \eta} = -\frac{1}{2}(1-\zeta_m^2)\frac{\partial Q}{\partial \eta} \tag{5}$$

$$0 = \frac{\partial \Pi}{\partial \zeta} = -\frac{1}{2}\Pi_S + \zeta_m Q \tag{6}$$

Equation (5) shows that the circumferential location of the minimum pressure is not dependent on Π_S. Equation (6) shows, however, that unless the condition

$$Q \geq \frac{1}{2}\Pi_S \tag{7}$$

Nomenclature

C = nominal radial clearance
D = bearing diameter
e = eccentricity
H = dimensionless film thickness, $1 - \epsilon\cos\eta$
L = bearing length
P = film pressure
Q = hydrodynamic wedge function, $\epsilon\sin\eta/(1-\epsilon\cos\eta)^3$
R = bearing radius, $D/2$
T = friction torque
W_R, W_T = radial and tangential force components
z = axial coordinate, measured from midplane
ϵ = eccentricity ratio, e/C
ζ = dimensionless axial coordinate, $2z/L$
ζ_m = dimensionless axial location of minimum pressure
$\Delta\zeta$ = scale of ζ in universal representation, Table 1
η = circumferential coordinate measured from minimum gap location
λ = length-to-diameter ratio, L/D
μ = viscosity coefficient of lubricant
ν = whirl frequency of damper
Π = dimensionless pressure, $p/\{6\mu\omega(R/C)^2(L/D)^2\}$ for journal bearing or $p/\{12\mu\nu(R/C)^2(L/D)^2\}$ for squeeze-film damper
Π_0, Π_1 = coefficients in short bearing solution, equation (2)
Π_C = dimensionless cavitation pressure measured from ambient
Π_S = dimensionless supply pressure measured from ambient
$\Delta\Pi$ = scale of Π in universal representation, Table 1
ψ = volume rate of lubricant through flow

Subscripts

b = breakup boundary
bi = breakup initiation
$b0$ = average value over the entire breakup boundary
i = cavitation incipience
0 = offset value
t = termination point of cavity
w = waist

Superscripts

$\bar{}$ = universal variable
$\tilde{}$ = dimensionless variable, applied to (W_R, W_T, T, ψ)

is satisfied, a true pressure minimum would not be present in the film. The minimum pressure location is always on the discharge side in the axial direction ($\zeta_m = \Pi_S/(2Q) > 0$). The special condition $Q = \Pi_S/2$ causes the minimum pressure to be located at the exit edge; i.e., $\zeta_m = 1$.

Forms of Cavitation. For a submerged bearing, previous work indicated the existence of two distinct cavitation patterns [1]. In the "0" cavitation pattern, the pressure in the cavitated region is maintained at Π_C; film breakup approaches the cavitation boundary with the modified Swift-Stieber boundary conditions [7, 8]. In the "Γ" cavitation pattern, the minimum pressure Π_C exists at an internal point; cavitation regions are connected to the ambient edges and thus are maintained at the ambient pressure. They are in effect "dry pockets."

With one edge of the bearing maintained at an elevated pressure, there are similarly these two major varieties of cavitation forms. Due to the elevated pressure at the supply edge, however, symmetry would be disrupted. If one makes the reasonable assumption that only the liquid lubricant flows through the feed line, then an edge cavity can only be present on the exit (ambient) edge. The entire periphery of the pressurized edge is thus fully effective as the inlet passage for lubricant through flow. The exit cavity may be either wet, such that the film approaches the cavitation boundary with the Swift-Stieber condition; or it may be dry, and the ambient cavity borders a film with some subambient region. The solution of the wet exit cavity turns out to be a special case of the internal cavitation. The dry exit cavitation problem requires separate attention.

If the exit cavity is dry, the film pressure near the cavity boundary is necessarily subambient. Therefore, there must be at least a local region along the exit edge, where the lubricant flows back from the "exit" edge into the film. At the same time, in the immediate neighborhood, a dry cavity interrupts the film. Such a special condition is possible if the lubricant level is maintained precisely at the initiation point of the dry cavity. Clearly, this is an unlikely situation except possibly in a deliberate laboratory setup; hence no further attention will be given to the dry exit cavity problem.

With a wet exit cavity, while a zero pressure gradient condition is satisfied at the breakup boundary, the film pressure is everywhere higher than the ambient. Thus, the lubricant always flows out along that portion of the exit edge which is reached by the fluid film. At the same time, the entire exit edge remains at the ambient pressure including that portion which borders the wet cavity. This is a "flow-through" condition typical of most bearing and seal installations; the film pressure is everywhere higher than the ambient even if the lubricant is physically capable of a subambient state. The exit edge can be flooded by the lubricant (for example by restricting the exit flow), then the cavity will be located inboard and the pressure in the cavity should be approximately at the effective vapor pressure of the lubricant and can be substantially subambient.

Cavitation Incipience. The full film solution, equation (4), is applicable so long as the minimum film pressure is higher than the cavitation pressure; i.e., $\Pi \geq \Pi_C$. The condition of cavitation incipience is reached when the minimum film pressure is exactly equal to the cavitation pressure.

According to equation (5), the circumferential location of the minimum pressure point (in a full film) is given by $\partial Q/\partial\eta = 0$. Since this condition does not depend on the values of Π_S and Π_C, the relationship between the circumferential location of cavitation incipience, η_i, and the incipience eccentricity ratio, ϵ_i, as determined in the previous study [2] remains valid. The value of ϵ_i, however, is now dependent on both Π_S and Π_C. Upon setting $Q = Q_i = Q(\epsilon_i, \eta_i)$ and $\zeta_m = \zeta$ in equation (6), one obtains

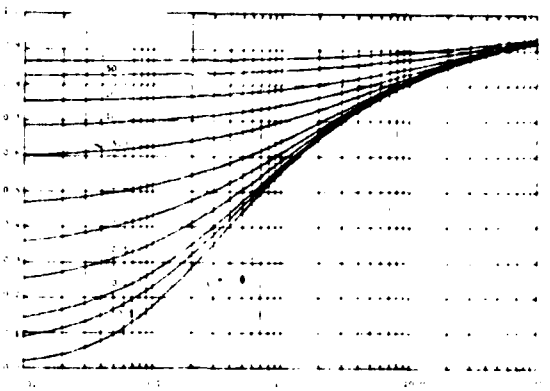

Fig. 1 Eccentricity ratio for cavitation incipience

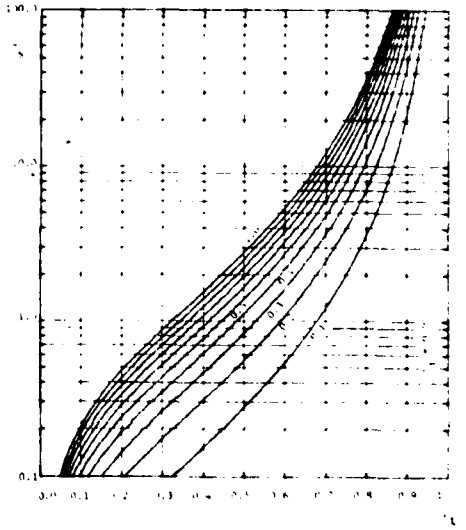

Fig. 2 Supply pressure level

$$\Pi_S = 2Q_i\zeta_i \tag{8}$$

Then substituting into equation (4) along with (Π, ζ, Q), respectively, identified as (Π_C, ζ_i, Q_i), it is found

$$-\Pi_C = Q_i(1-\zeta_i)^2/2 \tag{9}$$

Since η_i depends uniquely on ϵ_i, Q_i can be regarded as a function of ϵ_i also. Accordingly, equations (8) and (9) can be regarded as $\Pi_S(\epsilon_i, \zeta_i)$ and $-\Pi_C(\epsilon_i, \zeta_i)$.

Physically, it is more natural to regard (ϵ_i, ζ_i) as functions of ($-\Pi_C$, Π_S). To obtain such relationships, one can first eliminate Q_i between equations (8) and (9), then, after some rearrangements, it is found

$$\zeta_i = 1 + 2(-\Pi_C/\Pi_S)[1 - \sqrt{1 + (-\Pi_S/\Pi_C)}] \tag{10}$$

Then, substituting into equation (8), one obtains

$$Q_i = (\Pi_S/2) + (-\Pi_C) + \sqrt{(-\Pi_C)[(-\Pi_C) + \Pi_S]} \tag{11}$$

Since Q_i is a unique function of ϵ_i, the inverse would be true, so that equation (11) yields indirectly the function of $\epsilon_i(-\Pi_C, \Pi_S)$. Actual computation of $\epsilon_i(Q_i)$, however, requires a numerical procedure. Graphical representation of $\epsilon_i(-\Pi_C, \Pi_S)$ is given in Fig. 1.

$(-\Pi_C, \Pi_S)$ and (ζ_i, ϵ_i) are alternative parametric sets to specify the condition of cavitation incipience. Fig. 2 together

with Fig. 1 furnish the complete relationships among these parameters in the graphical form. In subsequent analysis to treat the cavitation problem, the condition $\epsilon > \epsilon_i$ is of interest. Thus the parametric set (ζ_i, ϵ_i) will be assumed to be given.

Universal Solution of the Cavitation Region. For any combination of a finite and positive (nonvanishing) value of $-\Pi_C$ together with a finite and non-negative value of Π_S, the axial location of the incipience point is internal; i.e., $0 \le \zeta_i < 1.0$.

The case ($\Pi_S = 0$, $\zeta_i = 0$) corresponds to the "0" cavitation prolem of a submerged journal which was treated previously [1]. If the eccentricity ratio exceeds the incipience value, $\epsilon > \epsilon_i$, then the cavitation pressure Π_C would be reached at $0 < \eta_{bi} < \eta_i$. The subscript "*bi*" designates the condition of "breakup in tiation." Since the breakup initiation should also be at the axial minimum of the film pressure, equation (6) must apply. Substituting $(\Pi_C, \zeta_{bi}, Q_{bi})$, respectively for (Π, ζ, Q) in equation (4), and (ζ_i, Q_{bi}), respectively, for (ζ_m, Q) in equation (6), one obtains

$$\Pi_C = \frac{1}{2}(1 - \zeta_{bi})\Pi_S - \frac{1}{2}(1 - \zeta_{bi}^2)Q_{bi} \tag{12}$$

$$\Pi_S = 2\zeta_{bi}Q_{bi} \tag{13}$$

Eliminating $-\Pi_S$, one obtains

$$-\Pi_C = Q_{bi}(1 - \zeta_{bi})^2/2 \tag{14}$$

Comparing equations (13) and (14) with equations (8) and (9), one concludes that since (ζ_{bi}, Q_{bi}) have the same functional relations of $(-\Pi_C, \Pi_S)$ as (ζ_i, Q_i), it follows

$$\zeta_{bi} = \zeta_i; \qquad Q_{bi} = Q_i \tag{15}$$

Noting that ζ_i depends only on the parameter $(-\Pi_C/\Pi_S)$ according to equation (10), the value of $\zeta_{bi} = \zeta_i$ is a direct indicator of the supply pressure (relative to the cavitation pressure). η_{bi}, on the other hand, can be solved from equation (3) upon substituting $Q_{bi} = Q_i(\epsilon_i)$ for Q, and therefore is dependent only on (ϵ, ϵ_i) in the explicit sense. Computation of $\eta_{bi}(\epsilon, \epsilon_i)$, however, has to be performed numerically since the governing re ationship is transcendental.

$$\epsilon \sin\eta_{bi} - Q_{bi}(1 - \epsilon\cos\eta_{bi})^3 = 0 \tag{16}$$

The break up process continues beyond η_{bi}. An internal cavitation domain separates the two "side bands" which border either end of the bearing. The pressure field in the sideband is universal because the pressure of either end of the bearing is constant, whereas the Swift-Stieber condition is applicable at the cavitation border. The universal pressure profile can thus be written as

$$\bar{\Pi} = (\hat{\zeta}_b - \hat{\zeta})^2 Q/Q_i; \qquad \hat{\zeta}_b = \sqrt{Q_i/Q} \tag{17}$$

($\bar{\Pi}$, $\hat{\zeta}$) are, respectively, the universal film pressure and the universal axial coordinate for either sideband. They are linearly related to (Π, ζ) with appropriate scale factors and offsets; i.e.,

$$\bar{\Pi} = (\Pi - \Pi_0)/\Delta\Pi; \qquad \hat{\zeta} = (\zeta - \zeta_0)/\Delta\zeta \tag{18}$$

The scale factors and the offsets are listed in Table 1.

In the universal representation, as shown by equation (17), the width of the sideband depends parametrically on (ϵ, ϵ_i) and is a function of η. It assumes its minimum value when Q reaches its maximum at

$$\eta_w = \cos^{-1}[(\sqrt{1 + 24\epsilon^2} - 1)/(4\epsilon)] \tag{19}$$

The subscript "w" refers to the "waist" of the sideband. If cavitation had not taken place, η_w would locate the minimum film pressure; η_w is functionally dependent on ϵ identically as η_i is on ϵ_i.

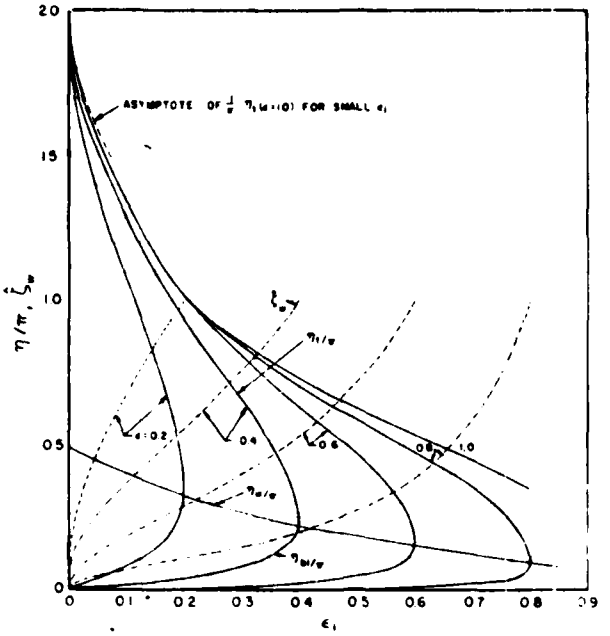

Fig. 3 Geometrical parameters of the universal cavitation pattern

Beyond η_w, the sideband widens with η as the axial flow, drawn in from the end adds to the circumferentially transported flow, through the internal cavity, to cause the film to fill back. The universal pressure profile is given by

$$\bar{\Pi} = -(\hat{\zeta} - \hat{\zeta}_f)/\hat{\zeta}_f + \hat{\zeta}(\hat{\zeta} - \hat{\zeta}_f)(Q/Q_i) \tag{20}$$

$\hat{\zeta}_f$ is the cavitation boundary in the "fill-back" region. Note that the boundary values of $\bar{\Pi}$ at $\hat{\zeta} = (0, \hat{\zeta}_f)$ are satisfied, whereas the Swift-Stieber condition is no longer enforced except at η_w where $\hat{\zeta}_f = \hat{\zeta}_w$.

At the fill-back boundary, flow transported through the cavity from $\eta(\hat{\zeta}_b = \hat{\zeta}_f)$, which is given by equation (17), combines with the axial in-flow through the widening sideband to fill the gap of the reformed film. For the short bearing approximation, only the Couette component is retained in the circumferential flow of the reformed film. The relation between $\hat{\zeta}_f$ and $\eta > \eta_w$ is same as that for the submerged bearing. Upon approximating the local, transported flow by the average value [1], and adopting the universal representation the formula of interest is

$$(H - H_{b0})\hat{\zeta}_f^2 = (H_w - H_{b0})Q_i/Q_w + [F(\eta) - F(\eta_w)]Q_i \tag{21}$$

where

$$F(\eta) = \int H^3 d\eta$$

$$= \left(1 + \frac{3}{2}\epsilon^2\right)\eta - 3\epsilon\left(1 + \frac{\epsilon^2}{4}\right)\sin\eta + \frac{3}{4}\epsilon^2\sin 2\eta - \frac{\epsilon^3}{12}\sin 3\eta \tag{22}$$

$$\cos\eta_{b0} = \frac{1}{(1 - \hat{\zeta}_w)}\int_{\hat{\zeta}_w}^{1} \cos\eta\, d\hat{\zeta}_b \tag{23}$$

and

$$H_{b0} = 1 - \epsilon\cos\eta_{b0} \tag{24}$$

The fill-back process is terminated when $\hat{\zeta}_f$ becomes unity. The universal form of $\hat{\zeta}_b$ and $\hat{\zeta}_f$ ensures that the internal

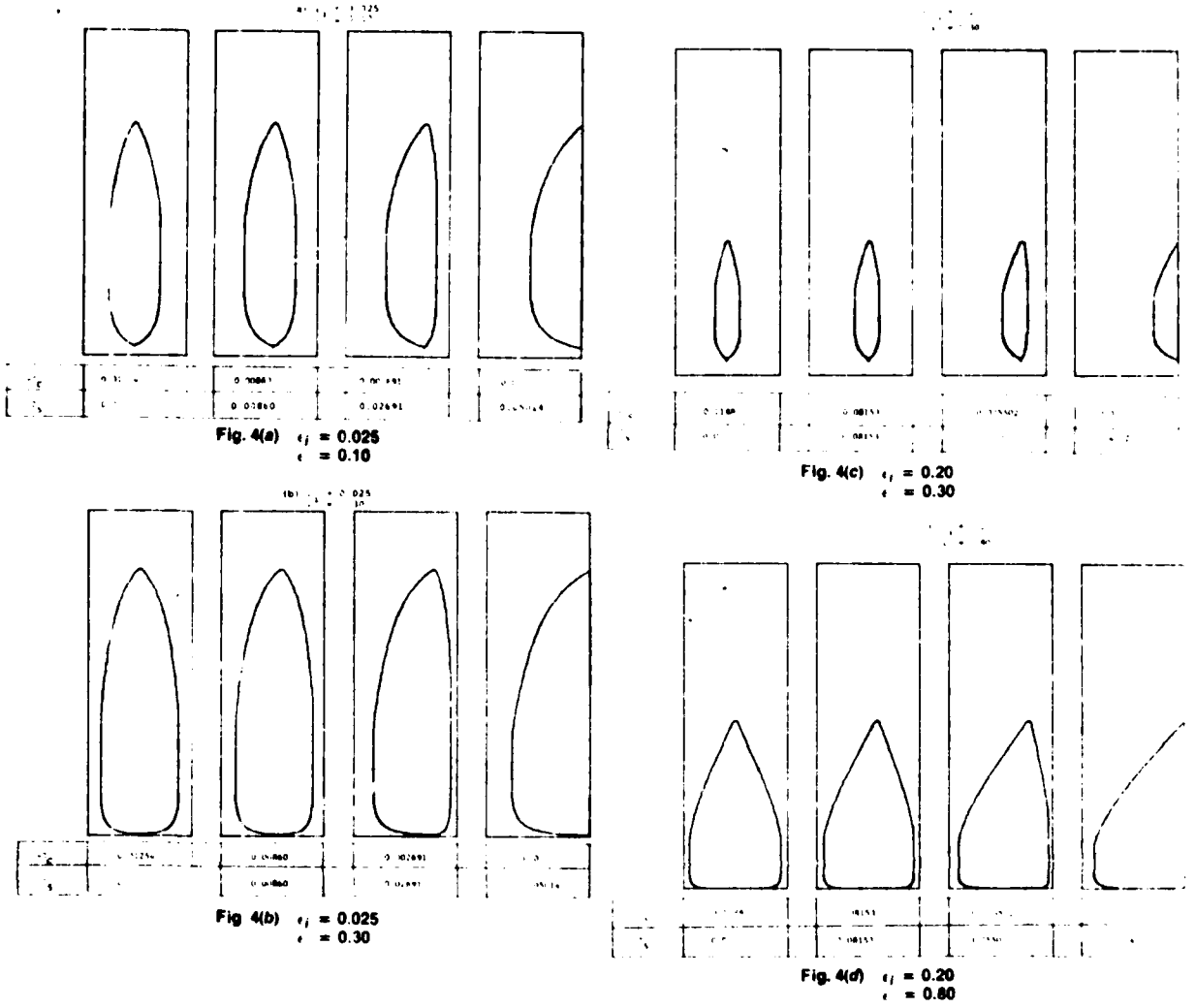

Fig. 4(a) $\epsilon_i = 0.025$, $\epsilon = 0.10$

Fig. 4(c) $\epsilon_i = 0.20$, $\epsilon = 0.30$

Fig 4(b) $\epsilon_i = 0.025$, $\epsilon = 0.30$

Fig. 4(d) $\epsilon_i = 0.20$, $\epsilon = 0.80$

Fig. 4 Cavitation patterns

cavitation begins and ends together. For convenience of future reference, the termination location is designated η_t. The computations previously performed for the "0" cavitation problem of the submerged bearing [1] are in fact directly applicable to the internal cavitation problem viewed in the universal form.

In the universal representation, geometrical parameters of the internal cavitation pattern can be summarized as the circumferential locations of the breakup initiation point, the film waist, and the cavitation termination point together with the width fraction of the film waist. They are uniquely defined by (ϵ_i, ϵ) as graphically shown in Fig. 3.

Table 1 Scale factors and offsets in side bands

Side band	Inlet	Exit
Pressure offset Π_0	Π_C	Π_C
Pressure scale $\Delta\Pi$	$\Pi_S - \Pi_C$	$-\Pi_C$
Axial offset ζ_0	-1	1
Axial scale $\Delta\zeta$	$\zeta_i + 1$	$\zeta_t - 1$

Results

Cavitation Patterns. The pressure parameters $(-\Pi_C, \Pi_S)$ affect the cavitation pattern in two ways. Firstly they determine ϵ_i according to Fig. 1. It may be noted that the lower bound of ϵ_i depends only on Π_S as given by the line $\zeta_i = 1.0$ in Fig. 2. ϵ_i together with the operating eccentricity ϵ fix the circumferential characteristics of the cavitation boundary; i.e., the locations of breakup initiation, the waist, and the termination point along with the waist width ratio ζ_w as shown in Fig. 3. Secondly, the two "halves" of the cavitation pattern divide at ζ_i; ζ_i being a function of the ratio $(-\Pi_C/\Pi_S)$ as given by equation (10), and $(1 + \zeta_i, 1 - \zeta_i)$ are, respectively, width scales of the two halves in the universal solution.

These effects are shown in Fig. 4. Figure 4 (*a*) corresponds to the condition ($\epsilon_i = 0.025$, $\epsilon = 0.10$). Four cavitation patterns are shown. Each plan form covers the entire developed film; the lower and upper boundaries are the minimum gap locations. From left to right the cavitation patterns correspond in sequence the ratio $-\Pi_C/\Pi_S = (\infty, 1.0, 0.1, 0.0)$. In this case, because ϵ_i is quite small (representing a lubricant with an effective vapor pressure very close to the ambient (and a very low feed pressure) the cavitation region spans about 2/3 of the total periphery even though the operating eccentricity is quite modest. In Fig. 4 (*b*), with ϵ_i staying at 0.025, ϵ is increased to 0.3. The four patterns correspond to the same sequence of the pressure ratio. The larger operating eccentricity is seen to be ac

companied by the enlargement of the cavity in both axial and circumferenctial directions. Figure 4 (*c*) corresponds to (ϵ_t = 0.2, ϵ = 0.3). The moderately large ϵ_t requires either a relatively low vapor pressure lubricant (about 10 times more remote from the ambient than the previous cases) or a moderately high feed pressure or some suitable combination of the two pressure parameters. Figure 4 (*d*) shows the cavitation paterns for a rather large operating eccentricity. Note that the length of the cavity remain at about 1/2 the total periphery while its width has increased substantially.

It is quite clear that the feed pressure is an effective means to limit the circumferential extent of cavitation.

Formulas for Global Characteristics. The essential performance parameters of a journal bearing include the force components,

$$(\bar{W}_R, \bar{W}_T) = \frac{(W_R, W_T)}{\left(\frac{3}{2}\right)\mu\omega\left(\frac{R}{C}\right)^2\left(\frac{L}{D}\right)^2(LD)} = \int_0^{2\pi}(\cos\eta, -\sin\eta)d\eta\int_{-1}^{1}\Pi d\zeta \tag{25}$$

the friction torque,

$$\bar{T} = \frac{TC}{\mu\omega R^2(\pi DL)} = \frac{1}{4\pi}\int_0^{2\pi}d\eta\int_{-1}^{1}\left(\frac{\tau C}{\mu\omega R}\right)d\zeta \tag{26}$$

and the supply flow,

$$\bar{\psi} = \frac{12\mu(L/D)\psi}{\pi C^3 p_S} = \frac{4\psi}{\omega R(\pi DC)(L/D)\Pi_S} \tag{27}$$

Because the integrands take on different functional forms in the full-film and cavitation regions, it is convenient to separate the integrals into parts pertaining to the two regions. One can therefore write

$$(\bar{W}_R, \bar{W}_T) = (\bar{W}_R, \bar{W}_T)_F + (\bar{W}_R, W_T)_C$$

$$\bar{T} = (\bar{T})_F + (\bar{T})_C \tag{28}$$

The terms associated with the subscript "*F*" are contributed by the full-film region, which spans $\eta_t - 2\pi \le \eta \le \eta_{bi}$. The subscript "*C*" identifies the contribution to the cavitation domain, $\eta_{bi} \le \eta \le \eta_t$. It is not necessary to separate the supply flow into two parts because the cavity blocks axial through flow so that $\bar{\psi}$ is entirely due to the full-film region.

For short bearings, contribution to friction torque by circumferential pressure gradient is of $0[(L/D)^2]$, and is commonly neglected. In the cavitated region, $\eta_{bi} \le \eta \le \eta_t$, the friction torque $(\bar{T})_C$ is made up from two parts; one part is due to the continuous films between either end of the bearing and the cavity border ($0 < \hat{\zeta} < \hat{\zeta}_b$ for $\eta_{bi} \le \eta \le \eta_w$ and $0 < \hat{\zeta} < \hat{\zeta}_f$ for $\eta_w \le \eta \le \eta_t$), the second part is due to the striated streamers within the cavity [9]. For computing the streamer contribution to $(\bar{T})_C$, the local gap at film breakup is used in the range $\eta_{bi} \le \eta \le \eta_w$, and the average value H_{b0} is used in the range $\eta_w \le \eta \le \eta_t$.

In summary, the global characteristics in the dimensionless form are

$$\bar{W}_R = W_R\left\{\frac{3}{2}\mu\omega\left(\frac{R}{C}\right)^2\left(\frac{L}{D}\right)^2(LD)\right\}^{-1}$$

$$= 2\left(\frac{1}{2}\Pi_S - \Pi_C\right)(\sin\eta_{bi} - \sin\eta_t) \tag{29a}$$

$$+ \frac{\epsilon(\cos\eta_{bi} - \cos\eta_t)(\cos\eta_{bi} + \cos\eta_t - 2\epsilon\cos\eta_{bi}\cos\eta_t)}{3(1-\epsilon\cos\eta_{bi})^2(1-\epsilon\cos\eta_t)^2} \tag{29b}$$

$$+ C_{II}\left\{\frac{1}{3}\int_{\eta_{bi}}^{\eta_w}\cos\eta\,\hat{\zeta}_b\,d\eta + \frac{1}{2}\int_{\eta_w}^{\eta_t}\hat{\zeta}_f\cos\eta\left(1 - \frac{\hat{\zeta}_f^2 Q}{3Q_t}\right)d\eta\right\} \tag{29c}$$

$$\bar{W}_T = W_T\left\{\frac{3}{2}\mu\omega\left(\frac{R}{C}\right)^2\left(\frac{L}{D}\right)^2(LD)\right\}^{-1}$$

$$= 2\left(\frac{1}{2}\Pi_S - \Pi_C\right)(\cos\eta_{bi} - \cos\eta_t) \tag{30a}$$

$$+ \frac{\epsilon[2\pi - (\chi_t - \chi_{bi}) + \sin\chi_t\cos\chi_t - \sin\chi_{bi}\cos\chi_{bi}]}{3(1-\epsilon^2)^{3/2}} \tag{30b}$$

$$- C_{II}\left\{\frac{1}{3}\int_{\eta_{bi}}^{\eta_w}\sin\eta\,\hat{\zeta}_b d\eta + \frac{1}{2}\int_{\eta_w}^{\eta_t}\hat{\zeta}_f\sin\eta\left(1 - \frac{\hat{\zeta}_f^2 Q}{3Q}\right)d\eta\right\} \tag{30c}$$

$$\bar{T} = \frac{TC}{\mu\omega R^2(\pi DL)}$$

$$= \frac{1}{2\pi(1-\epsilon^2)^{1/2}}\left\{2\pi - (\chi_t - \chi_{bi}) + \int_{\chi_{bi}}^{\chi_w}\left(\hat{\zeta}_b + \frac{1}{H}\int_{\hat{\zeta}_b}^{1}H_b d\hat{\zeta}\right)d\chi + \int_{\chi_w}^{\chi_t}\left[\hat{\zeta}_f + \frac{(1-\hat{\zeta}_f)H_{b0}}{H}\right]d\chi\right\} \tag{31}$$

$$\bar{\psi} = \frac{4\psi}{\omega R(\pi DC)(L/D)\Pi_S}$$

$$= \left(1 + \frac{3}{2}\epsilon^2\right) - \frac{1}{2\pi}\left\{\left(1 + \frac{3}{2}\epsilon^2\right)(\eta_t - \eta_{bi}) + \epsilon\left[\sin\eta_{bi}\left(3 + \epsilon^2 - \frac{3}{2}\epsilon\cos\eta_{bi} - \frac{\epsilon^2}{3}\sin^2\eta_{bi}\right) - \sin\eta_t\left(3 + \epsilon^2 - \frac{3}{2}\epsilon\cos\eta_t - \frac{\epsilon^2}{3}\sin^2\eta_t\right)\right]\right\} \tag{32}$$

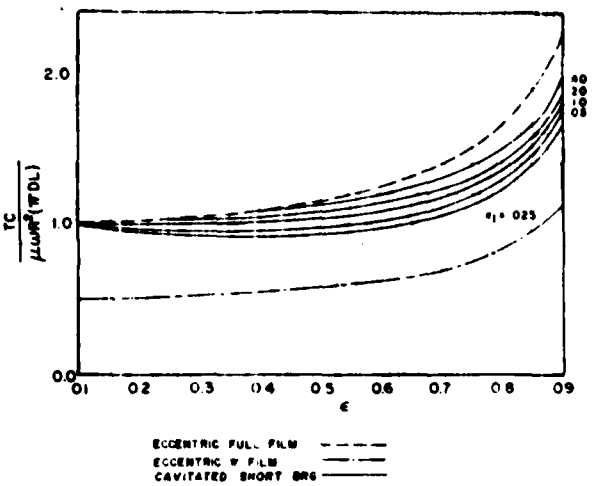

Fig. 5 Dimensionless friction

where

$$C_{\Pi} = 2\left\{\frac{(\Pi_S - \Pi_C)^{3/2} + (-\Pi_C)^{3/2}}{(\Pi_S - \Pi_C)^{1/2} + (-\Pi_C)^{1/2}}\right\} \tag{33}$$

and

$$\chi = 2\tan^{-1}\left\{\sqrt{\frac{1+\epsilon}{1-\epsilon}}\tan\left(\frac{\eta}{2}\right)\right\} \tag{34}$$

Various subscripts are used to designate the appropriate integration limit. One may note that $\bar{T}$ and $\bar{\psi}$ can be fully described in terms of (ϵ_i, ϵ), which uniquely determine (η_{b_i}, η_i) as well as $\hat{\zeta}_b(\eta_{b_i} \le \eta \le \eta_w)$ and $\hat{\zeta}_f(\eta_\pi \le \eta \le \eta_i)$, without further specification of (Π_S, Π_C). $(\bar{W}_R, \bar{W}_T)$, however, are influenced by (Π_S, Π_C), in addition to (ϵ, ϵ_i) because of the pressurization effects both in the full-film region, equations (29*a*) and (30*a*), and in the cavitation region, equations (29*c*) and (30*c*).

Representative Results. Graphs for the dimensionless friction torque are shown in Fig. 5. A value of unity indicates agreement with Petrov's law [10]. Upper and lower bounds are respectively full-film and π-film frictions with allowance for eccentricity. It is observed that even though the film may be extensively cavitated; for instance, for $(\epsilon_i = 0.025, \epsilon = 0.3)$, as shown by the cavitation pattern of Fig. 4 (*b*), the torque is substantially higher than π-film result. The effect of enlarging the cavity, however, is evident for $\epsilon_i = 0.025$, as the curve dips down and reaches a minimum value near $\epsilon = 0.4$. Competing effects of eccentricity and cavitation nullify each other such that near agreement with Petrov's law is indicated for $(0.025 \le \epsilon_i \le 0.20, 0 \le \epsilon \le 0.55)$.

Graphs for the flow function are shown in Fig. 6. The same results were previously obtained by Wakuri, et al., [2] with the interpretation restricted to the case of an ambient exit cavity, so that each value of ϵ_i is associated with a unique value of Π_S. It is clear, nevertheless, that these results remain applicable to the bearing with a flooded exit end, such that an internal cavity would sustain a subambient pressure. In the latter situation, if both $\bar{\psi}$ and ϵ are available from test data and Π_S is known; then Fig. 6 allows one to determine ϵ_i, and subsequently Fig. 1 can be used to determine $-\Pi_C$ for the particular combination of (Π_S, ϵ_i). In this manner, *a flow-eccentricity experiment would become a basis to determine the cavitation pressure.*

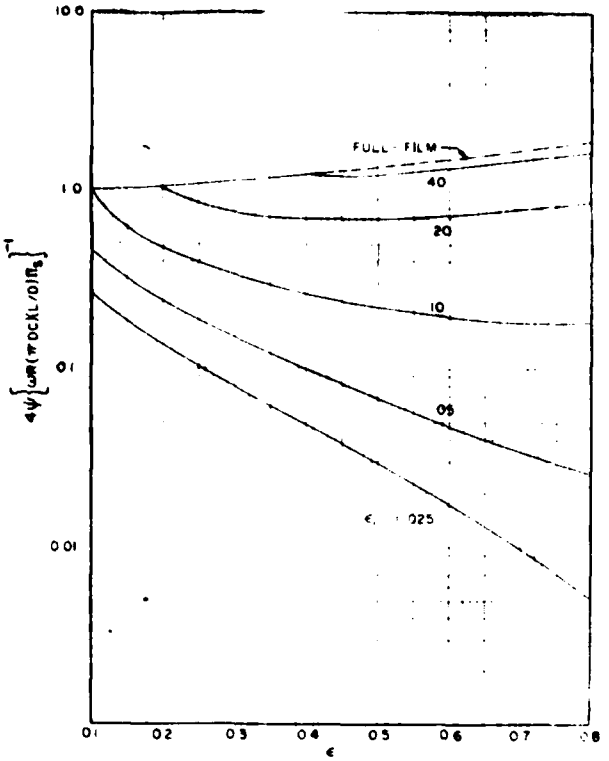

Fig. 6 Flow function

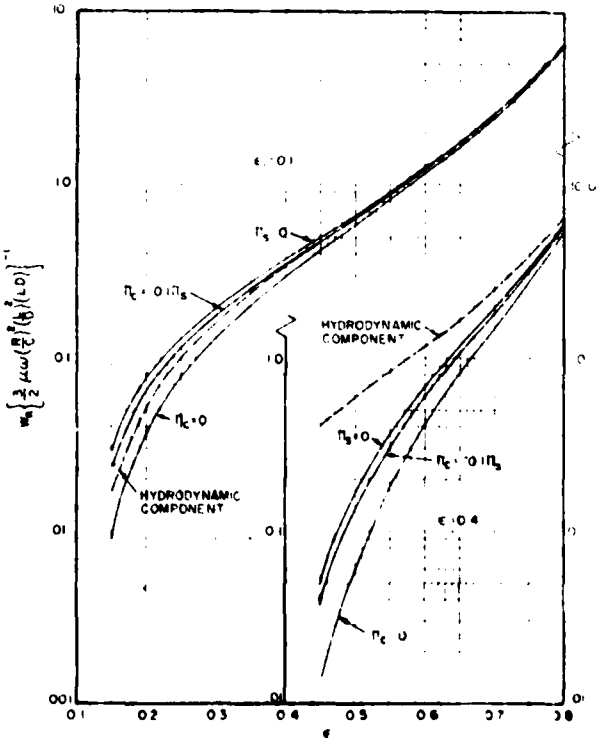

Fig. 7 Hydrostatic effects on radial force

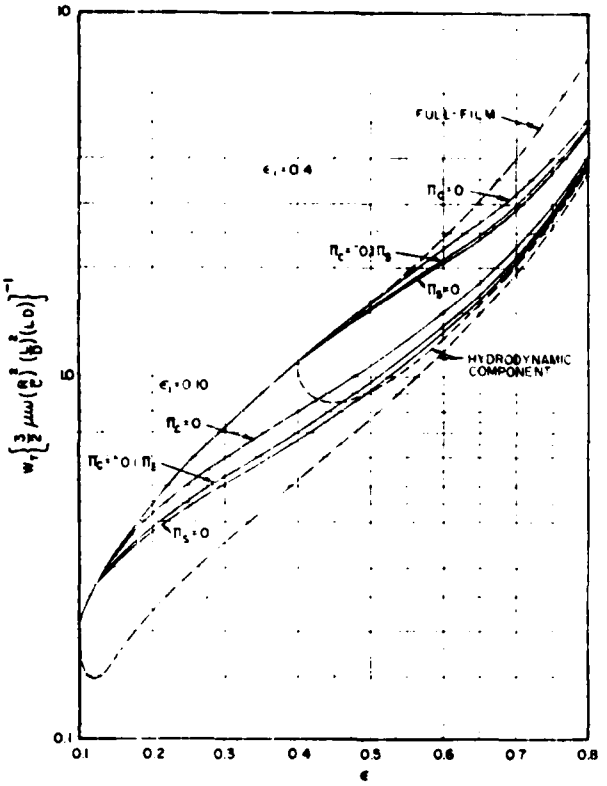

Fig. 8 Hydrostatic effects on tangential force

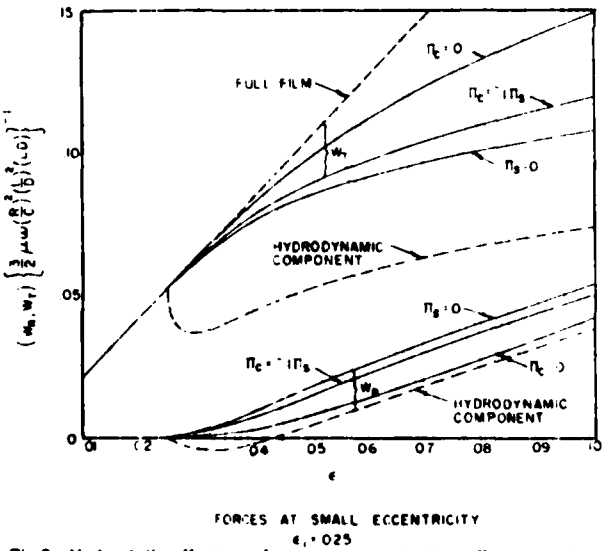

FORCES AT SMALL ECCENTRICITY
$\epsilon_i = .025$

Fig. 9 Hydrostatic effects on force components at small eccentricity for $\epsilon_i = .025$

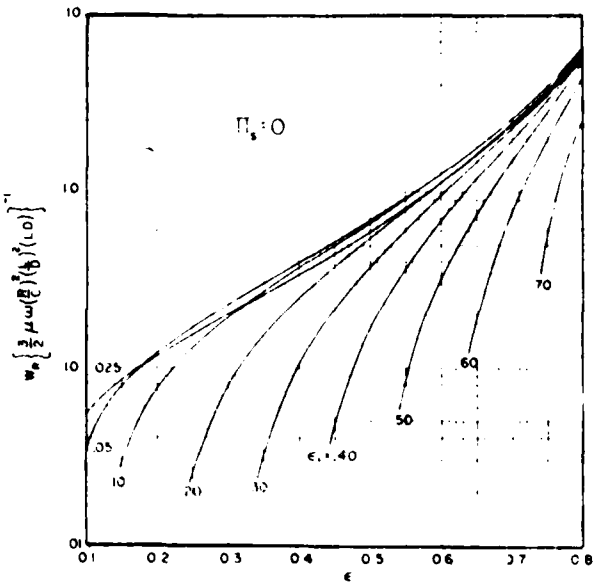

Fig. 10(a) Dimensionless radial force - submerged bearing

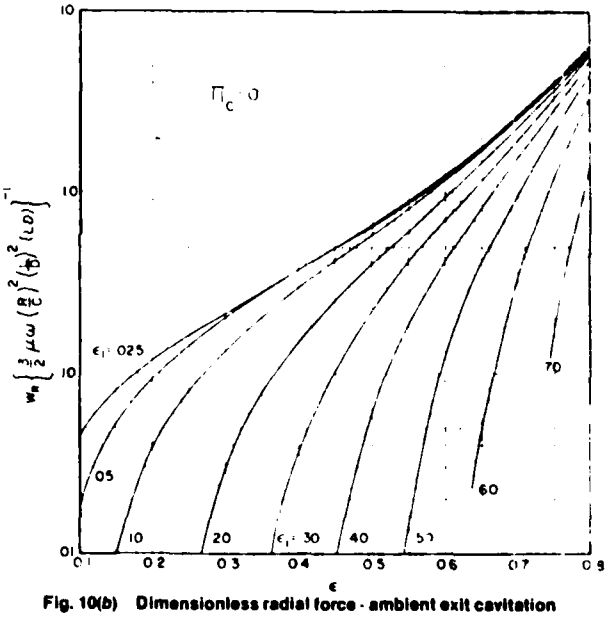

Fig. 10(b) Dimensionless radial force - ambient exit cavitation

It was noted previously that the force components cannot be uniquely specified in terms of (ϵ, ϵ_i). This is because the pressure profile in the cavitation domain takes on a drastically different character than that in a full-width film. In a full-film condition as shown by equation (4), the contribution of Π_s is rotationally symmetrical and thus would not result in a net force. The full-film journal bearing force is entirely due to the hydrodynamic wedge effect represented by Q. In a cavitated region, even if one continues to measure the pressure profile from the straight line which connects the pressure levels of the two ends, its characterization requires representation of the pressure and width scales as indicated in Table 1. The roles of $(\Pi_S, -\Pi_C)$ in the pressure scales are self-evident. The width scales contain the parameter ζ_i, which in turn is a function of the pressure ratio $(-\Pi_C/\Pi_S)$. Since ϵ_i already provides one constraint between $(\Pi_S, -\Pi_C)$, a second parameter is sufficient to specify both $(\Pi_S, -\Pi_C)$. For the latter purpose, three values of the pressure ratio, $-\Pi_C/\Pi_S = (\infty, 0.1, 0)$, are used to examine the effects on the forces which are not included in the hydrodynamic components as represented by equations (29*b*) and (30*b*). The same conditions were used to illustrate the sequence of successively increasing asymmetry in the cavitation pattern in Figs. 4(*a*) through 4(*d*). In Figs. 7 and 8, radial and tangential forces are, respectively, plotted against ϵ in two groups, each of which includes the three

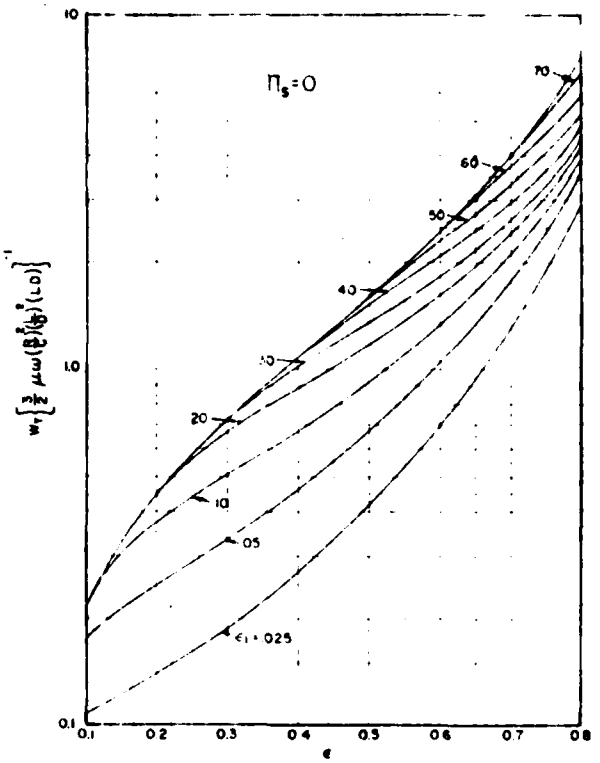

Fig. 11(a) Dimensionless tangential force - submerged bearing

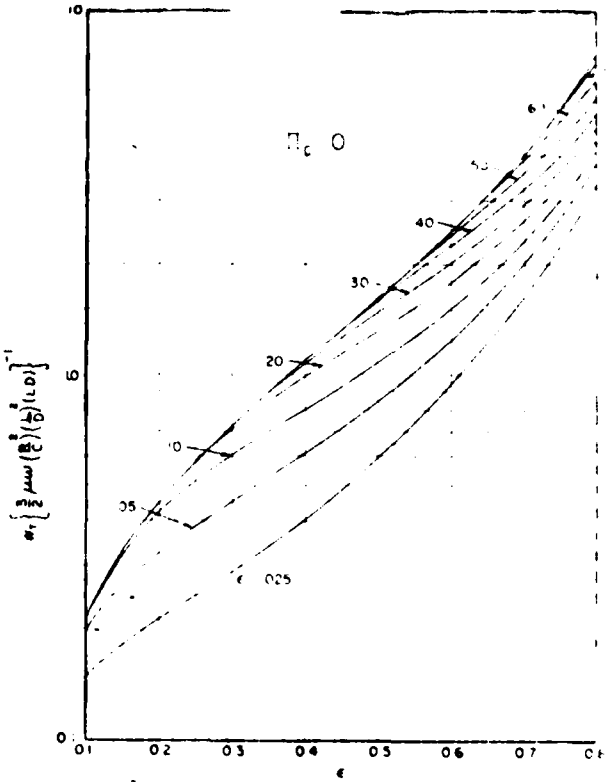

Fig. 11(b) Dimensionless tangential force - ambient exit cavitation

values of the pressure ratio for a given ϵ_i. The two values of ϵ_i are (0.1, 0.4). For comparison, the hydrodynamic component is drawn in dashes. Both radial and tangential forces show moderate spreads among various values of the pressure ratio at moderate values of $\epsilon > \epsilon_i$. In the same range of ϵ, the hydrodynamic components are not good approximations of the actual forces. Further scrutiny of this question at small (ϵ_i, ϵ) is referred to Fig. 9. So far as the radial force is concerned (for $\epsilon \geq \epsilon_i$), the hydrodynamic component is lower than the full force at a small ϵ_i and can be an order of magnitude too large at moderately large values of ϵ_i. The hydrodynamic component of the tangential force is always smaller than the full value, it breaks away from the full-film value too rapidly. The two conditions ($\Pi_S = 0$, $\Pi_C = 0$) represent the extreme conditions of symmetry. For any combination of (ϵ_i, ϵ), all solutions of the forces are somewhere between those corresponding to the extreme conditions. Figures 10 (*a*) and (*b*) contain curves for the radial force for the two respective conditions ($\Pi_S = 0$, $\Pi_C = 0$). Curves for the tangential force are given in Figs. 11 (*a*) and (*b*). It turns out that for any finite, combinations of (Π_S, Π_C), the following empirical formula yields very accurate results:

$$(\bar{W})_{\epsilon_i,\epsilon;\Pi_S,\Pi_C} = \frac{24.72(-\Pi_C)(\bar{W})_{\epsilon_i,\epsilon;\Pi_S=0} + \Pi_S(\bar{W})_{\epsilon_i,\epsilon;\Pi_C=0}}{\Pi_S + 24.72(-\Pi_C)}$$

where $\bar{W}$ may be either $\bar{W}_R$ or $\bar{W}_T$.

Conclusions

Pressurization of lubricant supply at one end of a short bearing would shift the cavitation pattern toward the discharge side. For the same cavitation (subambient) pressure, the eccentricity ratio for cavitation incipience would be increased by supply pressurization.

Size parameters of the cavitation pattern are dependent on (ϵ_i, ϵ) only, so long as the short bearing theory is valid. Axial location of the cavity and the degree of geometrical asymmetry are dependent on the supply/cavitation pressure ratio (both pressures are measured above the ambient). For any finite $\epsilon_i > 0$, there is an upper bound of the extent of cavitation as $\epsilon \to 1.0$.

The cavity can occupy an internal domain only when the exit edge is flooded by lubricant (with negligible pressurization), and the cavity pressure would then be necessarily subambient. If the cavitation pressure is precisely equal to the ambient pressure or if the exit lubricant is allowed to drain away freely, then the exit edge would be only partially connected to the fluid film and the cavity must communicate to the ambient directly. The drain away condition enforces an ambient condition of the cavity even if the lubricant can inherently sustain a subambient condition.

Dimensionless friction and through-flow function can be fully defined by (ϵ_i, ϵ). Competitive effects of eccentricity and cavitation on friction results in the near agreement with Pehrov's law for a wide range of conditions. The through-flow function is strongly dependent on the value of ϵ_i in practical operating condition of ϵ. Thus, validity of the present analysis can be verified by correlating the mutual dependence between the cavitation pressure and the through-flow function at fixed supply pressure and the operating eccentricity.

Radial and tangential force components (as functions of operating eccentricity ϵ) are dependent on the supply/cavitation pressure ratio in addition to the determination of the cavitation incipience eccentricity ϵ_i by the supply and cavitation pressures. An accurate empirical formula for both force components has been found to permit simple interpolation from their respective values at the extreme conditions of zero supply pressure and zero cavitation pressure.

Acknowledgment

This work was supported by the U.S. Army Research Office under Contract Number DAAG29-78-C-0027, Project Number P-15657-E.

References

1 Pan, C. H. T., "An Improved Short Bearing Analysis for the Submerged Operation of Plain Journal Bearings and Squeeze-film Dampers," ASME Paper No. 79-Lub 33, Presented at the ASME-ASLE Lubrication Conference, Dayton, Ohio, October 16-18, 1979, also to be published in the JOURNAL OF LUBRICATION TECHNOLOGY.

2 Wakuri, Tutaro et. al., "Oil Flow in Short Bearing with Circumferential Groove," *Bulletin of the JSME*, Vol. 16.

3 Dubois, G. B., and Ocvirk, "Analytical Derivation of Short Bearing Approximation for Full Journal Bearings," NACA Report 1157, 1953.

4 "Cavitation and Related Phenomena in Lubrication," *Proceedings of the First Leeds-Lyon Symposium on Tribology*, The University of Leeds Symposium, Edited by Dowson, M. Godet, and C. M. Taylor Mechanical Engineering Publications for the Institute of Tribology, Leed University and the Institut National des Sciences Appliquees Lyon, London.

5 Nakahara, T., Kobayashi, T., and Masuko, M., "The Influences of Air Content of Lubricant on Cavitation in the Thrust Bearing with Closed Recesses," *Proceedings of JSLE-ASLE International Lubrication Conference*, Tokyo, Japan, June 9-11, 1975, Ed. T. Sakurai, Elsvier Scientific Publishing Co., New York, 1976, pp. 204-211.

6 Jakobsson, B., and Floberg, L., "The Finite Journal Bearing, Considering Vaporization," *Trans. Chalmers University Tech.*, Nr. 190, Goteborg, 1957.

7 Swift, H. W., "The Stability of Lubricating Films in Journal Bearings," *Proceedings Institute of Civil Engineers* (London), Vol. 233, 1932, pp. 267-288.

8 Stieber, W., "Das Schwimmlager," VDI, Berlin, 1933.

9 Floberg, L., "On Hydrodynamic Lubrication with Special Reference of Sub-Cavity Pressures and Number of Streamers in Cavitation Regions," *Acta Poly. Scan.*, 1965, ME 19.

10 Petrov, N. P., "Friction in Machines and the Effect of the Lubricant," *Inzhernui Zhurnal*, St. Petersburg, 1883, Vol. 1, pp. 71-140; Vol. 2, pp. 227-279; Vol. 3, pp. 377-463; Vol. 4, pp. 535-564.

DISCUSSION

I. Etsion[2]

The authors have presented a valuable solution to the problem of short journal bearings fed from either one or two ends. This problem is also of great interest in squeeze film dampers and mechanical face seals. The exact solution for the cavitation shape and bearing performance, as derived by the authors, is quite complex. However, such exact solutions are essential as a basis for assessment of less accurate, simpler solutions that may be used for practical purposes.

A possible simpler solution, for example, is the one based on equation (4) with an additional condition replacing any $\Pi < \Pi_c$ by $\Pi = \Pi_c$ (the half Sommerfeld condition). The cavitation shape $\zeta(\eta)$ in this case is found from a solution of equation (4) with $\Pi = \Pi_c$. The accurate shape of the cavity and, more important, the flow continuity on the cavitation boundaries are not preserved by this simple solution. Nevertheless, the overall results, especially for friction torque and load carrying capacity, may be fairly close to these obtained from the much more complex, exact solution presented in this paper. The authors have apparently attempted a comparison between their exact solution and available aproximations. In Fig. 5, for example, the results for the friction torque are compared with these obtained for eccentric full film and eccentric π film. The latter is basically the half Sommerfeld solution for the case $-\Pi_c = \Pi_c = 0$. Unfortunately, the π film results, shown in Fig. 5, do not account for the striation affect on the friction torque, leading to the erroneous conclusion that ". . . .the torque is substantially higher than π film result. . . .". Table 2 presents results of the dimensionless friction torque for the π film with the striation effect included. These results were obtained by dividing the dimensionless friction force $\bar{F}$ of reference [11] by 2π.

From the results in Table 2 and those in Fig. 5, it is clear that the π film, or the half Sommerfeld solution for $-\Pi_c = \Pi_c = 0$, approximates very well the exact solution in cases of suitable caviation incipient (e.g. $\epsilon_t = 0.025$ and $\epsilon_t = 0.05$). The exact solution for higher values of ϵ_t can be well approximated if more realistic (less than ambient) cavitation pressures are used in the half Sommerfeld solution. Hence, it can be concluded that the half Sommerfeld solution based on equation (4) approximates quite well the exact friction torque.

With regard to the lubricant through flow it can be shown that the half Sommerfeld solution yields the same results as the exact solution. This is due to the fact that the net hydrodynamic component of the flow in a submerged bearing is zero and the through flow is exclusively a result of the hydrostatic pressure differential across the bearing.

It would be interesting to compare the results of the radial and tangenial forces obtained from the half Sommerfeld solution with these obtained from the present exact solution. Such a comparison would settle the yet unresolved issue of the accuracy of using the half Sommerfeld condition for approximating cavitation in narrow configurations like face seals and squeeze film dampers.

Another problem, which was not given much attention in the past, is the assumption of constant pressure inside the cavitation zone and on its boundaries. This assumption which is used here by the authors and was used extensively by other researchers in the past may not be correct for enclosed cavities such as in submerged journal bearings. In a recent work [12], where the pressure field in the cavitation zone of a submerged journal bearing was maped, it was found that significant pressure variations occur inside the cavity. In cases where the full film formation point penetrates into the converging portion of the bearing clearance, high cavity pressures were recorded that exceeded even the elevated pressure at the ends of the bearing. This phenomenon was attributed to air solubility of the lubricating oil which probably plays an important role in the cavitation mechanism.

Additional References

11 Etsion, I., and Pinkus, O., "Analysis of Short Journal Bearings With New Upstream Boundary Condition," ASME JOURNAL OF LUBRICATION TECHNOLOGY, Vol. 96, No. 3, July 1974, pp. 489-496.

12 Etsion, I., and Ludwig, L. P., "Observation of Pressure Variation in the Cavitation Region of Submerged Journal Bearings," NASA TM-81582

Table 2 Dimensionless friction torque for π film with striation effect included

ϵ_t	0.1	0.2	0.3	0.4	0.5	0.6	0.7	0.8	0.9
$TC/\mu WR^2(\pi DL)$	0.96	0.94	0.93	0.93	0.96	1.02	1.11	1.29	1.75

[2] Department of Mechanical Engineering, Technion, Haifa, Israel.

Author's Closure

The authors concur with Dr. Etsion that if one allows for the contribution of shear from striations in the divergent portion of the gap, the π-film analysis yields rather satisfactory results. However, one may justifiably argue that the striation correction itself implies the need to obey overall continuity of flow; otherwise, as indicated by Fig. 5, the friction torque would be consistently and substantially underestimated. The important message revealed by the more cautious calculation is that the simultaneous effects of eccentricity, cavitation, and striation tend to balance one another such that Petrov's law is quite satisfactory in its simplest form.

It is quite natural to query to what extent film force calculations may be adequately approximated by the π-film results. This question was examined for the submerged journal bearing [1] and graphical comparisons were separately presented for the tangential and radial force components. These graphs are reproduced as Figs. A-1 and A-2. If one modifies the Ocvirk-Gumbel approximation by requiring $\Pi \geq \Pi_c$ with a suitably selected value of $\Pi_c < 0$, then the corresponding results would be between those of the standard π-film results ($\Pi_c = 0$) and the full film results ($\Pi_c < \Pi_{min}$). It is clear that since some of the curves in these figures are not contained between these "extreme cases," the modified Ocvirk-Gumbel approximation has limited usefulness. The basic fault of the Gumbel approximation is its inability to describe the boundary of the re-established film, which can reach into the convergent portion of the bearing gap. This conclusion remains valid even if one edge of the bearing is pressurized.

Dr. Etsion's comments regarding the hydrostatic through flow prompted the author to re-examine the role of cavitation in this respect. Equation (32) and Fig. 6 are based on the axial flow in the full-film ($\eta_i - 2\pi \leq \eta \leq \eta_h$) at the mid plane ($\zeta = 0$). With pressurization of one edge of the bearing, however, the "cavitation axis" is shifted to $\zeta_i > 0$. Accordingly, the correct hydrostatic through flow should be calculated as the axial flow in the full film at ζ_i and equation (32) should be corrected by a "cavitation leakage" term:

$$(\Delta\bar{\psi})_{\text{cavitation leakage}} = \frac{2\zeta_i}{\Pi_s}\epsilon(\cos\eta_{h_i} - \cos\eta_i) = \epsilon(\cos\eta_{c_i} - \cos\eta_i)/Q_i \qquad \text{(A-1)}$$

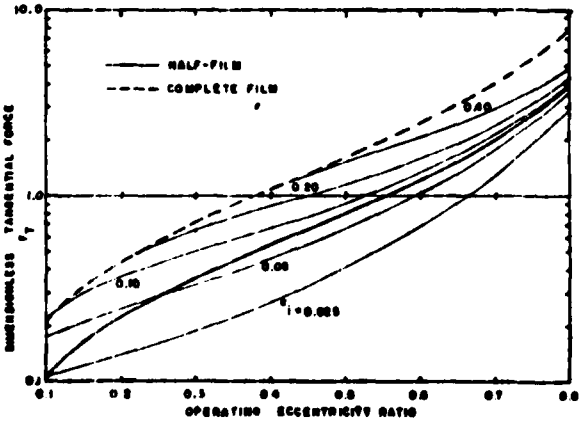

Fig. A-1 Tangential force for "O" cavitation

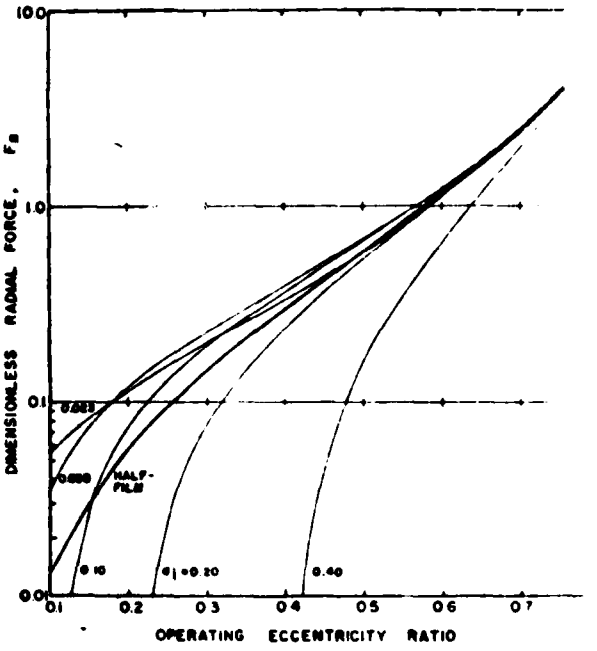

Fig. A-2 Radial-force for "O" cavitation

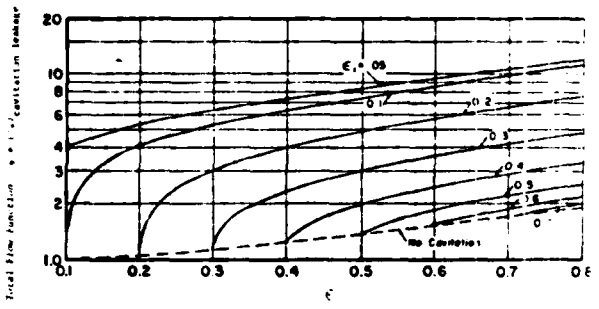

Fig. A-3 Total flow function equations (32) and (A-1)

With the addition of "cavitation leakage," the total flow function is as shown in Fig. A-3.

The formal simplicity of Equation (A-1) motivated a search for similarly simple formulae for the effects of pressurization on the force components. This was found possible upon recognizing

$$\Pi_s - 2\Pi_c = (1 + \zeta_i^2)Q_i \qquad \text{(A-2)}$$

$$C_{\Pi} = (1 + 3\zeta_i^2)Q_i \qquad \text{(A-3)}$$

ζ_i as a function of $(\Pi_s - \Pi_c)$ can be readily calculated with the aid of Equation (10). Therefore, in place of the empirical formula given in the original text, the following exact formula is obtained:

$$\bar{W}_{\Pi_s,\Pi_c} = \bar{W}_{\Pi_s\ 0} + \zeta_i^2(\bar{W}_{\Pi_c\ 0} - \bar{W}_{\Pi_s\ 0}) \qquad \text{(A-4)}$$

A further refinement of the present analysis is the discovery of an exact integral for the cavitation boundary, without invoking the "mean transport approximation" [1] yielding

$$\zeta_B^2 = \frac{Q_i}{(H_B - H_h)}\int_{\eta_h}^{\eta_B} H^3\, d\eta \qquad \text{(A-5)}$$

where the subscript "B" refers to the cavitation boundary either in the break-up or in the fill-back region. For the break-up boundary, the right-hand side of equation (A-5) reduces to Q_i/Q_h in agreement with equation (17) by the limiting process

$\eta_B - \eta_b$. For the fill-back boundary, the subscript "B" is replaced by "f" for (ζ, H, η). (H_b, η_b) refer to the break-up boundary at ζ_B. Equation (A-5) thus becomes a transcendental relationship between ζ_f and η_f, and can be solved only numerically. The actual discrepancy between equation (21), which is based on the "mean transport approximation," and equation (A-5) is quite minute in *all* physically significant aspects.

It is understandable that the analytical content of the present work should be regarded as being too complex for practical use. However, it is because of the fully analytical treatment that very complete numerical results can be compiled. In view of their universal applicability, tabulations for the full range of (ϵ, ϵ_c) are furnished with this closure. It is hoped that the availability of the numerical tables will encourage judicial use of these results in pertinent engineering activities. The headings used in these tables are defined as follows:

E-INC	ϵ
ECC	ϵ
BEG	η_{in}/π
END	η_f/π
WAIST	$\bar{\xi}_w$
FRICTION	$\bar{T}$
FLOW	$\bar{V} + (\Delta\bar{V})_{\text{cavitation leakage}}$
R-FORCE	$(\bar{W}_R)_{\Pi_\zeta = 0}$
T-FORCE	$(\bar{W}_T)_{\Pi_\zeta = 0}$
R-INCR	$(\bar{W}_R)_{\Pi_\zeta = 0} - (\bar{W}_R)_{\Pi_\zeta = 0}$
T-INCR	$(\bar{W}_T)_{\Pi_\zeta = 0} - (\bar{W}_T)_{\Pi_\zeta = 0}$

The interesting experimental results reported by Dr. Etsion will no doubt enhance our knowledge of the cavitation process in fluid film bearings. This author looks forward to the full publication of his findings. In the context of the present discussion, this author would suggest that hydrodynamic action in the gaseous phase, along with inertia effects and mass transfer related to gas phase solubility may be all associated with the interesting observations reported by Dr. Etsion. It should be clear that the details of the cavitation process must depend on other thermodynamic and fluid dynamic parameters which are overlooked in conventional lubrication studies. For this reason, in terms of details of the cavitation process, universality among journal bearings, seals, and dampers will cease to exist.

Table A-1 Numerical results

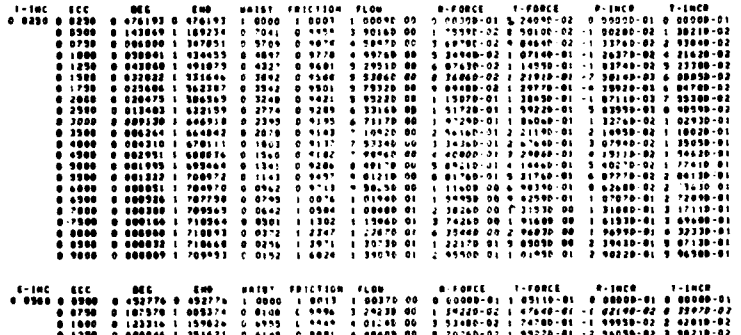

(Sheet 1 of 5)

Table A-1 (cont.)

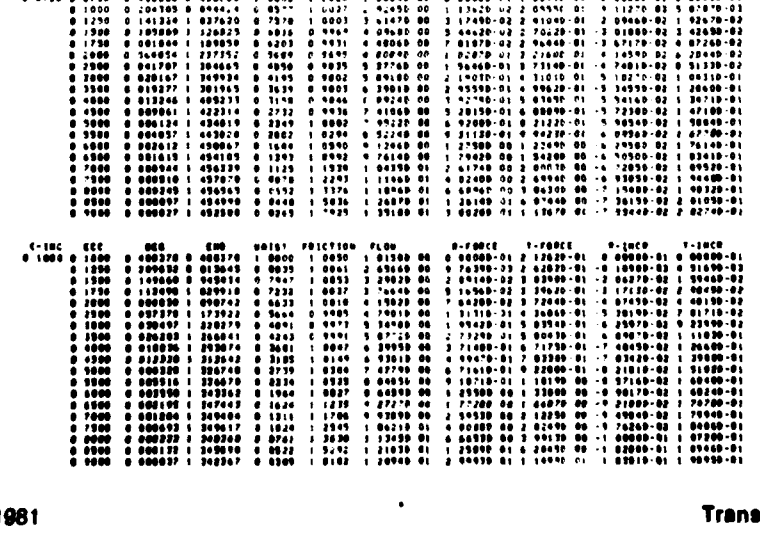

Table A-1 (cont.)

E-INC	ECC	DEG	END	WAIST	FRICTION	FLOW	R-FORCE	T-FORCE	R-INCR	T-INCR
0 2000	0 2000	0 333333	0 333333	1 0000	1 0266	1 0600D 00	0 0000D-01	4 4533D-01	0 0000D-01	0 0000D-01
	0 2500	0 146400	0 700503	0 8539	1 0209	2 4256D 00	2 5711D-02	5 6343D-01	-2 0498D-02	1 1040D-02
	0 3000	0 092912	0 822412	0 7372	1 0396	3 0929D 00	7 6640D-02	6 7012D-01	-5 0760D-02	3 6797D-02
	0 3500	0 061327	0 890642	0 6396	1 0432	3 5656D 00	1 5321D-01	7 7507D-01	-7 0141D-02	6 6350D 02
	0 4000	0 041661	0 936026	0 5550	1 0531	4 0306D 00	2 4912D-01	8 0925D-01	-1 0142D-01	9 9222D 02
	0 4500	0 030270	0 967546	0 4901	1 0664	4 4763D 00	3 7550D-01	1 0181D 00	-1 2121D-01	1 2100D-01
	0 5000	0 019020	0 989797	0 4129	1 0845	4 9108D 00	5 4619D-01	1 1714D 00	-1 3029D-01	1 4395D 01
	0 5500	0 012969	1 005402	0 3319	1 1004	5 3449D 00	7 0302D-01	1 3613D 00	-1 5329D-01	1 6746D-01
	0 6000	0 008000	1 016335	0 2961	1 1400	5 7833D 00	1 1260D 00	1 6069D 00	-1 6633D-01	1 0462D 01
	0 6500	0 004992	1 023539	0 2440	1 1818	6 2279D 00	1 4424D 00	1 9592D 00	-1 7042D-01	2 0365D 01
	0 7000	0 002910	1 027940	0 1977	1 2376	6 6000D 00	2 4418D 00	2 4017D 00	-1 8911D-01	2 1077D 01
	0 7500	0 001576	1 030164	0 1543	1 3140	7 1403D 00	3 6679D 00	3 1075D 00	-1 9070D-01	2 3210D-01
	0 8000	0 000796	1 030606	0 1147	1 4227	7 6093D 00	6 9311D 00	4 2759D 00	-2 0729D-01	2 4405D 01
	0 8500	0 000300	1 029075	0 0787	1 5009	8 0068D 00	1 2454D 01	6 4908D 00	-2 1474D-01	2 5450D-01
	0 9000	0 000084	1 020021	0 0466	1 0778	8 5729D 00	2 4057D 01	1 1704D 01	-2 2113D-01	2 6364D-01

E-INC	ECC	DEG	END	WAIST	FRICTION	FLOW	R-FORCE	T-FORCE	R-INCR	T-INCR
0 3000	0 3000	0 275592	0 275592	1 0000	1 0403	1 1390D 00	0 0000D-01	7 2300D-01	0 0000D-01	0 0000D-01
	0 3500	0 126911	0 569757	0 8676	1 0642	1 9507D 00	3 1129D-02	8 7021D-01	-2 5904D-02	1 1409D-02
	0 4000	0 080922	0 662260	0 7527	1 0796	2 3604D 00	1 0946D-01	1 0293D 00	-6 9947D-02	4 1349D 02
	0 4500	0 053402	0 719159	0 6312	1 0969	2 7075D 00	2 1952D-01	1 1872D 00	-1 1409D-01	7 9501D-02
	0 5000	0 035586	0 757058	0 5600	1 1170	3 0278D 00	3 0152D 01	1 3633D 00	-1 5963D-01	1 2025D-01
	0 5500	0 023296	0 785349	0 4772	1 1430	3 3357D 00	6 1273D-01	1 5715D 00	-1 9971D-01	1 6046D-01
	0 6000	0 014917	0 805323	0 4015	1 1769	3 6307D 00	9 5047D-01	1 8311D 00	-2 3629D-01	1 9003D-01
	0 6500	0 009199	0 819960	0 3320	1 2190	3 939[illegible] 00	1 4629D 00	2 1727D 00	-2 6960D-01	2 3473D-01
	0 7000	0 005371	0 830404	0 2681	1 2763	4 2023D 00	2 2799D 00	2 6494D 00	-2 9906D-01	2 6790D-01
	0 7500	0 002859	0 838472	0 2093	1 3532	4 5478D 00	[illegible] 6010D 00	3 3630D 00	-3 2726D-01	2 9829D 01
	0 8000	0 001391	0 844019	0 1555	1 4622	4 8572D 00	6 3416D 00	4 5393D 00	-3 5181D-01	3 2591D 01
	0 8500	0 000552	0 847030	0 1067	1 6206	5 1712D 00	1 2262D 01	6 7595D 00	-3 7356D-01	3 5082D 01
	0 9000	0 000155	0 850116	0 0633	1 9175	5 4902D 00	2 9664D 01	1 2059D 01	-3 9229D-01	3 7306D-01

E-INC	ECC	DEG	END	WAIST	FRICTION	FLOW	R-FORCE	T-FORCE	R-INCR	T-INCR
0 4000	0 4000	0 230053	0 230053	1 0000	1 0911	1 2400D 00	0 0000D 01	1 0882D 00	0 0000D-01	0 0000D-01
	0 4500	0 105319	0 475041	0 8451	1 1162	1 7309D 00	6 7200D 02	1 3055D 00	-3 0433D 02	1 4924D 02
	0 5000	0 065064	0 554656	0 7440	1 1422	2 0017D 00	1 7000D 01	1 5310D 00	-1 1070D-01	5 6297D 02
	0 5500	0 042121	0 604137	0 6340	1 1719	2 2407D 00	3 7430D 01	1 7794D 00	-1 5137D-01	1 1201D-01
	0 6000	0 026636	0 630541	0 5335	1 2076	2 4675D 00	6 9174D-01	2 0724D 00	-2 7391D-01	1 7390D-01
	0 6500	0 016322	0 663632	0 4411	1 2523	2 6890D 00	1 1076D 00	2 4421D 00	-3 4900D-01	2 3726D-01
	0 7000	0 009501	0 682420	0 3562	1 3103	2 9115D 00	1 4437D 00	2 9420D 00	-4 2123D-01	2 9934D-01
	0 7500	0 005121	0 696746	0 2781	1 3881	3 1350D 00	3 1016D 00	3 6770D 00	-4 8794D-01	3 5850D 01
	0 8000	0 002496	0 707767	0 2066	1 4900	3 3617D 00	6 0327D 00	4 8711D 00	-5 4060D-01	4 1106D-01
	0 8500	0 000975	0 716309	0 1410	1 6649	3 5926D 00	1 1945D 01	7 1067D 00	-6 0382D-01	4 6521D-01
	0 9000	0 000273	0 722962	0 0840	1 9541	3 8204D 00	2 9340D 01	1 2419D 01	-6 5035D-01	5 1167D 01

Table A-1 (cont.)

E-INC	ECC	DEG	END	WAIST	FRICTION	FLOW	R-FORCE	T-FORCE	R-INCR	T-INCR
0 5000	0 5000	0 192360	0 192360	1 0000	1 1547	1 3750D 00	0 0000D-01	1 6123D 00	0 0000D-01	0 0000D-01
	0 5500	0 084264	0 409702	0 8322	1 1929	1 6773D 00	5 5070D-02	1 9408D 00	-6 0162D-02	2 3540D-02
	0 6000	0 050215	0 474099	0 7170	1 2341	1 8690D 00	3 2622D-01	2 3100D 00	-2 0165D-01	9 0174D-02
	0 6500	0 030034	0 510912	0 5929	1 2830	2 0479D 00	7 6512D-01	2 7525D 00	-3 5610D-01	1 0195D-01
	0 7000	0 017295	0 550036	0 4707	1 3437	2 2229D 00	1 5640D 00	3 3009D 00	-5 1455D-01	2 0501D-01
	0 7500	0 009270	0 573107	0 3737	1 4237	2 3992D 00	2 0767D 00	4 0922D 00	-6 6045D-01	3 9354D-01
	0 8000	0 004441	0 590945	0 2777	1 5350	2 5767D 00	5 4966D 00	5 3277D 00	-8 1324D-01	4 9991D-01
	0 8500	0 001767	0 604062	0 1905	1 7031	2 7626D 00	1 1703D 01	7 6002D 00	-9 4370D-01	6 0154D-01
	0 9000	0 000493	0 615951	0 1130	1 9932	2 9515D 00	2 8756D 01	1 2945D 01	-1 0630D 00	6 9480D-01

E-INC	ECC	DEG	END	WAIST	FRICTION	FLOW	R-FORCE	T-FORCE	R-INCR	T-INCR
0 6000	0 6000	0 159532	0 159532	1 0000	1 2500	1 5400D 00	0 0000D-01	2 4344D 00	0 0000D-01	0 0000D-01
	0 6500	0 061961	0 349296	0 8369	1 3095	1 7394D 00	1 9094D-01	3 0449D 00	-1 4380D-01	4 5222D-02
	0 7000	0 030730	0 410030	0 6676	1 3773	1 8908D 00	7 7005D-01	3 7399D 00	-4 1541D-01	1 7250D-01
	0 7500	0 016258	0 450337	0 5313	1 4619	2 0399D 00	2 0084D 00	4 6449D 00	-7 7464D-01	3 4806D-01
	0 8000	0 008667	0 470601	0 3073	1 5767	2 1914D 00	4 5125D 00	5 9060D 00	-1 1223D 00	5 0430D-01
	0 8500	0 003429	0 499945	0 2657	1 7472	2 3474D 00	1 0389D 01	8 3536D 00	-1 4389D 00	7 3077D-01
	0 9000	0 000959	0 516639	0 1576	2 0392	2 5000D 00	2 7609D 01	1 3701D 01	-1 7659D 00	9 4961D-01

E-INC	ECC	DEG	END	WAIST	FRICTION	FLOW	R-FORCE	T-FORCE	R-INCR	T-INCR
0 7000	0 7000	0 129311	0 129311	1 0000	1 4003	1 7750D 00	0 0000D-01	4 0233D 00	0 0000D-01	0 0000D-01
	0 7250	0 065919	0 255500	0 8800	1 4409	1 8169D 00	1 4907D 01	4 6169D 00	-1 2352D-01	2 6426D-02
	0 7500	0 044033	0 300410	0 7007	1 5000	1 8056D 00	5 7516D-01	5 2754D 00	-4 0478D-01	1 1290D-01
	0 7750	0 029709	0 331500	0 6701	1 5506	1 9535D 00	1 3527D 00	6 0296D 00	-7 7032D-01	2 4775D-01
	0 8000	0 019023	0 355391	0 5000	1 6252	2 0219D 00	2 6271D 00	6 9305D 00	-1 1905D 00	4 1965D-01
	0 8250	0 012720	0 374690	0 4067	1 7046	2 0912D 00	4 6705D 00	8 0620D 00	-1 6505D 00	6 1749D-01
	0 8500	0 007725	0 390709	0 3980	1 8022	2 1617D 00	8 0564D 00	9 5769D 00	-2 1161D 00	8 3246D-01
	0 8750	0 004329	0 404400	0 3100	1 9279	2 2337D 00	1 3916D 01	1 1762D 01	-2 5760D 00	1 0573D 00
	0 9000	0 002152	0 416341	0 2360	2 0987	2 3071D 00	2 5096D 01	1 5253D 01	-3 0251D 00	1 2860D 00

E-INC	ECC	DEG	END	WAIST	FRICTION	FLOW	R-FORCE	T-FORCE	R-INCR	T-INCR
0 7250	0 7250	0 121924	0 121924	1 0000	1 4519	1 7004D 00	0 0000D-01	4 6474D 00	0 0000D-01	0 0000D-01
	0 7500	0 068123	0 269106	0 8792	1 5003	1 0654D 00	2 0301D-01	5 3066D 00	-1 6954D-01	3 9367D-02
	0 7750	0 039040	0 280036	0 7636	1 5696	1 9328D 00	6 1171D-01	6 2224D 00	-5 9329D-01	1 6940D-01
	0 8000	0 025532	0 319041	0 6532	1 6300	2 0000D 00	1 9457D 00	7 2813D 00	-1 0360D 00	3 2729D-01
	0 8250	0 016240	0 342330	0 5400	1 7191	2 0600D 00	3 0787D 00	8 4074D 00	-1 6294D 00	5 5107D-01
	0 8500	0 009027	0 360905	0 4402	1 8183	2 1372D 00	7 1419D 00	9 9911D 00	-2 2376D 00	8 0004D-01
	0 8750	0 005496	0 376620	0 3500	1 9451	2 2070D 00	1 2900D 01	1 2243D 01	-2 8571D 00	1 0063D 00
	0 9000	0 002730	0 389940	0 2637	2 1164	2 2799D 00	2 3450D 01	1 5797D 01	-3 4605D 00	1 3764D 00

Table A-1 (cont.)

E-INC	ECC	DEG	END	WAIST	FRICTION	FLOW	R-FORCE	T-FORCE	R-INCR	T-INCR
0 7500	0 7500	0 114932	0 114932	1 0000	1 5118	[illegible]	0 0000D 01	9 4262D 00	0 0000D-01	0 0000D-01
	0 7750	0 090206	0 230900	[illegible] 0605	1 5706	[illegible]	2 9472D 01	6 3732D 00	-2 0027D-01	0 0029D-02
	0 8000	0 036067	0 277379	[illegible]	1 6905	[illegible]	1 1402D 00	7 0617D 00	[illegible]	2 0025D-01
	0 8250	0 021304	0 306690	0 6253	1 7362	[illegible]	2 9725D 00	[illegible] 7720D 00	-1 0042D 00	0 0467D-01
	0 8500	0 012706	0 329195	0 5090	1 8150	[illegible]	6 3170D 00	1 0550D 01	[illegible]	7 4579D-01
	0 8750	0 007136	0 347370	0 4026	1 9639	2 1401D 00	1 1026D 01	1 2003D 01	-3 1107D 00	1 0076D 00
	0 9000	0 003374	0 362553	0 3023	2 1370	[illegible]	2 2500D 01	1 6007D 01	-3 9446D 00	1 4533D 00

E-INC	ECC	DEG	END	WAIST	FRICTION	FLOW	R-FORCE	T-FORCE	R-INCR	T-INCR
0 7750	0 7750	0 107894	0 107894	1 0000	1 5020	[illegible]	0 0000D 01	6 4312D 00	0 0000D-01	0 0000D-01
	0 8000	0 048370	0 224005	0 0556	1 6612	[illegible]	4 4482D 01	[illegible]	1 9377D-01	6 9942D-02
	0 8250	0 029036	0 265996	[illegible]	1 7491	2 0106D 00	1 0295D 00	9 1769D 00	-1 1410D 00	2 0949D-01
	0 8500	0 017130	0 290376	0 5070	1 8530	[illegible]	4 6362D 00	[illegible] 01	-2 1997D 00	6 2499D-01
	0 8750	0 009400	0 310161	0 4616	1 9961	[illegible]	9 9417D 00	[illegible] 01	-3 3009D 00	1 0400D 00
	0 9000	0 004691	0 333772	0 3400	2 1593	[illegible]	2 0001D 01	[illegible] 01	-4 0907D 00	1 5002D 00

E-INC	ECC	DEG	END	WAIST	FRICTION	FLOW	R-FORCE	T-FORCE	R-INCR	T-INCR
0 8000	0 8000	0 099930	0 099930	1 0000	1 6667	[illegible]	0 0000D 01	7 7870D 00	0 0000D-01	0 0000D-01
	0 8250	0 062371	0 214030	0 8190	1 7626	[illegible]	6 9093D 01	9 4431D 00	-3 4982D-01	1 0600D-01
	0 8500	0 023005	0 254070	[illegible]	1 8710	[illegible]	[illegible]	1 1495D 01	-1 7436D 00	6 2791D-01
	0 8750	0 013074	0 281960	0 5020	2 0061	[illegible]	[illegible]	1 4190D 01	-3 2013D 00	9 1659D-01
	0 9000	0 006420	[illegible]	[illegible]	[illegible]	[illegible]	[illegible]	[illegible] 01	-4 9006D 00	1 5100D 00

(Sheet 3 of 3)

81-LUB-24

THE AMERICAN SOC OF MECHANICAL ENGINEERS
345 E 47 St., New York, ...Y. 10017

Dynamic Analysis of Rupture in Thin Fluid Films. I—A Noninertial Theory[1]

C. H. T. Pan
Professor of Mechanical Engineering
Columbia University
New York, NY 10027
Consultant
David W. Taylor Naval Ship R&D Center
Annapolis, MD 21402
Formerly,
Shaker Research Corporation,
Ballston Lake, NY 12019

A noninertial theoretical model for the dynamics of film rupture has been formulated. Under the transient condition, movement of the rupture boundary is governed by the condition of flow continuity between the film flux and adhered film transport in the cavitation domain. The traditional Swift-Stieber condition for film breakup is shown to be valid upon reaching steady-state. Generalization is extended to allow consideration of two sliding surfaces and the pure squeeze-film. The possibility of subcavitation film pressure is shown to result in dry regions in the cavitation domain.

1 Introduction

In the lubricant film of a self-acting bearing, surface sliding in the presence of spatial variation of the bearing gap constitutes the hydrodynamic wedge action, which is responsible for the load carrying pressure in the bearing film. If surface sliding is in the direction of gap divergence, then the pressure in the lubricant film tends to decrease. With the proper gap distribution, the reduced pressure in the diverging gap can combine with the elevated pressure in the convergent gap to form the overall load capacity of the bearing as illustrated by the classical Sommerfeld solution of the infinitely long journal bearing [1]. Although a reduced film pressure in a bearing may not be undesirable, it hardly ever happens in reality. It is usually found that the pressure in a conventional lubricant film cannot fall substantially below the atmospheric level. Presumably, lubricant used in real environments always contains some dissolved ambient gas, volatile constituents of moderately high vapor pressure, and sometimes even entrained gas phase in suspension. Thus, as surface sliding enters into a divergent region, the void fraction in the bearing gap will rapidly increase through a combination of physical and chemical processes. As a result, this region of high void fraction will prevent further reduction of the film pressure according to the hydrodynamic lubrication theory, instead, expansibility and a relatively low viscosity of the gas phase allow a zone of nearly uniform pressure to be formed. Among workers in the field of lubrication research, this process is interchangeably known as cavitation or film rupture.

A totally rigorous treatment of the film rupture process should give some attention to the thermodynamic and chemical behaviors of the liquid lubricant. The present work is a less ambitious undertaking by assuming a purely mechanistic viewpoint. Allowing sufficient time lapse, phase equilibrium may be considered to have been established. The pressure level in the cavitated lubricant film should in some way be related to the physical chemistry of the lubricant, and may be regarded as a constant parameter in the context of a mechanistic study. The detail flow structure of the ruptured film, viewed in the scale of the film thickness, is quite intricate. Liquid-solid-gas interfacial effects, free surface curvature, and fluid inertia are simultaneously interacting with the viscous stress which is dominating in the remote regions (from the rupture boundary). Meniscus features and/or striation fingers are merely particular features of the flow field here. The present work shuns involvement in this fine-scale point of view and will deal mainly with gross features on either side of the rupture boundary. Surface tension, for a film thickness of the submicron level, can also manifest itself in a subcavitation pressure in the immediate upstream of the rupture boundary. In the gross scale, one can accommodate this phenomenon by assigning a pressure jump at the rupture boundary. For common situations associated with bearings and dampers, the amount of this pressure jump is quite small when compared with the film pressure associated with hydrodynamic wedge and/or squeeze effects, and thus can justifiably be neglected. Pressure level alone, however, does not uniquely define the theoretical problem of a ruptured lubricant film; thus, the zero pressure gradient condition [2,3] has been regarded as the rigorous rupture condition. Use of the latter condition to analyze a one-dimensional bearing film (infinitely long) is a common practice. Two dimensional problems are less frequently treated with the same degree of care, due to the extreme complexity in computational undertaking required. The work of Jakobsson and Floberg [4] is an exemplifying exception; it brought out the need to satisfy the continuity condition throughout the cavitation domain. In lieu of satisfying the rigorous rupture condition, it is a common approximation to treat the film rupture problem with the Gümbel hypotheses [5]; such that the film pressure is first solved with no regard for film rupture, then all subambient pressure values are

[1] Supported in part by the U.S. Army Research Office under Contract Number DAAG29-78-C-0027, Project Number P-15657-E.

Contributed by the Lubrication Division of THE AMERICAN SOCIETY OF MECHANICAL ENGINEERS for presentation at the ASLE-ASME Joint Lubrication Conference, New Orleans, La., October 4-7, 1981. Manuscript received by the Lubrication Division March 5, 1981. Paper No. 81-Lub-24.

Copies will be available until June, 1982.

replaced by the ambient pressure. Such an approach is particularly popular in connection with the short bearing approximation [6] under the dynamic condition. More recently, the Swift-Stieber condition of film rupture has been adapted to study short bearing configurations [7-10]; in comparison with the Gümbel approximation, significantly different results were obtained [9,10].

While there is now a thorough understanding of the issues associated with a steady-state film rupture process, relatively little attention has been given to the time-dependent counterpart. Elrod [11] proposed a computational procedure for the time-dependent cavitation according to a derivation due to Olsson [12]. Fill fraction of the gap was identified as the state variable in a ruptured film, and any movement of the boundary between the full-film and the ruptured film was treated as a time rate of change of the fill fraction. Choosing to rely on a single algorithm for both the full film and the cavitation domains, the concept of fill fraction was retained for the full film via the use of fluid compressibility so that pressure elevation above the cavitation pressure was associated with a fill fraction in excess of unity. In the present work, the problem of a time dependent film rupture problem is examined analytically in a manner consistent with the established lubrication theory of the full film.

Primary emphasis of the present work will deal with the self-acting bearing, in which a closed cavitation domain limits the lower bound of the film pressure. Wedge action and squeeze film together determine the film pressure according to the lubrication theory. The sliding motion, traversing between rupture boundaries, dominates the flow distribution within the cavitation domain.

Film rupture is known to exist in squeeze bearings with or without simultaneous sliding. In particular, a complete mathematical equivalence exists between a squeeze-film damper in a circular whirl condition and a statically loaded journal bearing, including the global structure of cavitation. The absence of a sliding motion, however, brings about a different situation in the flow balance at the rupture boundary. Therefore, film rupture dynamics in the squeeze film will be given separate attention.

Since film rupture is generally regarded as a mechanism to limit an excessive reduction of film pressure, the cavitation pressure is usually assumed to be lower than the film pressure in the interior. However, there is no fundamental argument to rule out a subcavitation film pressure in the absolute sense, particularly under a dynamic environment. Therefore, in the present study, the consequence of a subcavitation film pressure will be examined.

As the first of several articles, the author intends to expound problems related to the dynamics of ruptured fluid films; he chooses not to invoke computed examples. It is hoped that broadly applicable conclusions can be firmly established in the qualitative sense. Subsequent efforts can then be properly channeled to seek specific results of significance.

Five major assumptions will be observed in subsequent derivations. They are briefly stated as follows:

- Standard approximations of the lubrication theory are retained for the unruptured domain.
- A constant and uniform pressure exists in the ruptured domain.
- A homogenous flow structure is assumed in the ruptured domain.
- An abrupt change in the flow structure occurs at the rupture boundary. Surface tension is neglected, and pressure continuity is assumed.
- Inertial effects are neglected in the ruptured domain.

2 The Self-Acting Bearing

The self-acting bearing of the conventional type is considered here. The adjective, "conventional," is emphasized to exclude the absence of a surface velocity and such special bearings which have nonvanishing sliding velocities at both surfaces.

With only one sliding surface, the flow field in the cavitation domain will be modeled as a layer of fluid which is adhered to the sliding surface. The adhered fluid layer will be called the "adhered film." No interaction between the adhered film and the stationary surface is allowed to cause

Nomenclature

B = a functional form of the external boundary condition
C = nominal gap
e = journal bearing eccentricity
h = gap or film thickness
h_a = thickness of adhered film
h_r^* = film thickness at a rupture point
$\mathbf{n}_r^*$ = unit outward normal of the rupture boundary
p = film pressure
p_c = pressure in the cavitation domain
p_s = lubricant supply pressure
Q = film flux
$\mathbf{r}_B$ = vector coordinate of the external boundary
$\mathbf{r}_r$ = vector coordinate of the rupture boundary
R = journal radius
t = time
t_b = birth time of adhered film
t_f = final time of adhered film
t_0 = characteristic time
U_r = sweeping speed of the rupture boundary
$\mathbf{U}_r$ = sweeping velocity of a rupture point
V = sliding speed
$\mathbf{V}$ = sliding velocity
x = circumferential coordinate on a journal bearing surface
x_0 = characteristic circumferential coordinate
x_r^* = circumferential coordinate of a rupture point; function of (z, t)
z = axial coordinate of a journal bearing
z_r^* = axial coordinate of a rupture point; function of (x, t)

Symbols

β = inclination of the rupture boundary to the surface velocity
μ = fluid viscosity
σ = striation fraction
ω = rotation speed

Subscripts

a = adhered film
b = breakup (of full-film)
c = cavitation
f = fill-back (of full-film)
I = rupture initiation
0 = reference point of the transport characteristics
p = related to the pressure (Poiseuille) effect
r = rupture boundary
R = film reestablishment
V = related to the sliding effect
W = widest point of cavitation
∇ = two-dimensional gradient operator on the bearing surface
$(\hat{\ })$ = variable ( ) view in a frame of reference fixed to surface 1
1, 2 = surfaces 1 and 2

*When subscript "r" is replaced by "b" or "f," a breakup point or a fill-back point is indicated.

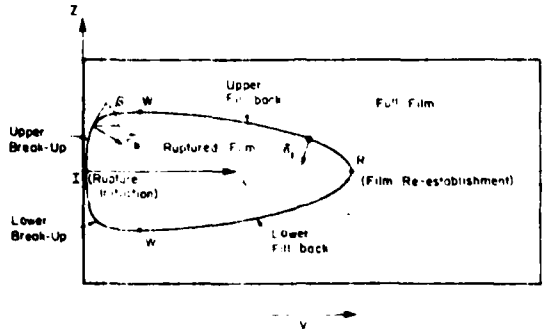

Fig. 1 Geometry of an enclosed cavitation domain

pressure variation in the cavitation domain. As a consequence, upon neglecting any inertia effects, the adhered film can be regarded to be fully quiescent relative to the sliding surface.

This model can be generalized to consider the bearing with two sliding surfaces provided

- a frame of reference can be used so that one of the two surfaces is not sliding with respect to the moving frame of reference,
- the second surface has a nonvanishing sliding velocity relative to the moving frame of reference, and
- the sum of the sliding velocities does not vanish.

Rules to be followed in order to achieve this generalization will be discussed at a later time. The immediate derivations will apply only to the case of a conventional self-acting bearing with a single sliding surface. The presence of (time dependent) squeeze effect, in addition to the wedge effect of the sliding surface, however, may be considered with the usual inclusion of the squeeze term in the treatment of the film pressure and by using the instantaneous gap for the fluid film at the rupture boundary.

(A) Geometrical Description of a Closed Cavitation Domain. If the cavitation domain should be enclosed by a full-film on all sides, as in the case of a journal bearing with both ends flooded or supplied with fluid, the rupture boundary can be divided into upper and lower branches for the convenience of analytical treatment. In the case of a self-acting bearing, each branch, in turn, can be divided into a breakup portion and a fill-back portion. The four parts of the rupture boundary can be identified with the inclination of its outward normal (pointing into the cavitation domain) relative to the surface velocity. According to the present convention, the surface velocity being aimed along the positive x-axis, the inclination of the outward normal has the following indicated property on each of the four parts of the rupture boundary:

	Breakup	Fill-back
Upper branch	− acute	− obtuse
Lower branch	+ acute	+ obtuse

As illustrated in Fig. 1, the upper and lower branches of the rupture boundary part from each other at the rupture initiation point "*I*" and continue on their respective breakup portions moving laterally away from each other. Each breakup boundary becomes more and more aligned with the surface velocity vector until it reaches point "*W*," where the boundary grazes the surface velocity vector. Beyond point "*W*," the boundary turns back in becoming a fill-back line. The fill-back lines eventually meet again at the film reestablishment point "*R*."

While a rectangular pl. orm is illustrated in Fig. 1, these features of the cavitation domain and its boundry are generally valid. For example, the bearing plan form may be annular, such that the surface velocity is a curved field.

(B) Fluid Transport in the Cavitation Domain. In a cavitated or ruptured domain of a self-acting bearing, the concept of an adhered film may be used to describe the fluid transport process. Explicitly, the adhered film thickness may be designated h_a; which can also be used for a striated film and be related to the striation fraction σ according to

$$h_a = \sigma h \tag{1}$$

Thus, subsequent discussions regarding fluid transport are applicable to both an adhered film in reality or the striated film by analogy.[1]

One may reasonably postulate that the gaseous constituents within the void regions do not influence the motion of the adhered film. Accordingly, the fluid transport law for the adhered film can be stated as

$$\left(\frac{\partial}{\partial t} + \mathbf{V}\cdot\nabla\right)h_a = 0 \tag{2}$$

This is a first order partial differential equation of the hyperbolic type, which possesses one real characteristic equation [13]. For the particular situation on hand, using the uniform field $\mathbf{V}$ of the cylindrical journal bearing for illustration, the characteristic equation is

$$x - x_0 = V(t - t_0) \tag{3}$$

The axial coordinate does not appear explicitly in the characteristic equation because equation (2) makes no reference to the direction transverse to the surface velocity. For the same reason, the characteristic equation is meaningful only when the axial coordinate is fixed. t_0 may be zero, then x_0 refers to an element of the adhered film in its initial field $h_a(x_0, z, 0)$. Or, for $t_0 = t_b > 0$, x_0 is to be identified with the breakup point $x_b(z, t_b)$ on the rupture boundary. The characteristic equation is the trajectory of an element of the adhered film in the $x-t$ plane for a fixed axial location. This trajectory terminates as the element of the adhered film meets a fill-back point on the rupture boundary $x_f(z, t)$.

(C) Sweeping Motion of the Rupture Boundary. The rupture boundary, which separates the full-film and the cavitation domains, may not be stationary. Its motion is dictated by the balance of flux between the full-film and the adhered film. By definition, the sweeping velocity $\mathbf{U}_r$ is aimed along the outward normal $\mathbf{n}_r$. As illustrated in Fig. 2, which depicts the displacement by the sweeping motion for an infinitesimal duration Δt, continuity consideration yields

$$U_r(h_r - h_a) = \left(-\left(\frac{h_r^3}{12\mu}\right)(\nabla p)_r + \frac{h_r}{2}\mathbf{V} - h_a\mathbf{V}\right)\cdot\mathbf{n}_r \tag{4}$$

The first term on the right-hand side is the Poiseuille flow. Because the rupture boundary is an isobar, it is always perpendicular to the Poiseuille flow. If the film pressure is higher than the cavitation pressure, then the Poiseuille flow tends to cause the rupture boundary to contract; the reverse is true if the film pressure is lower. The second and third terms are, respectively, the Couette flow and the transport of the adhered film. Being directionally controlled by the surface velocity, they contribute to the motion of the rupture boundary through the normal component (to the rupture boundary) of the surface velocity. Depending on the balance

[1] A fundamental distinction between an adhered film and a striated film is the ability of the latter to sustain a shear stress. This distinction is important only when attempts to calculate friction are made, but is irrelevant to equations of pressure, flow, and the geometry of the rupture boundary.

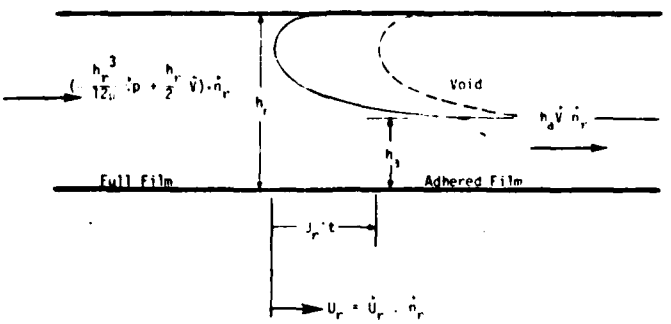

Fig. 2 Displacement of a sweeping rupture point

between the Couette flow and the adhered film transport, as well as the inclination of the surface velocity relative to the rupture boundary, the net effect of these two terms may also cause the rupture boundary to contract or to enlarge.

For a cylindrical journal bearing, the inclination of the rupture boundary is $\beta = \pi/2 - \tan^{-1}(\partial x_r/\partial z)$ and that of the outward normal is $\beta \mp \pi/2$, the alternative signs of the latter angle apply, respectively, to the upper and lower branches of the rupture boundary. Hence equation (4) becomes

$$U_r(h_r - h_a) = \pm\left(\frac{h_r^3}{12\mu}\right)\left(\frac{\partial p}{\partial z}\right)_r \cos\beta$$

$$\pm\left(-\left(\frac{h_r^3}{12\mu}\right)\left(\frac{\partial p}{\partial x}\right)_r + V\left(\frac{h_r}{2} - h_a\right)\right)\sin\beta \qquad (5)$$

The foregoing equation encompasses the special case of a stationary rupture boundary, for which the breakup point requires

$$h_a = \frac{h_b}{2}; \quad \left(\frac{\partial p}{\partial x}\right)_b = \left(\frac{\partial p}{\partial z}\right)_b = 0 \qquad (6a,b)$$

while the fill-back point requires

$$\left(\frac{h_f^3}{12\mu}\right)\left(\frac{\partial p}{\partial z}\right)_f\left(\frac{\partial x_f}{\partial z}\right) - \left(\frac{h_f^3}{12\mu}\right)\left(\frac{\partial p}{\partial x}\right)_f + V\left(\frac{h_f}{2} - h_a\right) = 0 \qquad (7)$$

Equation (6*b*) may be recognized as the Swift-Stieber condition [2,3]. The steady-state problem for a journal bearing of finite length was solved by Jakobsson and Floberg [4]. The short-bearing version of the steady-state problem was treated by Wakurai, et al. [7], with respect to the flow requirement of a short journal bearing, by Findlay [8] concerning the operation of a wavy face seal, and by Pan [9, 10] regarding the load characteristics of a short-bearing or a squeeze-film damper.

For a time-dependent problem, an important issue is the appropriate relationship between h_b, the film thickness of the full-film approaching the breakup boundary, and $h_a(x_b, t_f)$, the thickness of the adhered film immediately downstream. This question must be resolved in the context of providing a consistent link between the full-film and the adhered film across the breakup boundary. Since the adhered film introduces the point of view of a characteristic line at a fixed z, equation (3), it is useful to rewrite equation (5) into

$$\frac{\partial x_r}{\partial t} = U_r \sec\left(\beta \mp \frac{\pi}{2}\right)$$

$$= (h_r - h_a)^{-1}\left(\left(\frac{h_r^3}{12\mu}\right)\left(\frac{\partial p}{\partial z}\right)_r\left(\frac{\partial x_r}{\partial z}\right) - \left(\frac{h_r^3}{12\mu}\right)\left(\frac{\partial p}{\partial x}\right)_r + V\left(\frac{h_r}{2} - h_a\right)\right) \qquad (8)$$

The subscript "r" indicates that equation (8) is in a form which is applicable to either a breakup point or a fill-back point. However, for the breakup point, a relationship between h_b and h_a (z_b, t_b) must somehow be established; while for the fill-back point, h_a (x_f, t_f) is to be consistent with the transport law for the adhered film.

Actual implementation of equation (8) would become difficult in the neighborhood of point W, where $(\partial x_r/\partial z)$ becomes unbounded. This difficulty can be avoided by considering the rupture boundary as z_r (x, t) in this vicinity. Then, instead of equation (8), one can write

$$\frac{\partial z_r}{\partial t} = \mp U_r \sec\beta$$

$$= (h_r - h_a)^{-1}\left(-\left(\frac{h_r^3}{12\mu}\right)\left(\frac{\partial p}{\partial z}\right)_r + \left[\left(\frac{h_r^3}{12\mu}\right)\left(\frac{\partial p}{\partial x}\right)_r - V\left(\frac{h_r}{2} - h_a\right)\right]\left(\frac{\partial z_r}{\partial x}\right)\right) \qquad (9)$$

(D) World Diagrams of the Adhered Film. The transport process of the adhered film, as described by the characteristic equation, can be effectively presented in terms of the world diagram which traces the space-time relationships of pertinent phenomena. As an illustrative example, a model problem will be described to depict the evolution of the cavitation domain from that of a "half Sommerfeld film" to the steady-state solution which rigorously satisfy the Swift-Stieber condition and the adhered film transport law. For this purpose, the bearing gap h (x, y) is assumed to be time-independent. The initial state of the full-film domain is that portion of the "full Sommerfeld" solution where p $(x, y) \geq p_c$, p_c being the assumed cavitation pressure. Within the rupture boundary x_r $(z, t = 0)$ which encloses the subcavitation domain of the full Sommerfeld solution, a suitable initial field of the adhered film is presumably known, i.e., h_a $(x, z, t = 0)$ has been specified. For a fixed value of z, one is thus given the complete distribution of h_a $(t = 0)$ over the span x_b $(z, t = 0) < x \leq x_f$ $(z, t = 0)$. A series of characteristic lines can be drawn in the $x - t$ plane as described by the characteristic equation

$$x(t) - x(0) = Vt \qquad (10)$$

Along each characteristic line, h_a retains its value as specified in h_a $(x, z, t = 0)$. The world diagram is bounded on the left by the history of the breakup point x_b (z, t) and on the right by the history of the fill-back point x_f (z, t). x_b and x_f are obtained by the time-domain integrations of $(\partial x_b/\partial t)$ and $(\partial x_f/\partial t)$, respectively.

The left boundary of the world diagram, x_b, immediately brings up the question regarding the proper value of h_a (x_b, z, t_b), in order to initiate the analysis of the transport process. Previously, it was shown that a stationary breakup boundary requires that both equations (6*a*) and (6*b*) be satisfied. Violation of equation (6*b*) causes the breakup boundary to move. However, so long as the breakup boundary lags behind

the sliding surface (subcritical feeding), equation (6*b*) can be retained; thus,

$$h_a(x_h, z, t_h) = \frac{1}{2}h_h$$

for subcritical feeding (11*a*, *b*)

$$\frac{\partial x_h}{\partial t} = \left(\frac{h_h^2}{6\mu}\right)\left[\left(\frac{\partial p}{\partial z}\right)_h\left(\frac{\partial x_h}{\partial z}\right) - \left(\frac{\partial p}{\partial x}\right)_h\right]$$

This set of results cannot be universally valid, because, in the vicinity of point W where $\partial x_h/\partial z \to \infty$, equation (11*b*) would become unbounded. Before the latter condition prevails, $\partial x_h/\partial t$ would exceed V so that whatever may be $h_a(x_h, z, t_h)$, the motion of the breakup point would sweep ahead the adhered film such that h_a would have to be associated with the characteristic field of prior time, i.e., the adhered film at the point immediately downstream of the breakup point has existed prior to the approach of the rupture boundary. Thus the last term on the right-hand side of equation (8), which was omitted on account of equation (11*a*), would have to be retained. Thus, the subcritical feeding condition must obey the constraint

$$\left(\frac{h_h^2}{6\mu}\right)\left[\left(\frac{\partial p}{\partial z}\right)_h\left(\frac{\partial x_h}{\partial z}\right) - \left(\frac{\partial p}{\partial x}\right)_h\right] \le V \qquad (12)$$

A supercritical feeding condition is indicated if

$$\left(\frac{h_h^2}{6\mu}\right)\left[\left(\frac{\partial p}{\partial z}\right)_h\left(\frac{\partial x_h}{\partial z}\right) - \left(\frac{\partial p}{\partial x}\right)_h\right] = V + \Delta V;\ \Delta V > 0 \qquad (13)$$

Substituting into equation (8) with h_a identified with the prior time characteristics, one obtains

$$\frac{\partial x_h}{\partial t} = V + \frac{h_h \Delta V}{2(h_h - h_a)} \qquad (14)$$

which assures that the breakup point would indeed sweep ahead the adhered film regardless of the specific value of h_a. Since the condition of supercritical feeding is most likely induced by a large magnitude of $(\partial x_r/\partial z)$, the sweeping motion should be calculated in terms of $(\partial z_r/\partial t)$ according to equation (9). However, the test for the critical feeding condition should still be performed in terms of equation (13). Subsequently,

$$\frac{\partial z_r}{\partial t} = \begin{cases} -\left(\frac{h_h^2}{6\mu}\right)\left[\left(\frac{\partial p}{\partial z}\right)_h - \left(\frac{\partial p}{\partial x}\right)_h\left(\frac{\partial z_h}{\partial x}\right)\right], \\ \qquad \text{for subcritical feeding} \\ (h_h - h_a)^{-1}\left(-\left(\frac{h_h^3}{12\mu}\right)\left(\frac{\partial p}{\partial z}\right)_h\right. \\ \left. + \left[\left(\frac{h_h^3}{12\mu}\right)\left(\frac{\partial p}{\partial x}\right)_h - V\left(\frac{h_h}{2} - h_a\right)\right]\left(\frac{\partial z_h}{\partial x}\right)\right) \\ \qquad \text{for supercritical feeding} \end{cases} \qquad (15a, b)$$

The right boundary of the world diagram has a motion described by equation (8) if one merely replaces the subscript r by f. It may be regarded to be the sum of a pressure component $(\partial x_f/\partial t)_p$ and a sliding component $(\partial x_f/\partial t)_s$:

$$\frac{\partial x_f}{\partial t} = \left(\frac{\partial x_f}{\partial t}\right)_p + \left(\frac{\partial x_f}{\partial t}\right)_s$$

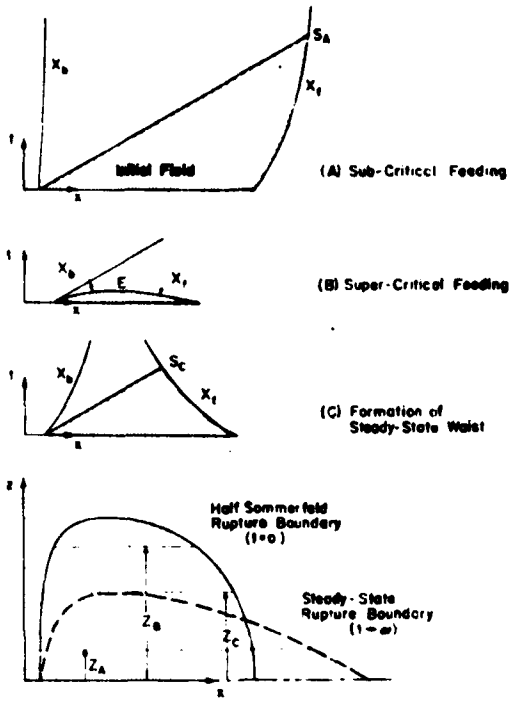

Fig. 3 World diagrams of rupture transition

$$\left(\frac{\partial x_f}{\partial t}\right)_p = \frac{h_f^3}{12\mu(h_f - h_a)}\left(\left(\frac{\partial p}{\partial z}\right)_f\left(\frac{\partial x_f}{\partial z}\right) - \left(\frac{\partial p}{\partial x}\right)_f\right)$$

$$\left(\frac{\partial x_f}{\partial t}\right)_s = \frac{V(h_f - 2h_a)}{2(h_f - h_a)} = V\left(1 - \frac{h_f}{2(h_f - h_a)}\right) \qquad (16a, b, c)$$

If the film pressure is assumed to be above p_a at all times, then $(\partial x_r/\partial t)_p$ is always negative. Now that $(\partial x_f/\partial t)_s$ is always less than V; therefore $(\partial x_f/\partial t)$ is always algebraically less than V so that one can be certain that the fill-back point is always overtaken by the adhered film. Again, where the magnitude of $(\partial x_f/\partial z)$ is large, it is better to treat the fill-back boundary as $z_f(x, t)$ in numerical implementation:

$$\frac{\partial z_f}{\partial t} = (h_f - h_a)^{-1}\left(-\left(\frac{h_f^3}{12\mu}\right)\left(\frac{\partial p}{\partial z}\right)_f + \left[\left(\frac{h_f^3}{12\mu}\right)\left(\frac{\partial p}{\partial x}\right)_f - V\left(\frac{h_f}{2} - h_a\right)\right]\left(\frac{\partial z_f}{\partial x}\right)\right) \qquad (17)$$

Representative world diagrams showing the transition of the cavitation domain in a journal bearing film from the half Sommerfeld state to the steady-state Swift-Stieber state are given in Fig. 3. Each world diagram describes the history of the adhered film at a particular axial location. At the bottom of Fig. 3, solid and dashed outlines, respectively, depict the initial and final rupture boundaries. Three horizontal lines are drawn through both boundaries. z_4 is near the central region of the cavitation domain. In this case, the breakup point feeds at a subcritical condition. The fill-back point moves under the influence of the initial field $h_a(x, z_4, 0)$ until it arrives at point S_4, where the earliest characteristic line from x_h intersects x_f. Both x_h and x_f have vertical asymptotes which mark the steady-state boundary points. z_B is close to the initial zero slope point. The breakup point moves ahead of its own characteristic lines. The fill-back point, with $\partial x_f/\partial t$ dominated by its pressure component, moves backward and meets the breakup point at "*E*." The world diagram ends here because the rupture boundary has swept below z_f. z_C grazes

point W of the final rupture boundary. The breakup point moves forward rapidly at first, albeit at a subcritical feeding condition. The fill-back point moves back quite rapidly in the initial period, dominated by the pressure component under the influence of the initial field $h_u(x, z_r, 0)$ until point "S_c," where x_r meets the earliest characteristic line from x_b. In the late period, as both x_b and x_r approach the final location of point W, the magnitude of the normal pressure gradient in the fluid film at the rupture boundary reduces to a negligible level; they both turn toward the vertical direction, reflecting slowing down of the sweeping motion and eventually they approach the same asymptote and coalesce into the final location of point W.

(E) The Initial Field. The true initial period of void generation and growth must necessarily involve mass transfer between liquid and gas phases so that thermodynamic and chemical parameters may not be negligible. The purely mechanistic model, therefore, may not be applicable until a later time, when the status quo of a relatively extensive void fraction prevails in the cavitation domain. The initial field of the thickness distribution of the adhered film, $h_u(x, z, 0)$, must be reconcilable with the initial film pressure. If one accepts the constraint that the film pressure cannot fall below the cavitation level, then it is necessary to exclude the possibility of a fully filled gap as the initial condition, which requires $h_u(x, z, t-0) = h(x, z, t-0)$. For this reason, the pseudo steady-state condition to be defined as follows is proposed to be the initial state of the adhered film. Given the description of the rupture boundary at the initial instant, $x_r(z, 0)$, the pseudo steady-state thickness of the adhered film is

$$h_u(x_b < x < x_r, z, 0) = \frac{1}{2} h(x_r, z, 0) \tag{18}$$

It should be recognized, however, the constraint that the film pressure cannot be subambient may not be realistic. There may be circumstances for which such an assumption should be relaxed. This issue will be further discussed at a later section.

(F) Interfacing with Film Pressure Calculation. Analysis of the adhered-film transport problem cannot be performed without dealing with the surrounding fluid film pressure at the same time. In fact, the starting point is most likely a half Sommerfeld type pressure field which is the solution of the conventional Reynolds' equation. Steps of computation required to perform the overall analysis are outlined in the following.

- Solve the appropriate form of Reynolds' equation, e.g.,

$$\nabla \cdot \left\{ -\left(\frac{h^3}{12\mu}\right) \nabla p + \frac{1}{2} \mathbf{V} h \right\} = 0 \tag{19}$$

Requisite boundary conditions include both external ones, e.g., those associated with bearing ends and feed slots, which can be expressed in the form

$$B[\mathbf{r}_B;\ p, p_s] = 0 \tag{20}$$

$\mathbf{r}_B$ is the vector coordinate of the external boundary and p_s is the applicable supply pressure, and also the pressure of the rupture boundary

$$p(\mathbf{r}_r,\ t) = p_c \tag{21}$$

$\mathbf{r}_r$ is the vector coordinate of the rupture boundary. An initial estimate of the rupture boundary may be determined from the half Sommerfeld solution. Pressure gradient at the rupture boundary, $\nabla p(\mathbf{r}_r, t)$, is to be established.

- Subdivide the rupture boundary into upper and lower branches, and for each branch into breakup and fill-back portions.

- Calculate the sweeping rates of the rupture boundary, using equations (8) and (9) as may be appropriate. Initially, a starting distribution of the adhered film thickness, $h_u(\mathbf{r}, t=0)$ in the cavitation domain is to be furnished, e.g., equation (18).

- Step in time to update the geometry of the rupture boundary. Subsequently, the full cycle of computations can be repeated as many times as necessary. To enhance the overall accuracy of the time-stepping operation, the Runge-Kutta method and/or the predictor corrector method [14] may be adopted. The size of time step should reflect the resolution required to depict the time-dependence of p.

3 Two Sliding Surfaces

There are self-acting bearings with two sliding surfaces. For instance, both the shaft and the bushing may be rotating, each at a different speed, while their centers are kept at a fixed displacement from each other. The applicable equations for such a bearing are

$$h = C - e\cos\left(\frac{x}{R}\right)$$

$$\frac{\partial}{\partial z}\left[\left(\frac{h^3}{12\mu}\right)\left(\frac{\partial p}{\partial z}\right)\right] + \frac{\partial}{\partial x}\left[\left(\frac{h^3}{12\mu}\right)\left(\frac{\partial p}{\partial x}\right) - \frac{1}{2}(V_1 + V_2)h\right]$$

$$= \left(\frac{\partial h}{\partial t}\right)_{x,z} = 0$$

$$(V_1, V_2) = (\omega_1, \omega_2)R \tag{22a, b, c}$$

In order to describe the adhered film in the cavitation domain, it is necessary to assume a frame of reference such that one of the surfaces does not have a sliding velocity. Such a frame of reference may be rotating at ω_1, and in such a frame of reference, the bearing gap is no longer time-independent. The required transformation is

$$\hat{x} = x - V_1 t \tag{23}$$

Accordingly, equations (22*a*, *b*) become

$$h = C - e\cos\left(\frac{\hat{x} + V_1 t}{R}\right)$$

$$\frac{\partial}{\partial z}\left[\left(\frac{h^3}{12\mu}\right)\left(\frac{\partial p}{\partial z}\right)\right] + \frac{\partial}{\partial \hat{x}}\left[\left(\frac{h^3}{12\mu}\right)\left(\frac{\partial p}{\partial \hat{x}}\right) - \frac{1}{2}(V_2 - V_1)h\right]$$

$$= \left(\frac{\partial h}{\partial t}\right)_{\hat{x},z} = V_1\left(\frac{\partial h}{\partial \hat{x}}\right) \tag{24a, b}$$

The difference between equations (22*b*) and (24*b*) is only in appearance so far as the pressure field is concerned. However, the Couette flux now becomes $1/2\,(V_2 - V_1)h$ so that the sweeping motion of the rupture boundary is governed by

$$\hat{U}_r(h_r - \hat{h}_u) = \pm\left(\frac{h_r^3}{12\mu}\right)\left(\frac{\partial p}{\partial z}\right)_r \cos\beta \pm \left[-\left(\frac{h_r^3}{12\mu}\right)\left(\frac{\partial p}{\partial \hat{x}}\right)_r + (V_2 - V_1)\left(\frac{h_r}{2} - \hat{h}_u\right)\right]\sin\beta \tag{25}$$

$\hat{U}_r$ is the sweeping speed viewed in the rotating frame of reference. $\hat{h}_u$ is the thickness of the adhered film which is attached to the moving surface (in the rotating frame of reference). And, in terms of the coordinates of the rupture point,

$$(h_r - \hat{h}_u)\frac{\partial x_r}{\partial t} = \left[\left(\frac{h_r^3}{12\mu}\right)\left(\frac{\partial p}{\partial z}\right)_r \left(\frac{\partial x_r}{\partial z}\right) - \left(\frac{h_r^3}{12\mu}\right)\left(\frac{\partial p}{\partial \hat{x}}\right)_r + (V_2 - V_1)\left(\frac{h_r}{2} - \hat{h}_u\right)\right]$$

$$(h_r - \hat{h}_a)\frac{\partial z_r}{\partial t} = -\left(\frac{h_r^3}{12\mu}\right)\left(\frac{\partial p}{\partial z}\right)_r + \left[\left(\frac{h_r^3}{12\mu}\right)\left(\frac{\partial p}{\partial \hat{x}}\right)_r - (V_2 - V_1)\left(\frac{h_r}{2} - \hat{h}_a\right)\frac{\partial z_r}{\partial \hat{x}}\right] \quad (26a, b)$$

At the steady-state condition, $t \to \infty$, the rupture boundary should become stationary in the space fixed coordinate system, i.e.,

$$\lim_{t\to\infty} \frac{\partial \hat{x}_r}{\partial t} = -V_1$$

Accordingly, equation (26*a*) becomes

$$\lim_{t\to\infty} \left(\frac{h_r^3}{12\mu}\right)\left[\left(\frac{\partial p}{\partial z}\right)_r\left(\frac{\partial \hat{x}_r}{\partial z}\right) - \left(\frac{\partial p}{\partial \hat{x}}\right)_r\right] + \frac{1}{2}(V_1 + V_2)h_r - V_2\hat{h}_a = 0 \quad (27)$$

At the breakup point, equation (27) is satisfied by

$$\left(\frac{\partial p}{\partial z}\right)_b = \left(\frac{\partial p}{\partial \hat{x}}\right)_b = 0$$

$$\hat{h}_a = \frac{1}{2}\left(\frac{V_1 + V_2}{V_2}\right)h_b \quad (28a, b)$$

Since $\hat{h}_a$ cannot exceed h_b, it is necessary to impose the constraint

$$|V_2| > |V_1| \quad (29)$$

This means the choice of the rotating frame of reference is not arbitrary, it must be fixed to the slower surface. Accordingly, the adhered film must be attached to the faster surface.

Having established the "birth value" of the adhered film and its transport speed, it is not necessary to retain the rotating frame of reference in subsequent analysis. One can now return to the space-fixed coordinate system to describe the sweeping motion of the rupture boundary:

$$U_r(h_r - h_a) = \pm\left(\left(\frac{h_r^3}{12\mu}\right)\left[\left(\frac{\partial p}{\partial z}\right)_r\cos\beta - \left(\frac{\partial p}{\partial x}\right)_r\sin\beta\right] + \left[\frac{1}{2}(V_1 + V_2)h_r - V_2h_a\right]\sin\beta\right) \quad (30)$$

where

$$\beta = \cos^{-1}(\mathbf{V}_2\cdot\mathbf{n}_r/V_2) \pm \pi/2$$

$$\frac{\partial x_r}{\partial t} = (h_r - h_a)\left(\left(\frac{h_r^3}{12\mu}\right)\left[\left(\frac{\partial p}{\partial z}\right)_r\left(\frac{\partial x_r}{\partial z}\right) - \left(\frac{\partial p}{\partial x}\right)_r\right] + \left[\frac{1}{2}(V_1 + V_2)h_r - V_2h_a\right]\right) \quad (31)$$

$$\frac{\partial z_r}{\partial t} = -(h_r - h_a)\left(\left(\frac{h_r^3}{12\mu}\right)\left[\left(\frac{\partial p}{\partial z}\right)_r - \left(\frac{\partial p}{\partial x}\right)_r\left(\frac{\partial z_r}{\partial x}\right)\right] + \left[\frac{1}{2}(V_1 + V_2)h_r - V_2h_a\right]\left(\frac{\partial z_r}{\partial x}\right)\right) \quad (32)$$

At a subcritical breakup point

$$\frac{\partial x_b}{\partial t} = \left(\frac{V_2}{V_2 - V_1}\right)\left(\frac{h_r^3}{6\mu}\right)\left[\left(\frac{\partial p}{\partial z}\right)_b\left(\frac{\partial x_b}{\partial z}\right) - \left(\frac{\partial p}{\partial x}\right)_b\right] \le V_2 \quad (33)$$

The adhered film is formed with its "birth" thickness

$$h_a = \left(\frac{V_1 + V_2}{V_2}\right)\left(\frac{h_b}{2}\right) \quad (34)$$

At a subcritical breakup point, h_a of prior time applies in equations (30-32). The characteristic equation in the cavitation domain is

$$x(t) - x(0) = V_2 t \quad (35)$$

Equations (30-35) are seen to include the "conventional" self-acting bearing ($V_1 = 0$, $V_2 = V$) as a special case, corresponding to equations (5, 8, 9, 12, 11*a*, 10), respectively.

The counter-rotating bearing ($V_1 = -V_2$) without squeeze is of no interest. The film pressure does not develop any circumferential variation, and therefore its film does not rupture.

The corotational bearing ($V_1 = V_2$) yields the special birth thickness of the adhered film

$$h_a = h_b \quad (36)$$

and the sweeping motion at a breakup point is preempted by the Swift-Stieber condition

$$\left(\frac{\partial p}{\partial z}\right)_b = \left(\frac{\partial p}{\partial x}\right)_b = 0 \quad (37)$$

4 Squeeze Film without Sliding

The pressure of a pure squeeze-film satisfies

$$\nabla\cdot\left[\left(\frac{h^3}{12\mu}\right)\nabla p\right] = \frac{\partial h}{\partial t} \quad (38)$$

and a suitable set of external boundary conditions, e.g., equation (20). Rupture may also take place as a mechanism to limit the lower bound of the squeeze-film pressure. Because the surfaces have no sliding motion, fluid left in the cavitation domain is "trapped." The motion of the rupture boundary is given by equation (4) upon setting $\mathbf{V}$ to zero:

$$U_r(h_r - h_a) = -\left(\frac{h_r^3}{12\mu}\right)(\nabla p)_r\cdot\mathbf{n}_r \quad (39)$$

The geometry of the cavitation domain can still be represented by Fig. 1; however, in the absence of the sliding velocity, the concepts of breakup and fill-back must be reexamined.

If the film pressure is above the cavitation pressure, then the right-hand side is positive. Since the cavitation domain is generally not filled, $(h_r - h_a)$ would be positive, so that U_r would also be positive. Thus the rupture boundary would move into the cavitation domain and the trapped fluid of prior time would become a part of the squeeze film. This is a fill-back point, and h_a represents the amount of trapped fluid already existing on the cavitation side of the rupture boundary.

Under certain circumstances, the constraint on the lower bound of the film pressure may dictate that U_r be negative, so that the rupture boundary would recede, leaving behind new fluid to become trapped in the cavitation domain. But the right-hand side of equation (39) must be nonnegative. Consequently, h_a must equal the film thickness to reconcile the two sides of equation (39), while the Swift-Stieber condition is to be satisfied by the squeeze film. The receding rupture boundary of a squeeze film can therefore be regarded as a breakup point. The corresponding birth value of h_a is

$$h_a = h_b;\ (\nabla p)_b = 0 \text{ if } U_b < 0 \quad (40a, b)$$

It is possible for a pure squeeze-film to have a fully receding rupture boundary. This usually happens when the film thickness is increasing with time for the entire cavitation domain. Thus one can have a filled cavitation domain as the initial state, so long as the Swift-Stieber condition is enforced on the entire rupture boundary in the film pressure.

The half Sommerfeld film pressure may also be used as the initial condition. When this is done, a partially scavenged initial cavitation domain, $h_a(x, z, 0) < h(x, z, 0)$, must be

assumed. Otherwise U_r would be infinite, rendering the initial state meaningless.

To consider a whirling squeeze-film, equation (39) can be replaced by the components

$$\left(\frac{\partial x_r}{\partial t}\right)(h_r - h_a) = \left(\frac{h_r^3}{12\mu}\right)\left[\left(\frac{\partial p}{\partial z}\right)_r \left(\frac{\partial x_r}{\partial z}\right) - \left(\frac{\partial p}{\partial x}\right)_r\right]$$

or

$$\left(\frac{\partial z_r}{\partial t}\right)(h_r - h_a) = -\left(\frac{h_r^3}{12\mu}\right)\left[\left(\frac{\partial p}{\partial z}\right)_r - \left(\frac{\partial p}{\partial x}\right)_r \left(\frac{\partial z_r}{\partial x}\right)\right] \tag{41a, b}$$

Upon reaching a steady-whirl condition,

$$\lim_{t\to\infty} \frac{\partial x_r}{\partial t} = V$$

then equation (41a) becomes

$$\lim_{t\to\infty} \left(\frac{h_r^3}{12\mu}\right)\left[\left(\frac{\partial p}{\partial z}\right)_r \left(\frac{\partial x_r}{\partial z}\right) - \left(\frac{\partial p}{\partial x}\right)_r\right] - V(h_r - h_a) = 0$$

which is satisfied by

$$\lim_{t\to\infty} \left(\frac{\partial p}{\partial z}\right)_b = \left(\frac{\partial p}{\partial x}\right)_b = 0; \quad h_a = h_b$$

$$\lim_{t\to\infty} \left(\frac{\partial x_f}{\partial z}\right) + \frac{\left(\frac{12\mu V}{h_f^3}\right)(h_f - h_b) + \left(\frac{\partial p}{\partial x}\right)_f}{\left(\frac{\partial p}{\partial z}\right)_f} \tag{42a, b}$$

These relations represent a precise analog of the steadily whirling squeeze-film to a statically displaced self-acting journal in both the film pressure and the rupture boundary. However, in the latter case, $h_a = 1/2\ h_b$, i.e., the fluid content in the cavitation domain of the journal bearing is one-half of that of the whirling damper.

5 Subcavitation Film Pressure

The assumption of a constant and uniform pressure in the cavitation domain, p_c, does not necessarily mean it has to be a lower bound of the film pressure at the same time. The latter condition should be recognized as a conceptual artifact which is invoked to avoid a rigorous consideration of the thermodynamic and chemical processes which may be present. Such a posture can be justified if one is concerned with a steady-state situation and that thermodynamic and chemical equilibria can be assured. Unfortunately, thermodynamic and chemical equilibria hardly ever exist in the pure sense. In studying dynamic problems, it is quite possible that the rate of chemical kinetics associated with mass transfer between liquid and gaseous phases in a rupturing film may be quite small in comparison with the rate of mechanical phenomena of interest. Therefore, it may be necessary to abandon the constraint that p_c is the lower bound of the film pressure.

One approach to resolve the conceptual dilemma described earlier is to specify the existence of a cavitation domain, in which p_c prevails, but not to require a lower bound of the film pressure in the unruptured domain. Such a model may be justified by the following lines of reasoning.

- Void generation in the fluid film begin at internal nucleation sites of entrained bubbles, as well as surface nucleation sites.
- There are sufficient number of nucleation sites where the growth rate is high enough so that the voids merge, aggregate, and cumulate within the boundaries of the bearing film.
- After an adequate lapse time, which is short in comparison with the operation time of the bearing but long as compared with the growth-aggregation-cumulation processes, mass transfer between the phases become minimal and can be neglected.
- In the absence of significant mass transfer, residual void fraction in the fluid film is negligible. Pressure fluctuations within the fluid film can be sustained. In any case, with the presence of a cavitation domain, the pressure within the fluid film cannot fall substantially below p_c.

On the basis of these postulated ideas, one can proceed to examine the mathematical consequences of subcavitation pressure in the fluid film near the rupture boundary.

Consider first the self-acting bearing. With a subcavitation film pressure in the immediate vicinity of the rupture boundary, $(\nabla p)_r \cdot \mathbf{n}$, would be positive and the Poiseuille flux would aim away from the cavitation domain. The total flux toward a rupture boundary is

$$Q_r = \left[-\left(\frac{h_r^3}{12\mu}\right)(\nabla p)_r + \frac{1}{2}(\mathbf{V}_1 + \mathbf{V}_2)h_r\right]\cdot\mathbf{n}, \tag{43}$$

r may be replaced by b or f in reference to a breakup or a fill-back point. With a subcavitation film at a breakup point, Q_r can be negative. When this happens, the breakup boundary withdraws, leaving behind a dry region. Therefore, a drying up condition of a breakup point is due to

$$Q_b < 0$$

consequently,

$$h_a = 0; \quad U_b = Q_b/h_b < 0 \tag{44a, b}$$

If Q_b is positive, but less than the Couette flux due to a subcavitation film, then the adhered film thickness is still given by equation (34); in the meantime, as may be obtained from equation (30),

$$U_b = -\left(\frac{V_2}{V_2 - V_1}\right)\left(\frac{h_b^2}{6\mu}\right)(\nabla p)_b \cdot \mathbf{n}_b < 0 \tag{45}$$

indicating a receding motion. If the film pressure at a fill-back point is subcavitation, then a supercritical fill-back condition can exist:

$$(h_f - h_a)^{-1}\left(\left(\frac{h_f^3}{12\mu}\right)\left[\left(\frac{\partial p}{\partial z}\right)_f \left(\frac{\partial x_f}{\partial z}\right) - \left(\frac{\partial p}{\partial x}\right)_f\right] + \left[\frac{1}{2}(V_1 + V_2)h_f - V_2 h_a\right]\right) = V_2 + \Delta V > V_2 \tag{46}$$

The fill-back point would be moving ahead the transported adhered film, opening up a dry domain; accordingly, the supercritical sweeping speed of a fill-back point is obtained by setting h_a to zero in equation (30) yielding

$$U_f = Q_f/h_f < 0; \text{ where } Q_f/h_f = \sin\beta\left[V_2 + \left(\frac{h_f - h_a}{h_f}\right)\Delta V\right] \tag{47}$$

h_a being given in the prior time value.

The pure squeeze-film with subcavitation film pressure can be regarded as a special case of the self-acting bearing with the sliding velocities set to zero. The total flux is then identically the Poiseuille flux,

$$Q_r = -\left(\frac{h_r^3}{12\mu}\right)(\nabla p)_r \cdot \mathbf{n}, \tag{48}$$

and there is no distinction between breakup and fill-back points. The subcavitation film pressure automatically causes the drying up condition:

$$h_a = 0; \quad U_r = Q_r/h_r \text{ if } Q_r < 0 \tag{49a, b}$$

The possibility of dry regions due to the subcavitation film pressure may be described in the world diagram as shown in Fig. 4. The world diagram of a pure squeeze-film has vertical characteristic lines.

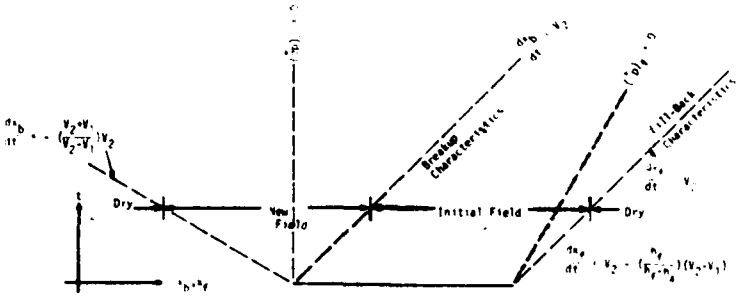

Fig. 4 World diagram with subcavitation film pressure

6 In Retrospect

The time dependent problem of film rupture can be analyzed in terms of the movement of the rupture boundary. The instantaneous motion of the rupture boundary is the result of flow balance between the full film on one side, which is described by the traditional lubrication theory, and the ruptured film on the other side, which is incapable of sustaining any significant pressure gradient due to the abundant presence of large scale voids.

Consistent with the lubrication analysis employed for the full film, inertia effects may be neglected for the ruptured film. Using a homogeneous model, the ruptured film may be regarded as a layer adhered to the sliding surface. The adhered film is transported through the cavitation domain with an invariant thickness which cannot exceed the local gap.

The adhered film next to a ruptured boundary may have one of three states, in reference to its thickness. The adhered film is in its *prior time state*, if the rupture boundary is advancing on the sliding surface; the thickness of the prior time adhered film is determined from past history of the ruptured film. The adhered film is in its *newly born state* if the rupture boundary is "subcritically fed" by the full film flux and lags behind the sliding surface; the thickness "at birth" of the adhered film is one-half of the local gap (if only one of the two surfaces has a sliding speed). The adhered film is in its *dry state* if the total film flux is directed away from the rupture boundary; the dry adhered film has no thickness. The dry adhered film always borders a full-film with a subcavitation pressure.

In mathematical terms, dynamics of the ruptured film is concerned with a mixed field initial value problem. In the model problem illustrated in this paper, the full-film domain is the outer field; the field variable is the film pressure, its governing equation is elliptical in character. The cavitation domain is the inner field; the field variable is the adhered film thickness, its governing equation is hyperbolic in character. Coupling between the two fields is maintained through

- the cavitation pressure as the internal boundary condition of the film pressure,
- birth of new adhered film at subcritically fed rupture point, and
- motion of the rupture boundary as determined by the states of the fields on both sides.

The initial value set includes the location of the rupture boundary and the distribution of the adhered film. The film pressure field at every instant can be computed according to Reynolds' equation with the cavitation pressure imposed at the rupture boundary. Birth values of adhered film thickness, as well as the sweeping speed of the rupture boundary, can be determined accordingly. Time domain integration of the motion of the rupture boundary allows incremental updating of both field variables and the rupture boundary. If the film pressure is not allowed to become lower than the cavitation pressure, the initial state of the adhered film cannot be a fully filled gap.

Generalization to the case of two sliding surfaces requires that the ruptured film be adhered to the faster-sliding surface. The birth value of the adhered film is thicker by an additional fraction, which is equal to the ratio of the slower sliding speed over the faster sliding speed, as compared to that for the case of a single sliding surface. The adhered film is transported by the faster sliding speed. The case of equal sliding speed, including the pure squeeze film with zero sliding of both surfaces, has a birth value of the adhered film equal to the full local gap, and the Swift-Stieber condition is to be satisfied at a subcritically fed rupture point.

References

1 Sommerfeld, A., "Zur hydrodynamischen theorie der Schmiermittelreibung," *Z. Math. Phys.*, Vol. 50, 1904, pp. 97-155.

2 Swift, H. W., "The Stability of Lubricating Films in Journal Bearings," *Proceedings Institution of Civil Engineers* (London), Vol. 233, 1932, pp. 267-288.

3 Stieber, W., "Das Schwimmlager," *VDI*, Berlin, 1933.

4 Jakobsson, B., and Floberg, L., "The Finite Journal Bearing, Considering Vaporization," *Trans. Chalmers University Tech.*, Nr. 190 Goteborg, 1957.

5 Gümbel, L., and Everling, E., "Das Problem der Lagerreibung," *VDI*, Vol. 5, 1914, pp. 87-104.

6 Dubois, G. B., and Ocvirk, F. W., "Analytical Derivation of Short Bearing Approximation for Full Journal Bearings," NACA Report 1157, 1953.

7 Wakurai, Y., et al., "Oil Flow in Short Bearing with Circumferential Groove," *Bulletin of the JSME*, Vol. 16, No. 92, Feb. 1973, pp. 441-446.

8 Findlay, J. A., "Cavitation in Mechanical Face Seals," ASME Journal of Lubrication Technology, Vol. 90, Apr. 1968, pp. 356-364.

9 Pan, C. H. T., "An Improved Short Bearing Analysis for the Submerged Operation of Plain Journal Bearings and Squeeze-Film Dampers," ASME Journal of Lubrication Technology, Vol. 102, No. 3, July 1980, pp. 320-332.

10 Pan, C. H. T., and Ibrahim, R. A., "Cavitation in a Short Bearing with Pressurized Lubricant Supply," ASME Journal of Lubrication Technology, Vol. 103, No. 3, July 1981, pp. 337-349.

11 Elrod, H. G., Jr., "A Cavitation Algorithm," ASME Journal of Lubrication Technology, Vol. 103, No. 3, July 1981, pp. 350-354.

12 Olsson, K., "Cavitation in Dynamically Loaded Bearings," *Trans. Chalmers Univ. Tech.*, 308, Goteborg, 1965.

13 Courant, R., and Hilbert, D., *Methoden der mathematischen Physik*, Vol. II, Springer, Berlin, 1937.

14 Seely, S., Tarnoff, N. H., and Holstein, D., *Digital Computers in Engineering*.

Printed in U.S.A.


DATE:
ILME